ABSTRACT

This report describes an investigation of the effects of tension strain on buckling of reinforcement. It will propose that the propensity for reinforcing bars to buckle under cyclic loading is tied directly to the amount of tension strain the bar is subjected to. This will be accomplished by, first conducting a literature review of past research to see what has been done in the way of predicting buckling. Then a buckling mechanism will be presented that evaluates buckling by the maximum tension strain a bar is subjected to before buckling in compression. In order to investigate the proposed buckling mechanism, a series of four large-scale column tests were conducted where the only variable in the tests was the loading history. The results from these tests will show that tension strain is an important factor in predicting the onset of buckling in reinforced concrete bridge columns.

INFLUENCE OF TENSION STRAIN ON BUCKLING OF REINFORCEMENT IN RC BRIDGE COLUMNS

by

MATTHEW JAMES MOYER

MERVYN KOWALSKY

CIVIL ENGINEERING

NORTH CAROLINA STATE UNIVERSITY

MAY 1, 2001

ACKNOWLEDGEMENTS

The research described in this report was supported jointly by a North Carolina State University Faculty Research and Professional Development Grant, and the Department of Civil Engineering. In addition, AmeriSteel of Raleigh and Steel Specialties of Mississippi provided support in the form of materials donations. Undergraduate student support was received from the NC State HMS-Rise program and NC State/National Taiwan University Exchange program that supported the contributions of Nathaniel Homer and Eddy Cheng. Lastly, the author would like to thank the technical staff of the NC State Constructed Facilities Laboratory – especially the efforts of Jerry Atkinson and Bill Dunleavy without whom this work would not have been possible.

TABLE OF CONTENTS

LIST OF TABLES

LIST OF FIGURES

1.0 Introduction

Properly detailed columns experience a flexural failure that is often accompanied by buckling of longitudinal reinforcement. Previous research has provided no reliable way to predict when this will occur. However, it is well established that the transverse steel details have a significant effect on the propensity for buckling. An increase in transverse steel will provide better confinement of the concrete core, delaying the initiation of buckling. Prediction of a column's performance based on concrete compression strain is not reliable due to the variability of the concrete compression strain capacity. Hence there is a need to find a reliable method of predicting column performance. This report will propose a method of evaluating buckling of longitudinal reinforcement, by the peak tension strain induced in the longitudinal bar.

There are three main motivating factors for this research. First, buckling of longitudinal reinforcement is a common mode of failure for properly detailed columns. Secondly, current buckling models are unreliable in predicting the onset of buckling. Thirdly, with seismic design moving more towards performance based methods, performance levels must be accurately defined.

This report has thirteen chapters to investigate the effects of tension strain on buckling. Lets first establish a need for the understanding why buckling occurs. With designing of bridge columns going more towards performance based engineering the performance levels need to be known with reliable results. Chapter 1 will discuss these prescribed performance levels and how to use them in designing bridge columns. A literature review will be conducted on past research to see what has been done in the way of predicting buckling of bridge column reinforcement. Chapter 2 will discuss past

buckling models and the inadequacies of these models to predict buckling of longitudinal reinforcement. A buckling mechanism will be presented that focuses on the peak allowable tension strain for predicting buckling of longitudinal reinforcement. Chapter 3 will present the proposed buckling mechanism for a reinforced concrete column. A second literature will be conducted of circular columns tested that have experienced a buckling failure. When these previous columns were tested it was not to investigate buckling as the failure mechanism, however, buckling did occur, thus making them useful for this report. Chapter 4 will present the information on these previous test columns and provide some preliminary insight on possible tension strain capabilities. Four identical columns with identical instrumentation and test setup will be presented. Chapters 5, 6, and 7 will discuss the details involved in designing, instrumentation, and test setup of the test columns. A series of four tests will be conducted to investigate the effects of tension strain on buckling of longitudinal reinforcement and determine the total tension strain that is associated with buckling of longitudinal reinforcement for these test columns. This total tension strain will be defined as the characteristic compression strain (ε_{scc}) of the column. This characteristic compression strain will be discussed in greater detail in chapter 12. Chapters 8, 9, 10, and 11 will discuss individually each test conducted with the variable between each test being the loading history of the column. An analysis all of the test data and how the characteristic compression strain of the column is used in design will be presented. The conclusion will summarize what was accomplished in this research and what steps need to be taken from here.

1.1 Scope and Objective of Research

A characteristic compression strain will be determined for the columns tested in this research. The characteristic compression strain will only be valid for columns with the same axial load ratio and transverse steel ratio of the specimens tested in this project. Columns must also be detailed in such a manner to prevent other types of failures, otherwise the characteristic compression strain is invalid. A change in the axial load ratio and transverse steel ratio of a column will change the characteristic compression strain. By knowing the characteristic compression strain of a column with specific axial load ratio and transverse steel ratio, the performance of the column can be predicted.

1.2 Research Significance

With design techniques moving more towards performance based design, it is important to establish reliable strain capacities for each level of performance. Strain levels can be defined based on compression limits for steel and concrete and tension limits for steel. In this report, the primary focus is on the ultimate limit state as defined by buckling of reinforcement. Historically, this has been defined by compression limits on steel and or concrete, however, it is postulated that a steel limit may be the more critical variable. Once performance levels such as ultimate are adequately defined, procedures such as Direct Displacement Based Design can be applied. The following section will provide some background information about limit states and Direct Displacement Based Design.

1.3 Seismic Design Concepts

When earthquakes occur they cause a wide variety of damage. Limit states are used to describe the level of damage a structure suffers during an earthquake. Typical limit states are serviceability, damage control, and survival. Reviewing these concepts is the first step in understanding the focus of performance based engineering.

1.4 Limit States

There are several limit states an engineer can use to quantify structural performance. The most common of the design limit states are defined as 1) serviceability 2) Damage Control 3) Survival. This is by no means an exhaustive list, however, they do represent important performance levels. Limit states such as cracking and yield are arguable less important for seismic design. The subsequent three sections will briefly discuss the key limit states and the strain limits typically associated with them.

1.4.1 Serviceability Limit State

"The serviceability concrete strain is defined as the strain at which crushing would occur, while the serviceability tension strain is defined as the strain at which residual crack widths would be over 1 mm, thus likely requiring repair and interrupting serviceability" (16). The structure that has reached this state performs in the inelastic range. Hence, there will be some residual deformation in the column and residual strains in the reinforcement. Concrete compression strains at the serviceability limit state are estimated to be around 0.004. Steel tension strains at this limit state are estimated to be around 0.015. (16)

1.4.2 Damage Control Limit State

"The damage control concrete strain has been defined based on conservative estimates of confined concrete strain capacity based on the Mander, Priestley, and Park energy balance approach (1988). The steel strain limit has been established based on experimental evidence and allows for cyclic damage to reinforcement" (16). Concrete compression strains at this limit state are estimated to be around 0.018. Steel tension strains at this limit state are estimated to be around 0.060. (16)

1.4.3 Survival Limit State

The survival limit state still remains somewhat of an unknown. A modern bridge column will likely suffer a flexural failure at this limit state, by buckling of the longitudinal reinforcement. The research in this report aims to develop a model for identifying strain limits for this limit state.

Tests conducted for this project together with previous tests will help provide more information about the survival limit state of reinforced concrete bridge columns. The development of the maximum allowable tension strain for the columns tested in this research will allow for the prediction of the ultimate displacement of columns with similar axial load ratio and transverse steel ratio.

1.5 Displacement Based Design

Once the limit states are defined, then they can be utilized in the Direct Displacement Based Design process. Direct Displacement Based Design allows engineers to design structures for a prescribed limit state. Instead of using forces, target displacements are used to design structures. Target displacements are chosen based on

the desired performance level of the structure. The following flow chart in conjunction with equations in chapter 4 shows the process for Displacement Based Design.

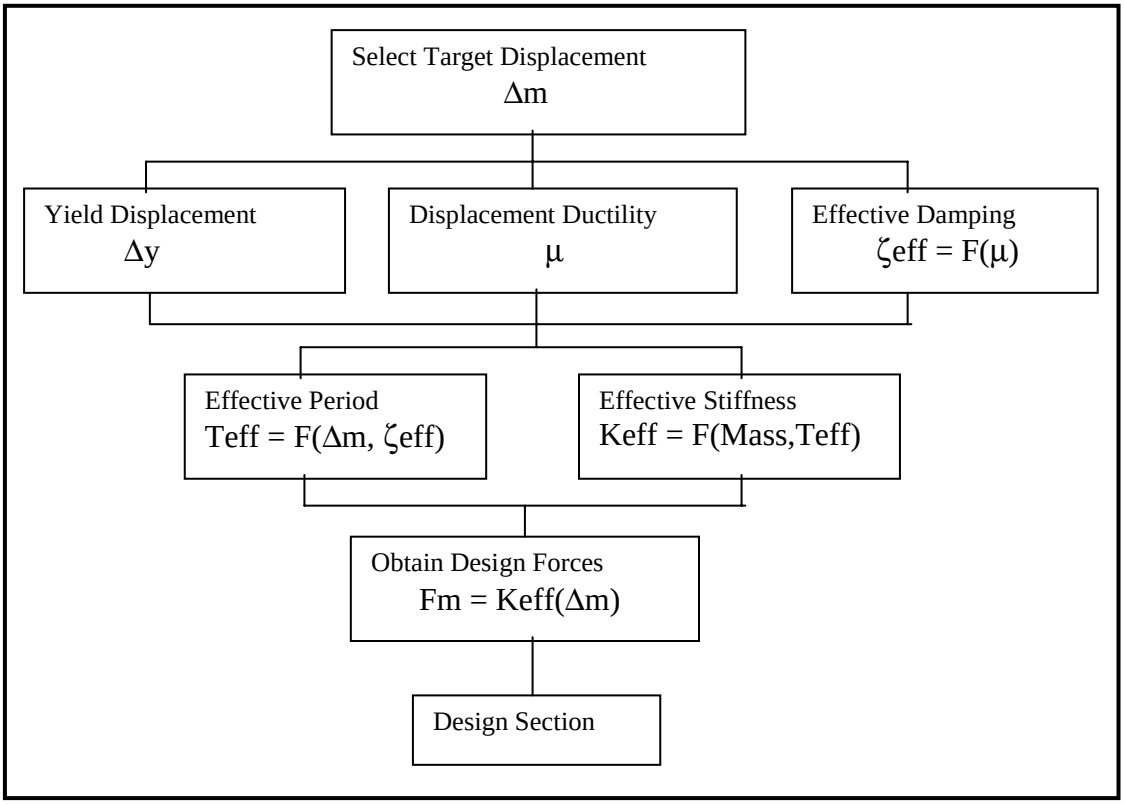

Figure 1.1 Displacement Based Design Flow Chart (8)

1.6 Non-Linear Behavior

In Displacement Based Design, a column will be allowed to perform in the inelastic range to achieve the target displacement. The exact force verses displacement response of a column is the solid curve shown in figure 1.2. To simplify the curve a bilinear approximation is used, this is represented by the two dashed lines in figure 1.2. The bilinear approximation is created by, first determining the equivalent yield displacement. The equivalent yield displacement is determined using equation 4.4. The bilinear approximation is formed by first connecting the origin of the two axes and the

equivalent yield point (Δ_y) with a line. Then the second line is drawn parallel to the displacement axis in the positive displacement direction.

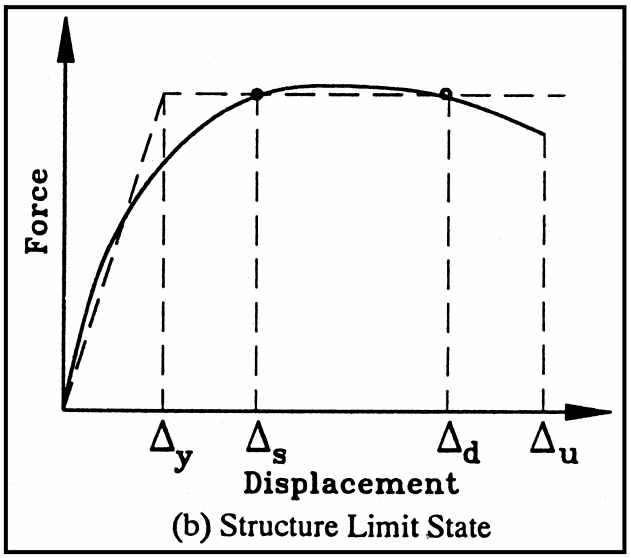

Figure 1.2 Structural Limit States (16)

2.0 Literature Review

Previous research has been done on buckling of longitudinal reinforcement in circular bridge columns. The main focus of the research has been on the compression strains in the longitudinal steel. It has also been noted that proper detailing of transverse steel is crucial in obtaining high levels of concrete strain. Some research has also been done in trying to establish a relationship between reduced modulus and concrete strain to model the performance of bridge columns during an earthquake. The most recent research focuses on the tension strain of the reinforcing bar before out of plain buckling in masonry walls (15). These different approaches try to answer the question of when buckling occurs. No single approach has the answer but each approach provides insight on the buckling phenomenon.

2.1 Past Research

This report will focus on investigating the influence of tension strain on buckling in circular bridge columns. The importance of compression capacity of the column still remains crucial because the bars will only buckle under compressive load. This report will present a hypothesis that the crucial point of buckling can best be described by the tension strain a bar is subjected too.

S.J. Pantazopoulou has conducted research in detail of reinforcement for stability in reinforced concrete members. In this research the following was observed. “The actual point of buckling initiation, which is identified in strain measurements as the point where strain in the bar deviates from the average strain in the surrounding concrete, often occurs earlier than the instant of reported visible buckling. Thus collapse occurs at

deformation levels larger than the point of deviation between the two strain measures (14)."

Researchers found that by adding larger amounts of transverse steel, they could increase the compression capacity of the concrete core. The detailing of the reinforcing bar is an important factor in achieving these higher concrete strain capacities. Researchers also found that the transverse steel should be no more than half the diameter of the longitudinal steel (18). The spacing can then be adjusted to achieve certain transverse steel ratios. As the spacing of the transverse steel decreases, the confinement of the concrete core is enhanced. This early research has lead to further investigation of how buckling occurs.

Another approach to predicting buckling is the reduced modulus approach. The reduced modulus is based on evaluating the section modulus at different levels of ductility. This reduced modulus is calculated as a function of the tangent modulus and Young's modulus of the reinforcement. Although this approach is somewhat more accurate than other approaches it only focuses on the steel capacity and does not take into account the effect of crack closure and the concrete core helping carry the load.

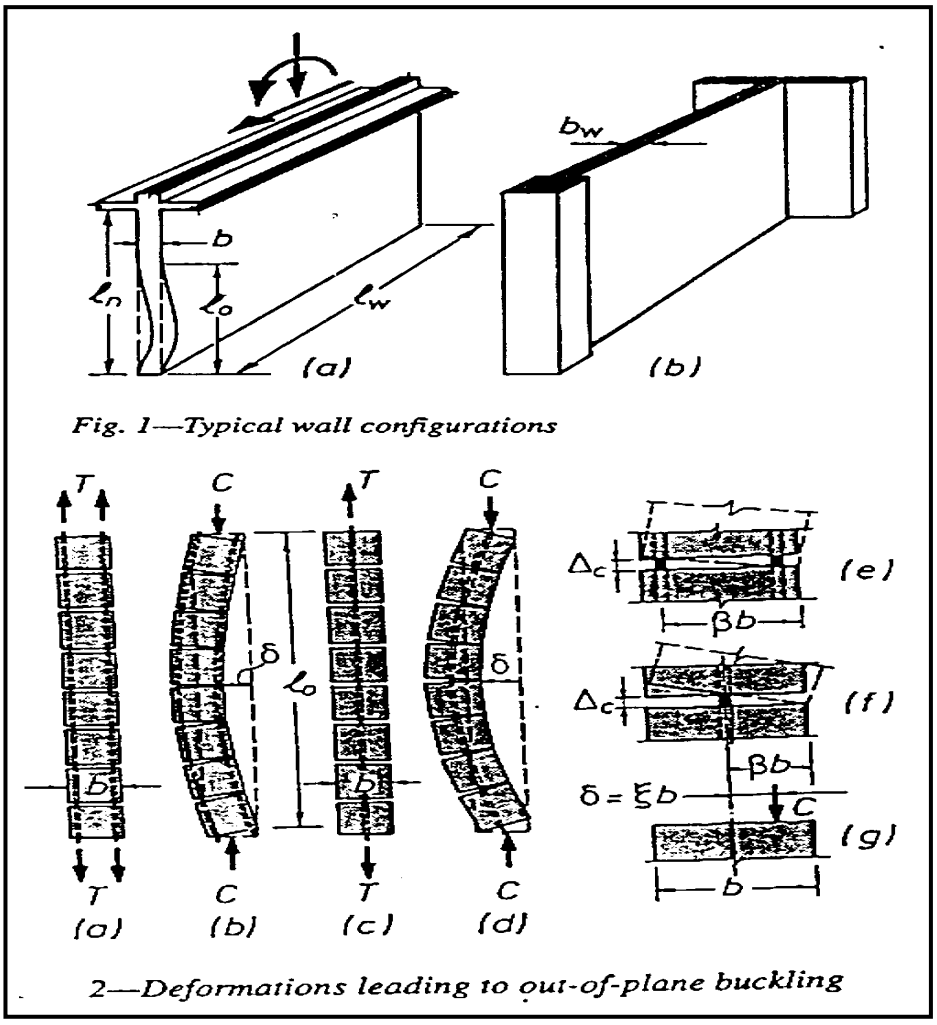

Figure 2.1 Paulay and Priestley out of Plane Buckling of Masonry Walls (15)

The influence of tension strain on buckling was first observed by Paulay and Preistley for the out of plane buckling of masonry walls (15). Their research has led to a method to predict out of plane buckling in masonry walls due to the flexural tension strain induced in the bar. They propose that the maximum tension strain and residual strain in a bar can be calculated by the following equations.

$$\varepsilon_{sm} = 8\beta\left(\frac{b}{L_o}\right)^2 \xi_c \qquad (Eq.3.1)$$

$$\varepsilon'_{sm} = \varepsilon_{s,\max} - \varepsilon_y \qquad (Eq.3.2)$$

In equation 3.1, L_o is the horizontal length of the wall section, b wall thickness, and ξ_c eccentricity ratio. In equation 3.2 $\varepsilon_{s,max}$ is the maximum tension strain the wall has been subjected to and ε_y is the yield strain (15). Y. H. Chai and D. T. Elayer have also done similar work with masonry walls. They proposed that the maximum tension strain that a wall may be exposed to is described in equation 3.3 (3).

$$\varepsilon_{sm} = \frac{\pi^2}{2}\left(\frac{b}{L_o}\right)^2 \xi_c + 3\varepsilon_y \qquad (Eq.3.3)$$

Although these models are for masonry walls and the mechanism is different than that of a circular bridge column, the effects of tension strain on buckling of reinforcement is the same, and as such provides a background for the mechanism discussed in this report.

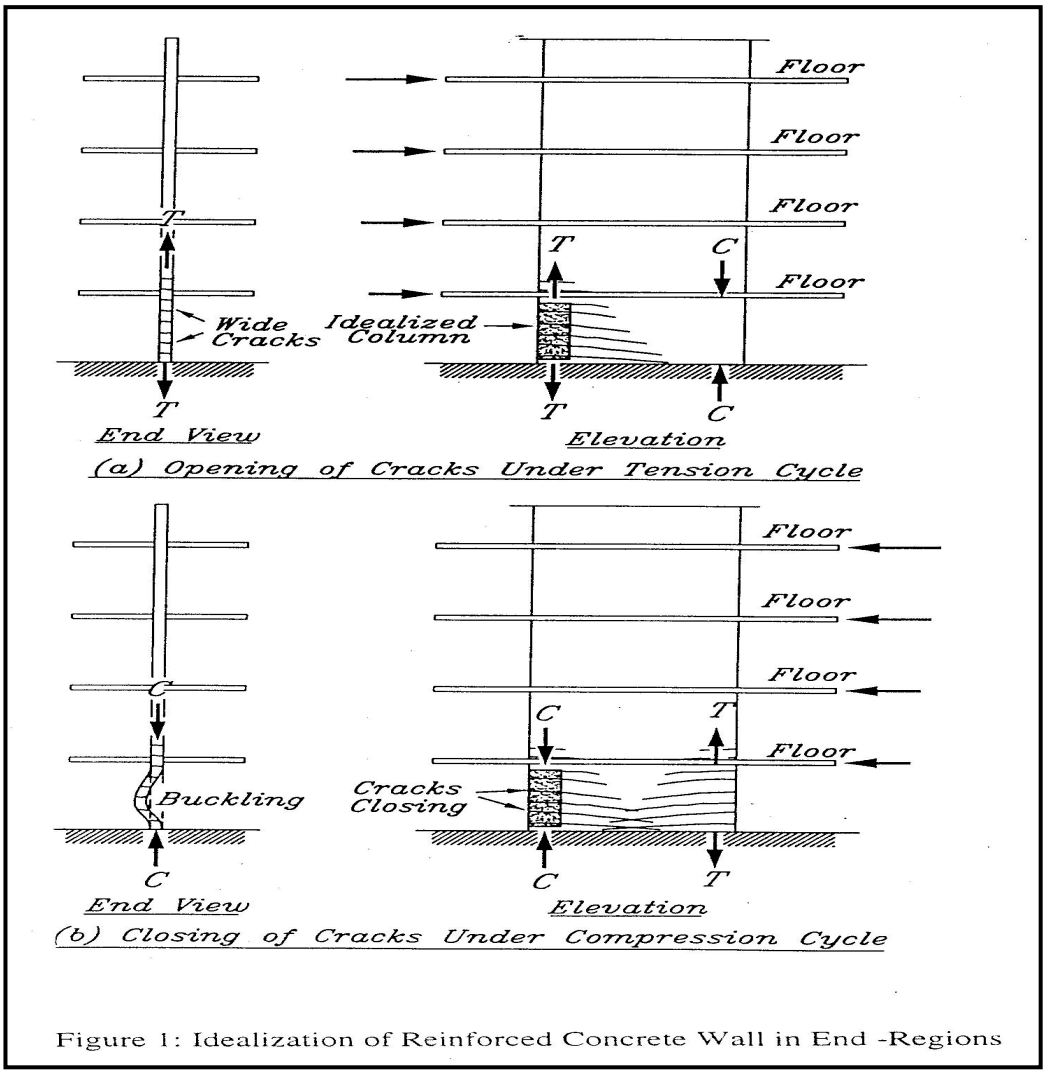

Figure 2.2 Chai and Elayer out of Plane Buckling of Masonry Walls (3)

3.0 Buckling Mechanism

There are five key strain variables in the proposed buckling model that must be described before the model can be discussed in detail. They are: (1) Peak steel compression strain, ε_{scp}. (2) Peak steel flexural tension strain, ε_{stp}. (3) Residual steel growth strain at zero column displacement, ε_{sgr}. (4) Total steel tension strain, ε_{stt}. (5) Characteristic steel compression strain capacity, ε_{scc}.

In order to define these strain parameters; consider Figure 3.1A, which represents an idealized reinforced concrete column subjected to lateral loading. The bar numbered 1 represents the bars subjected to compression for the direction of load shown, while the bar numbered 2 represents the bars subjected to tension for the direction of load shown. As the column displacement is increased to a value of Δ_a as shown at the location marked A in the force-displacement envelope of figure 3.1B, bar 2 is represented by the point marked A on the stress strain curves of figure 3.1B. From figure 3.1B the peak flexural steel tension strain, ε_{stp} is defined at displacement Δ_a.

Upon load reversal as the column displacement moves to point B in Figure 3.1C, the strain in bar 2 has not yet returned to zero. This residual growth strain is referred to as ε_{sgr} as shown by point B in figure 3.1C. As the column is loaded to zero displacement, the cracks are open on the bar 2 side (Point C figure3.1D), while the cracks on the bar 1 side are also open. Upon further loading to point D as shown in the force-displacement curve in figure 3.1E, the stress-strain condition in the reinforcing bars is now characterized by the stress-strain curve in figure 3.1E. If the cracks on bar 2 side close

before buckling of longitudinal reinforcement starts then the concrete core will help carry the compression load and buckling is delayed to a later cycle.

3.1 Model Description

The last of the variables is ε_{scc}, which represents the characteristic compression strain that a bar can sustain on its own before buckling occurs. This variable was not defined in the previous section. This variable is largely a function of transverse steel ratio, and its calculation is beyond the scope of this work. An exhaustive number of research efforts have been aimed at identifying it. It is also noted that the model described here does not contradict the many efforts aimed at identifying characteristic compression strain capacity. It rather incorporates the observation that reinforcing bars in a concrete section are required to deform in compression without the aid of the concrete for a period of time. This is directly related to the amount of tension strain the bars are first subjected to.

Consider the following scenario while referring to figure 3.1. Upon reversal from point A, bar 2, which was subjected to a tension strain of ε_{stp}, is immediately placed in compression. Similarly, bar 1, which was subjected to a compression strain of ε_{scp}, is immediately placed in tension, bar 2 must carry the entire compressive strain demand until the cracks in the section close at which time the concrete contributes to the compression zone stability and steel buckling is postponed. Therefore, the problem reduces to one of calculating the strain at which the cracks close. For bar 2, this is equal to the peak flexural tensile strain. As long as the peak flexural tensile strain is less than the characteristic compression strain capacity, ε_{scc}, buckling will not occur at this point on the bar 2 side.

Upon further loading the critical side becomes the bar 1 side. Referring to figure3.1E, bar 1 is now subjected to an effective total tension strain of ε_{stt} at a point beyond D on figure 3.1E. This total tension strain consists of two components, one due to bending, and one due to the residual growth strain, ε_{sgr}. The component due to bending is simply the tension strain obtained from flexural strength theory at the chosen displacement level. The component due to growth, ε_{sgr}, which manifests itself as an offset as shown in figures 3.1C, will be a function of the steel constitutive relationship. In order to avoid buckling upon reversal from a point beyond D bar 1 must be able to sustain in compression a strain equal to ε_{stt}.

One observation must be made at this point. First, note that if the column is cycled at the same level of displacement, thus resulting in the same level of induced flexural tension strain due to bending, the potential for buckling increases as the growth in the column increases with each cycle. It is also noted that the discussion of the experimental program in the remainder of the report aims to investigate these assumptions and develop a mechanism for its use in analysis and design.

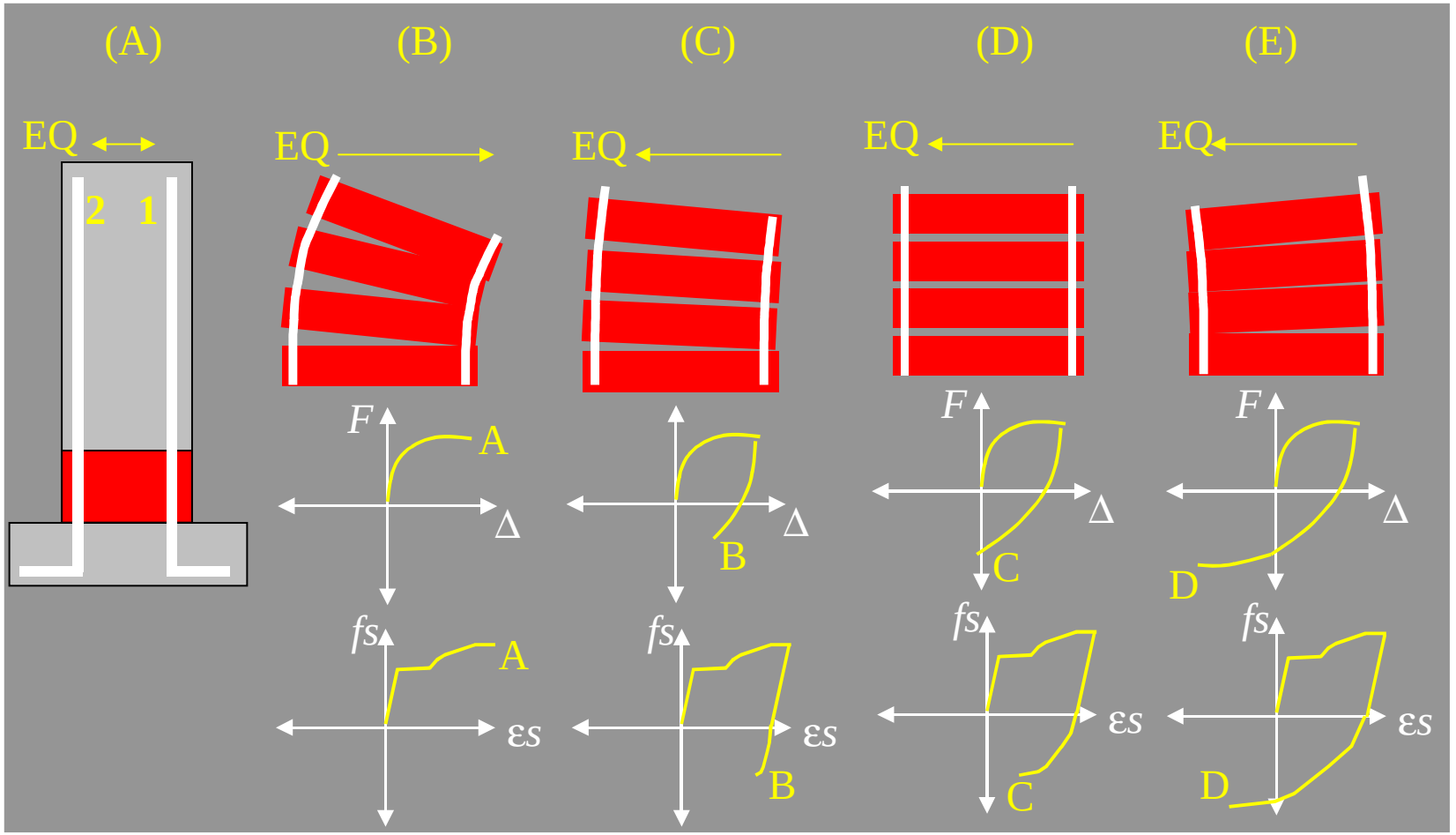

Figure 3.1 Proposed Buckling Mechanism

4.0 Database of Sample Columns

This database is a collection of circular test columns that experienced a flexural failure. The columns presented in this database have longitudinal steel that buckled in the plastic hinge region. Each column is different in percent steel areas and axial load ratio. A portion of this database was provided through personal communication with Professor Andrew Budek of Southwest Texas State University.

Not all of the columns presented in this database were tested to evaluate the buckling failure. Many of the test columns were experimental test that measured displacement ductility capacity but also experienced a flexural failure. Due to the elaborate description of the column performance during the tests the point at which buckling occurred was identified. This database is used to determine a range of possible tension strains in the longitudinal reinforcement of a column with a given axial load ratio and transverse steel ratio.

4.1 Sample Data

The columns in this database consist of tests from many sources. All of the columns experienced a flexural failure. From each article certain information had to be obtained. The results of the column failure were reviewed to ensure that the longitudinal steel did buckle. After ensuring the column failed due to buckling of longitudinal reinforcement, the ultimate lateral displacement of the column at failure was determined. Usually this information was given in the result section but sometimes it was read from graphs or calculated from displacement ductility at buckling. Information gathered about the columns material properties and section dimensions are listed below.

- Column diameter
- Aspect ratio (AR) – ratio of the column height over the column diameter
- Axial Load
- Concrete Strength
- Axial Load Ratio (ALR) – Axial load divided by the gross area of the section times the concrete strength
- Longitudinal steel – bar diameter, quantity per column, yield load, percent steel ratio
- Transverse Steel – bar diameter, pitch, yielding load, percent steel ratio

4.2 Analysis of Data

4.2.1 Calculation of Tension Strain

After all the information needed was collected, moment curvature analysis was performed and equations were used to determine the steel strain. The moment curvature analysis program gave the following information: neutral axis depth (c), maximum moment (M_{ideal}), yield curvature (ϕ_y), ultimate curvature (ϕ_u). Experimental information provides the ultimate displacement (Δ_u). The dimensions of the column section minus the cover concrete determine the depth (d) to the tension steel. The procedure in finding the maximum strain is as follows. Equations 4.2, 4.7, and 4.8 are for metric units all of the other equations work for both english and metric.

- Given – c, d, ϕ_y, Δ_u
- L_{col} = Length of the column

$$L_{col} = AR(Col.Dia) \qquad (Eq.4.1)$$

- L_{sp} = Length of strain penetration (16) (*dbl* – longitudinal bar diameter)

$$L_{sp} = 0.022(f_y)dbl \qquad (Eq.4.2)$$

- L_{eff} = effective length of the column

$$L_{eff} = L_{col} + L_{sp} \qquad (Eq.4.3)$$

- Δ_y = Yield displacement

$$\Delta_y = \frac{\phi_y (L_{eff})^2}{3} \qquad \textit{Single Bending} \qquad (Eq.4.4)$$

$$\Delta_y = \frac{\phi_y (L_{eff})^2}{6} \qquad \textit{Double Bending} \qquad (Eq.4.5)$$

- Δ_p = Plastic Deformation

$$\Delta_p = \Delta_u - \Delta_y \qquad (Eq.4.6)$$

- L_p = Plastic Hinge Length (16)

$$L_p = 0.044 F_y dbl \qquad (Eq.4.7)$$

$$L_p = 0.08(L_{col}) + 0.022 F_y dbl \qquad (Eq.4.8)$$

- ϕ_p = Plastic Rotation

$$\phi_p = \frac{\Delta_p}{L_p L_{col}} \qquad (Eq.4.9)$$

$$\phi_u = \phi_p + \phi_y \qquad (Eq.4.10)$$

- ϕ_u = Ultimate Rotation

- ε_s = Strain at extreme steel tension fiber

$$\varepsilon_s = \phi_u (d - c) \qquad (Eq.4.11)$$

- ε_{cu} = Strain at extreme concrete compression fiber

$$\varepsilon_{cu} = \phi_u (c) \qquad (Eq.4.12)$$

- ε'_s = Strain at extreme steel compression fiber

$$\varepsilon'_s = \phi_u (c - d') \qquad (Eq.4.13)$$

Table 4.1 Database of Test Columns

Name	Col.	Refernce	Single/	Dia.	Aspect	Pe	f'c	Axial Load
			Double	mm	ratio	kN	Mpa	Ratio
Ang - 1985	9	1	1	400	2.5	751	29.9	0.200
Ang -1981	1	2	2	400	4.0	680	26.0	0.208
Chai	3	3	1	610	6.0	1780	32.6	0.187
Hose	TU1	6	1	610	6.0	1780	41.1	0.148
Kowalsky	FL3	8	1	457	8.0	1780	38.6	0.281
Kowalsky	FL1	8	1	457	8.0	1780	36.6	0.297
Kunnath	A6	10	1	300	4.6	806	36.0	0.317
Kunnath	A5	10	1	300	4.6	806	36.0	0.317
Lehman	415	11	1	615	4	662	31	0.072
Lehman	815	11	1	615	8	662	31	0.072
Lehman	1015	11	1	615	10	662	31	0.072
Lehman	828	11	1	615	8	923	34.5	0.090
Lehman	1028	11	1	615	10	923	34.5	0.090
Lehman	328	11	1	615	3	923	34.5	0.090
NIST	FS FLEX	19	1	1520	6.00	4450	35.8	0.069
NIST	N3	19	1	250	6.00	120	25.4	0.096
NIST	N6	19	1	250	6.00	120	23.3	0.105
Sanchez	MG1	17	1	732	3.7	1780	37.0	0.114
Wong	1	20	1	400	2.00	907	38	0.190
Wong	3	20	1	400	2.00	1813	37	0.390
Wong	2	20	1	400	2.00	1813	37	0.390
Zahn	5	21	1	400	4.0	555	32.3	0.137

Name	Col.	long Rebar				Pitch
		Dia. m	Bars	fyl	Pt%	mm
Ang - 1985	9	0.016	20D16	448	3.2	30
Ang -1981	1	0.016	16D16	308	2.56	40
Chai	3	0.0191	26#6	315	2.53	127
Hose	TU1	0.0222	22#7	455	3	57
Kowalsky	FL3	0.016	30#5	477	3.62	76
Kowalsky	FL1	0.016	30#5	477	3.62	76
Kunnath	A6	0.0095	21#3	470	2.1	19
Kunnath	A5	0.0095	21#3	470	2.1	19
Lehman	415	0.016	22#5	462	1.5	32
Lehman	815	0.016	22#5	462	1.5	32
Lehman	1015	0.016	22#5	462	1.5	32
Lehman	828	0.0191	28#6	442	2.8	25.4
Lehman	1028	0.0191	28#6	442	2.8	25.4
Lehman	328	0.0191	28#6	442	2.8	25.4
NIST	FS FLEX	0.043	25D43	475	1.99	69
NIST	N3	0.007	25D7	446	1.99	14
NIST	N6	0.007	25D7	446	1.99	14
Sanchez	MG1	0.016	36#5	463	1.6	32
Wong	1	0.016	20D16	423	3.2	60
Wong	3	0.016	20D16	475	3.2	60
Wong	2	0.016	20D16	475	3.2	65
Zahn	5	0.016	16D16	337	2.43	135

Name	Col.	Trans Rebar			EXP	Moment	Curvature
		Bars	fyt	Pt%	Ue	kN - m	1/m
Ang - 1985	9	R6@30	372	1.02	66	334	0.146875
Ang -1981	1	R6@40	308	0.77	58.3	216	0.123749
Chai	3	#2@127	351	0.174	137.2	836	0.040388
Hose	TU1	#3@57	n/a	0.9	320	1255	0.089294
Kowalsky	FL3	#3@76	445	0.93	340	645	0.105988
Kowalsky	FL1	#3@76	445	0.93	332	638	0.104654
Kunnath	A6	R4@19	408	0.98	96	133	0.163374
Kunnath	A5	R4@19	408	0.98	75	133	0.163374
Lehman	415	#2@32	607	0.7	135	673	0.15731
Lehman	815	#2@32	607	0.7	411	673	0.15731
Lehman	1015	#2@32	607	0.7	658	673	0.15731
Lehman	828	#2@25.4	607	0.9	760	1064	0.146411
Lehman	1028	#2@25.4	607	0.9	980	1064	0.146411
Lehman	328	#2@25.4	607	0.9	133.4	1064	0.146411
NIST	FS FLEX	R15@69	493	0.65	510	13955	0.051921
NIST	N3	R2.7@14	476	0.69	73.2	46	0.292806
NIST	N6	R2.7@14	476	0.69	71.5	46	0.309964
Sanchez	MG1	#2@32	204	0.52	75	1402	0.054708
Wong	1	R10@60	323	1.45	42	350	0.154018
Wong	3	R10@60	300	1.45	28	399	0.108708
Wong	2	R6@65	340	0.48	12.5	377	0.060254
Zahn	5	R10@135	466	0.61	68.3	231	0.139623

Name	Col.	Force	Φ_y anal.	Φ_y appx.	C	d	d'	L col.
		kN	m	m	m	m	m	m
Ang - 1985	9	334.0	0.015223	0.01372	0.150	0.372	0.028	1.00
Ang -1981	1	135.0	0.010732	0.00943	0.145	0.372	0.028	3.20
Chai	3	228.4	0.008740	0.00633	0.223	0.5805	0.030	3.66
Hose	TU1	342.9	0.010350	0.00914	0.202	0.5789	0.031	3.66
Kowalsky	FL3	176.4	0.013017	0.01279	0.189	0.429	0.028	3.66
Kowalsky	FL1	174.5	0.013003	0.01279	0.191	0.429	0.028	3.66
Kunnath	A6	96.4	0.017723	0.01919	0.122	0.2753	0.025	1.38
Kunnath	A5	96.4	0.017723	0.01919	0.122	0.2753	0.025	1.38
Lehman	415	273.6	0.009014	0.00920	0.153	0.587	0.028	2.46
Lehman	815	136.8	0.009014	0.00920	0.153	0.587	0.028	4.92
Lehman	1015	109.4	0.009014	0.00920	0.153	0.587	0.028	6.15
Lehman	828	216.3	0.009397	0.00880	0.178	0.5855	0.030	4.92
Lehman	1028	173.0	0.009397	0.00880	0.178	0.5855	0.030	6.15
Lehman	328	576.7	0.009397	0.00880	0.178	0.5855	0.030	1.85
NIST	FS FLEX	1530.2	0.003872	0.00383	0.385	1.4785	0.042	9.12
NIST	N3	30.7	0.022331	0.02185	0.082	0.2265	0.024	1.50
NIST	N6	30.7	0.022652	0.02185	0.084	0.2265	0.024	1.50
Sanchez	MG1	521.9	0.007342	0.00775	0.219	0.704	0.028	2.69
Wong	1	437.5	0.014674	0.01295	0.143	0.372	0.028	0.80
Wong	3	498.8	0.013291	0.01455	0.184	0.372	0.028	0.80
Wong	2	471.3	0.015747	0.01455	0.199	0.372	0.028	0.80
Zahn	5	144.4	0.011281	0.01032	0.129	0.372	0.028	1.60

Name	Col.	L_{clear}	L_{sp}	L_{eff}	Δ y anal.	Δ y appx.
		m	m	m	m	m
Ang - 1985	9	1.00	0.158	1.158	0.0068	0.0061
Ang -1981	1	1.60	0.217	3.417	0.0209	0.0184
Chai	3	3.66	0.132	3.792	0.0419	0.0303
Hose	TU1	3.66	0.222	3.882	0.0520	0.0459
Kowalsky	FL3	3.66	0.168	3.824	0.0634	0.0623
Kowalsky	FL1	3.66	0.168	3.824	0.0634	0.0623
Kunnath	A6	1.38	0.098	1.478	0.0129	0.0140
Kunnath	A5	1.38	0.098	1.478	0.0129	0.0140
Lehman	415	2.46	0.163	2.623	0.0207	0.0211
Lehman	815	4.92	0.163	5.083	0.0776	0.0792
Lehman	1015	6.15	0.163	6.313	0.1197	0.1222
Lehman	828	4.92	0.186	5.106	0.0817	0.0765
Lehman	1028	6.15	0.186	6.336	0.1257	0.1178
Lehman	328	1.85	0.186	2.031	0.0129	0.0121
NIST	FS FLEX	9.12	0.449	9.569	0.1182	0.1169
NIST	N3	1.50	0.069	1.569	0.0183	0.0179
NIST	N6	1.50	0.069	1.569	0.0186	0.0179
Sanchez	MG1	2.69	0.163	2.849	0.0199	0.0210
Wong	1	0.80	0.149	0.949	0.0044	0.0039
Wong	3	0.80	0.167	0.967	0.0041	0.0045
Wong	2	0.80	0.167	0.967	0.0049	0.0045
Zahn	5	1.60	0.119	1.719	0.0111	0.0102

Name	Col.	Δ p	L_p	Φ p	Φ_u	ε_s	ε_s'
		m	m	1/m	1/m		
Ang - 1985	9	0.059	0.315	0.188	0.2029	0.0450	0.0248
Ang -1981	1	0.037	0.236	0.049	0.0602	0.0137	0.0087
Chai	3	0.095	0.425	0.061	0.0700	0.0250	0.0156
Hose	TU1	0.268	0.515	0.142	0.1525	0.0575	0.0308
Kowalsky	FL3	0.277	0.460	0.164	0.1773	0.0426	0.0335
Kowalsky	FL1	0.269	0.460	0.160	0.1726	0.0411	0.0330
Kunnath	A6	0.083	0.209	0.289	0.3063	0.0469	0.0374
Kunnath	A5	0.062	0.209	0.216	0.2334	0.0358	0.0285
Lehman	415	0.114	0.359	0.129	0.1383	0.0600	0.0212
Lehman	815	0.333	0.556	0.122	0.1308	0.0568	0.0200
Lehman	1015	0.538	0.655	0.134	0.1427	0.0619	0.0218
Lehman	828	0.678	0.579	0.238	0.2474	0.1008	0.0440
Lehman	1028	0.854	0.678	0.205	0.2144	0.0873	0.0382
Lehman	328	0.120	0.371	0.176	0.1852	0.0755	0.0330
NIST	FS FLEX	0.392	1.179	0.036	0.0403	0.0441	0.0155
NIST	N3	0.055	0.189	0.194	0.2162	0.0312	0.0177
NIST	N6	0.053	0.189	0.187	0.2096	0.0299	0.0176
Sanchez	MG1	0.055	0.378	0.054	0.0616	0.0299	0.0135
Wong	1	0.038	0.298	0.158	0.1725	0.0395	0.0247
Wong	3	0.024	0.334	0.089	0.1025	0.0193	0.0189
Wong	2	0.008	0.334	0.028	0.0441	0.0076	0.0088
Zahn	5	0.057	0.247	0.145	0.1562	0.0380	0.0202

The database presented here is a collection of columns with varying transverse and longitudinal steel ratios and axial load ratios. In chapter 12, this database in combination with the columns tested during this project will be discussed. A method of calculating the maximum tension strain for these columns will be proposed.

5.0 Test Specimen Design

Four columns were designed identically for the test conducted in this research. The detailing of the reinforcement in these columns was typical of columns in high seismic regions. With the columns being identical, the loading was changed for each test based on what was learned from the previous test.

5.1 Column Design

When designing the column it was important to ensure that a flexural failure would occur. There should not be appreciable footing deformation or rotation. The shear load on the footing was also considered to prevent extreme cracking or failure of the footing.

The layout of the lab limits the possible column and footing heights. The footing depth was chosen to be 18 inches, which allows for a column height of 8 feet. To insure a flexural failure, an aspect ratio greater than four will accommodate this need. This is not a dividing point between shear failure and flexural failure but just a conservative measure taken to ensure shear is not an issue. The column diameter was chosen to be 18 inches. The actual aspect ratio of the column was 5 1/3, which will allow for a flexural failure.

In the database there are several trends. These trends include certain transverse steel ratios and axial load ratios. The columns built in this project were designed to accommodate these trends so that the data collected could be compared with the database. After reviewing the database, a longitudinal steel ratio of 2% was chosen, as a target steel area. This resulted in twelve #6 bars equally spaced throughout the column. The target transverse steel ratio was chosen to be 1%. A #3 bar with a three inch pitch was chosen,

giving a .92% transverse steel ratio. Figure 5.1 shows the plan view of the column. Figure 5.8, which is located at the end of this chapter, shows an elevation view of the specimen reinforcement.

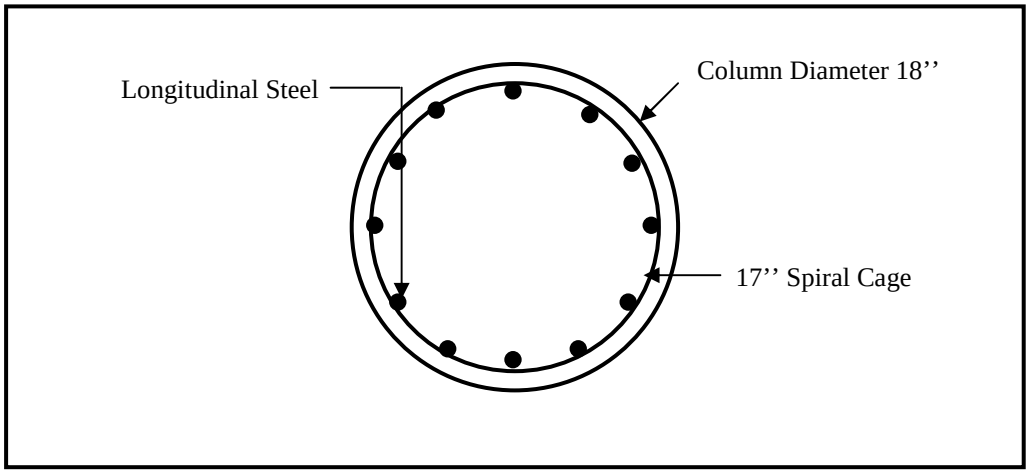

Figure 5.1 Plan View of Column Section

Figure 5.2 Column Reinforcement Spacing

The column was loaded with a 5.2% axial load ratio and considered to be concentrically loaded. With this assumption there was no initial moment due to the P-Δ effect. The column concrete 28-day strength was 4.5 ksi, the longitudinal steel yield

strength was 83 ksi, and the transverse steel yield strength was 63 ksi. Using these properties a moment curvature analysis of the column was performed. The King program (7) was used to perform the moment curvature analysis. The King program (7) uses the Mander model (12) for concrete confinement. The maximum moment of the column was 237 k-ft with an ultimate curvature of 0.05282511/ft and the neutral axis was located at 5.00 inches from the extreme compression fiber. Knowing the column capacity the footing can be designed to accommodate the column.

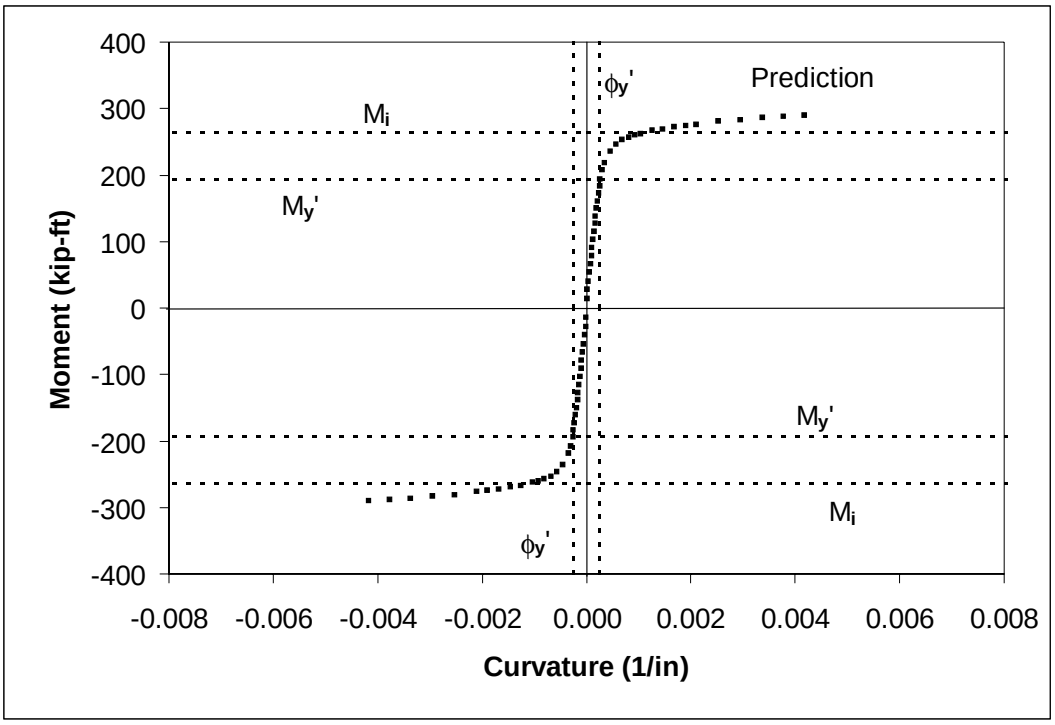

Figure 5.3 Results of Moment Curvature Analysis

5.2 Footing Design

The footing was designed to remain elastic under the column over strength moment. The axial load placed on the footing was 61.2 kips. The ultimate moment capacity of the column was 237 k-ft. The ultimate horizontal force can be found be dividing the moment by the height of the column, resulting in a force of 31.6 kips.

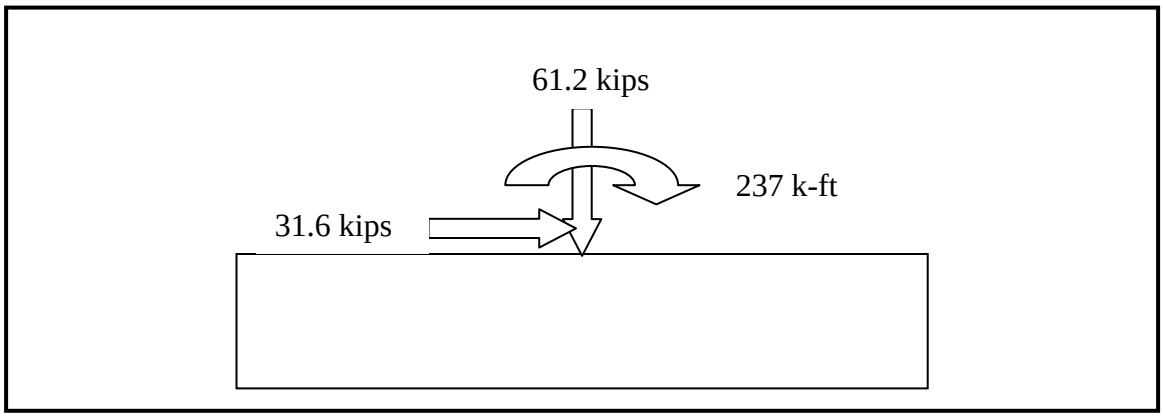

Figure 5.4 Ultimate Loads at the Base of the Column

The footing dimensions were four feet wide by eight feet long. The flexural reinforcement in the loading direction consisted of five #8 U1 bars in the bottom of the footing and seven #8 U1 bars in the top of the footing. There were also two sets of two #8 Z1 bars on each side of the column for shear strength and to limit joint rotation. The reinforcement in the direction perpendicular to loading consist of ten #4 bars at the top and ten #4 bars at the bottom of the footing. The longitudinal steel extended from the column into the footing and rest on top of the bottom flexural reinforcement of the footing. The spiral reinforcement also extended a distance of 1 foot into the footing and the pitch was decreased to 1½ inches to ensure that failure does not occur in the footing.

Figure 5.5 Footing Steel Picture 1

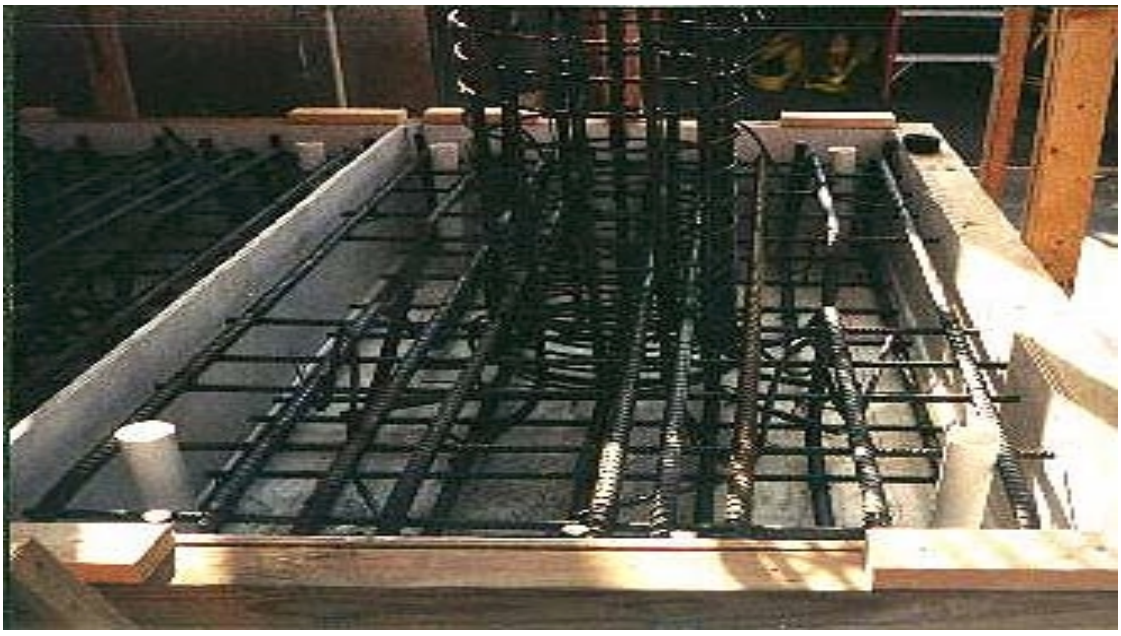

Figure 5.6 Footing Steel Picture 2

Section analysis of the footing found that the ultimate moment was approximately 2.5 times that of ultimate moment capacity of the column. Reinforcement strains in the footing were below yield at the ultimate moment capacity of the column. With steel

strains less than yield there is little rotation or deformation coming from the footing. The footing is adequately designed to ensure failure in plastic hinge region of the column.

5.3 Cap Design

The cap was where the actuator was mounted to apply the load to the column. The cap dimensions were two feet six inches square by two feet deep. The actuator was mounted to the center of the cap. There was a small moment and shear demand on the cap due to the loading from the actuator. There was also a crossbeam placed across the cap to apply the axial load on the column.

The stresses on the cap were low. The reinforcement cage was designed to control cracking and helps distribute the actuator loads into the column. The cage reinforcement consisted of six #4 U2 bars in the horizontal direction and ten #4 U2 bars in the vertical direction. Six of the twelve longitudinal bars from the column extended into the cap a distance of one foot nine inches. The spiral reinforcement was extended 1 ½ inches into the column with an extra 1 ½ turns.

5.4 Material Strength

Concrete cylinders were made when the footing and columns were cast. There was one set of three cylinders for the footing and one set of cylinders for each column to be tested on the day of testing plus a set for the 28-day strength. The following table shows the test results as the average of three cylinders.

Table 5.1 Concrete Strength Test Results

Speciemen	Footing	Column	Column 1	Column 2	Column 3	Column 4
	28 day	28 day	43 day	56 day	71 day	102 day
Strength in psi	5617	4532	4746	4964	4603	4913

The reinforcing steel was also tested to find its actual yield stress, ultimate stress and maximum elongation before rupture. The fabricator supplied this information for the footing and spiral but not for the longitudinal steel. Tests were conducted in the laboratory to find the yield stress and ultimate stress of the longitudinal steel. Table 5.2 lists the properties of the steel used in this project. Figure 5.7 illustrates the stress versus strain relationship for the longitudinal steel used in this project. Also plotted is the assumed stress versus strain relationship that is given by the Mander model (12) and used by the King program(7) to perform moment curvature analysis. The Mander model (12) defines ultimate steel stress of reinforcing steel as 1.5 times the yield stress, but this has been modified to 1.25 times the yield stress to model the actual ultimate steel stress of the reinforcing steel used in this project.

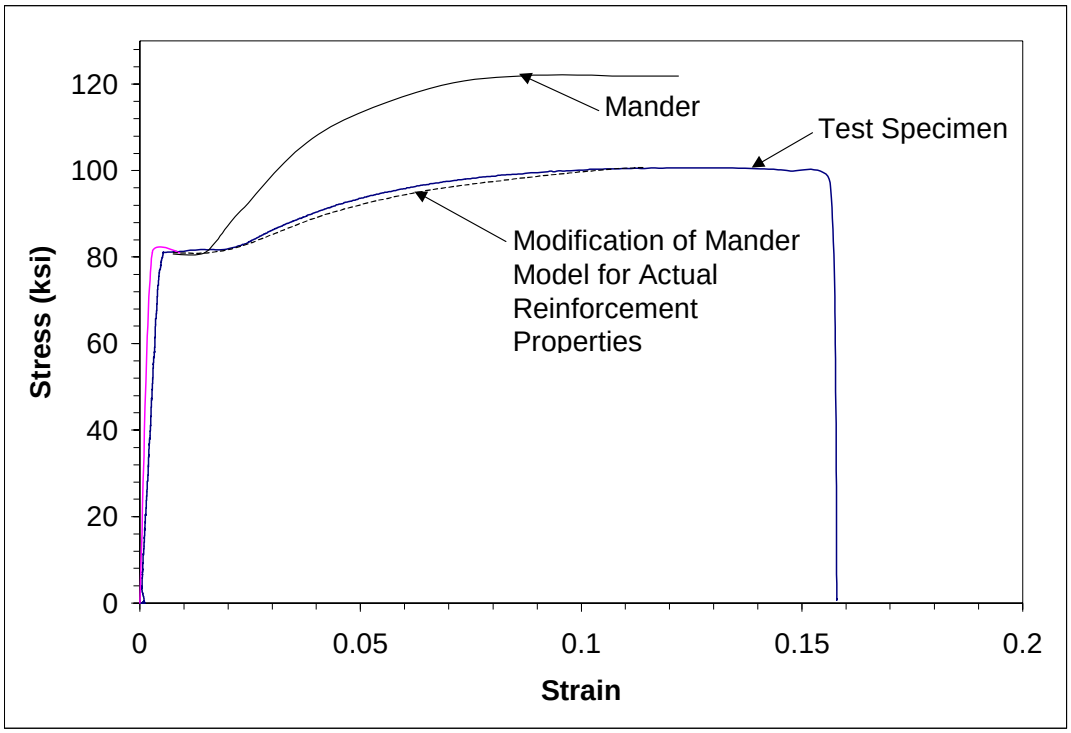

Figure 5.7 Tension Test of a Longitudinal Bar

Table 5.2 Actual Steel Strengths

	Yield Strength	Ultimate Strength	% elonagtion
	ksi	ksi	
Footing Steel	82	101	15
Transverse Steel	63	98	11.2
Longitudinal Steel	82	101	15

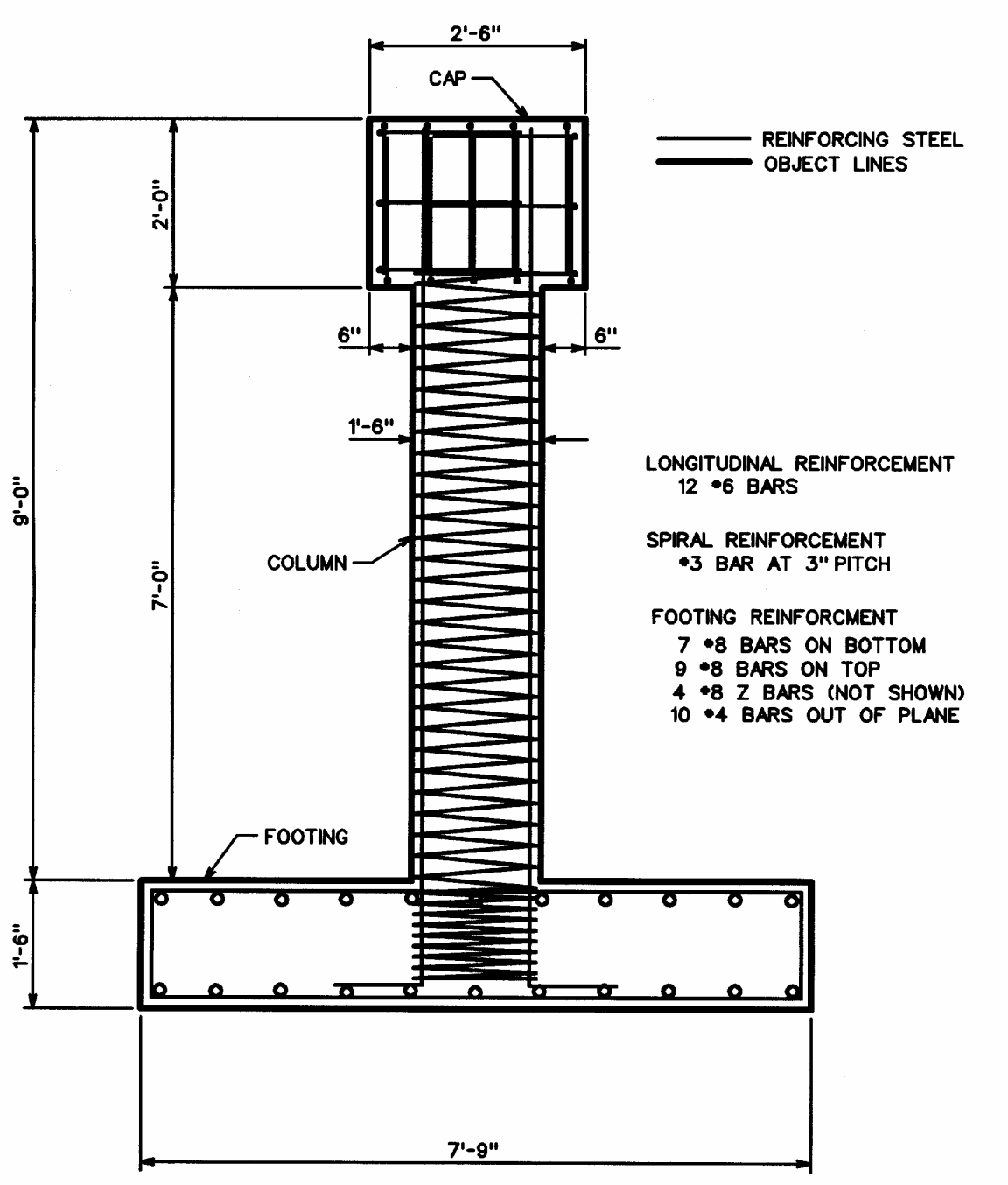

Figure 5.8 Elevation View of Test Specimens

6.0 Instrumentation

The test specimens had two types of gages: internal and external gages. The internal gages for these tests were strain gages applied directly to the reinforcing steel. The external gages consisted of linear potentiometers that measure displacement over a given distance and can be used to calculate other parameters. These gages will be discussed in four parts; strain gages, linear pots, string pots, and load cells. The gage application, location and calibration was the same for all four test specimen.

The gages were labeled according to their location on the specimen. The two primary directions were North and South. The first letter in the gage name tells what the gage was fastened to: L for longitudinal steel, T for transverse steel, and X for external gage. The next letter tells the direction, N for North and S for South. The next letter and number represents the distance of the gage from the top of the footing with P positive (up the column) and N for Negative (into the footing) with the distance in inches. An example of this is gage LNN04. This was located on the longitudinal steel (L) north side (N) four inches below (N04) the top of the footing. The external gages and transverse steel gages do not use the P and N sign convention because all of the gages were located in the positive direction. An example of this is gage XN16. This gage was located externally on the north side located at 16 inches up the column. The rest of the gages were labeled as follows: The string pot was labeled ST1 and the load cells were labeled LC1 and LC2.

6.1 Strain Gages

A TML strain gage, made by Tokyo Sokki Kenkyujo Co., Ltd., was used for these tests. All the strain gages had the same gage factor of 2.13 ±1%, and resistance of 122Ω. The gages came with wire leads already soldered on them.

The gages were applied to the reinforcing steel in the process described in the following steps.

1) A disk grinder was used to grind a flat spot on the reinforcing bar
2) 180 grit followed by 400 grit sand paper was used to polish the reinforcing bar surface
3) The surface was cleaned with Methyl Ethyl Keytone (MEK) to remove dirt and grease
4) The gage was checked to see if it worked by reading the resistance across its leads. This should read 122Ω
5) The gages were then glued to the reinforcement using Cyanoacrylate glue made by Tokyo Sokki Kenkyujo Co., Ltd.
6) A zip tie was placed on the lead to hold it in place.
7) The gage was checked to see if it worked by reading the resistance across its leads 122Ω.
8) M-Coat D, manufactured by Micro Measurements Group LTD, Raleigh, NC, was placed over the gage to protect it.
9) Finally the gage was covered with Scotch Seal 2229 compound made by 3M for a final layer of protection.
10) The gage was then labeled identifying its location on the bar.

Strain gages were placed on two longitudinal bars in each specimen. The longitudinal bars were the extreme north and south bar because these bars will experience the highest tension and compression strains. Figure 6.1 and Figure 6.2 show the location of the longitudinal steel strain gages.

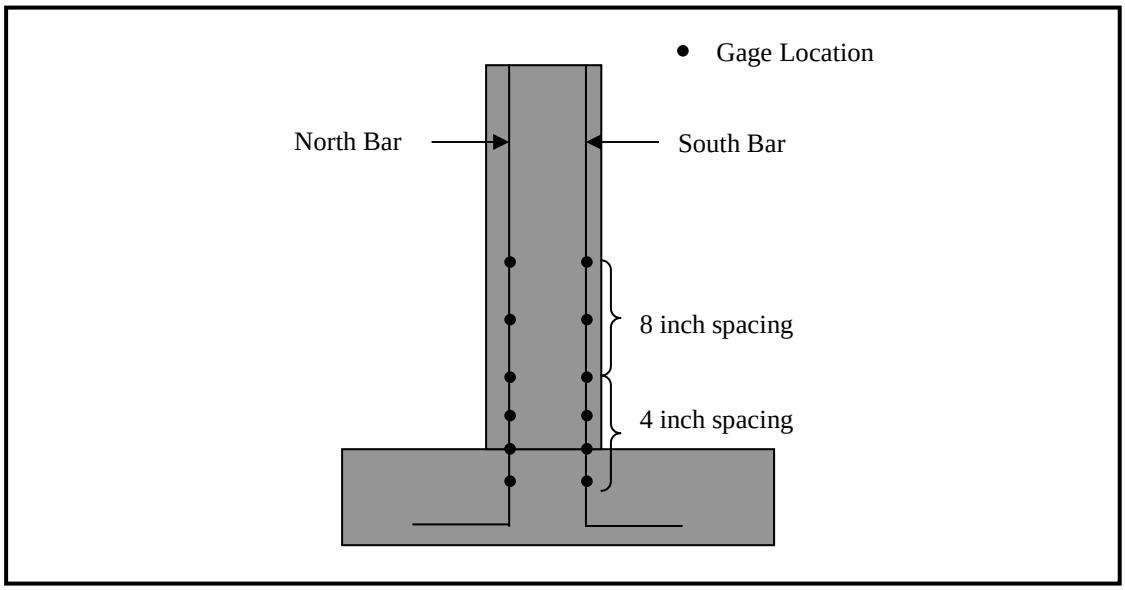

Figure 6.1 Location of Longitudinal Strain Gages

Figure 6.2 Picture of Longitudinal Strain Gages

Strain gages were placed on the outside of the bar on every other pitch of the transverse steel spiral cage. The transverse steel stain gages were located at 6, 12, 18, and 24 inches up the column on the north and south sides of the column. Figure 6.3 and Figure 6.4 show the location of the transverse steel strain gages.

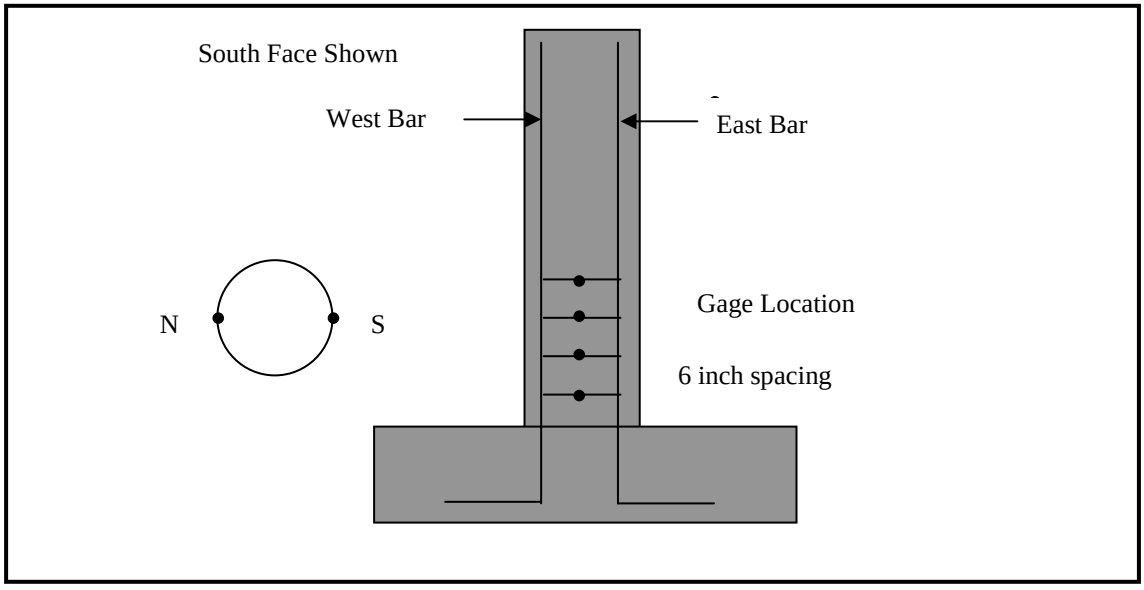

Figure 6.3 Location of Transverse Steel Strain Gages

Figure 6.4 Picture of Transverse Steel Strain Gages

6.2 Linear Potentiometers

A linear potentiometer is a device that measures displacement over a given gage length. There were four of these gages on the north and south side of the column. These gages measured displacement over an eight-inch gage length. Thread rods where placed in the column during construction for mounting these gages.

When constructing the columns two ¼ inch threaded rods at four different heights were placed through the sonotube with 6 inches protruding out on each side. The rods were spaced eight inches apart measuring from the top of the footing up to the first set of rods and then eight inches to the next set and so on. The rods were spaced six inches east and west of the north and south faces of the columns.

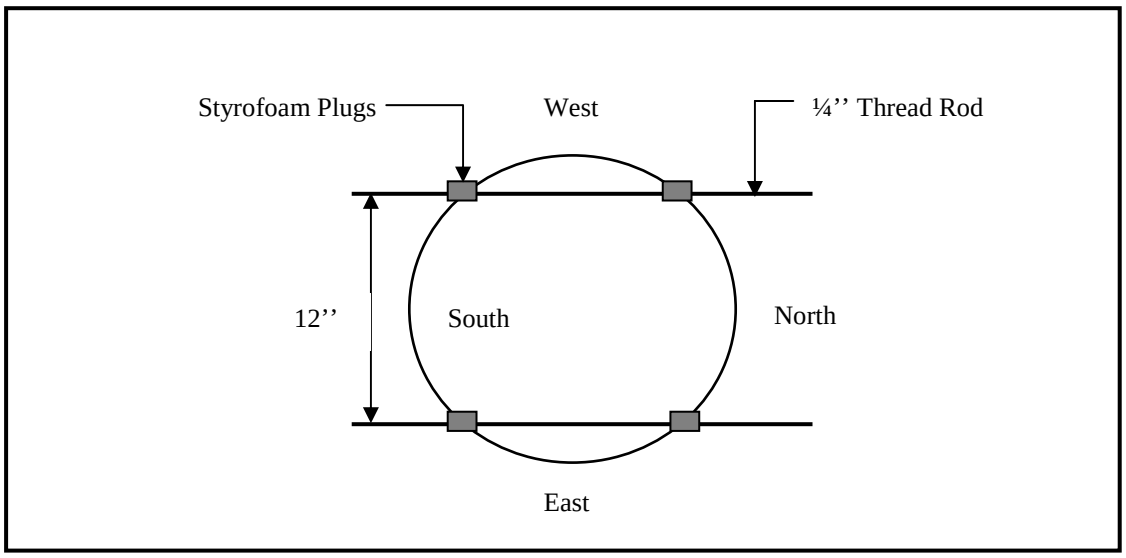

Figure 6.5 Plan View of Threaded Rods

Angle brackets were mounted to the rods with a linear potentiometer extending down to the angle bracket below it. Except for the first linear potentiometer a piece of aluminum foil tape had been placed on the top of the footing for the gage to rest on. The linear potentiometer measures displacement as its stem moves in or out depending on whether it was being compressed or tensioned.

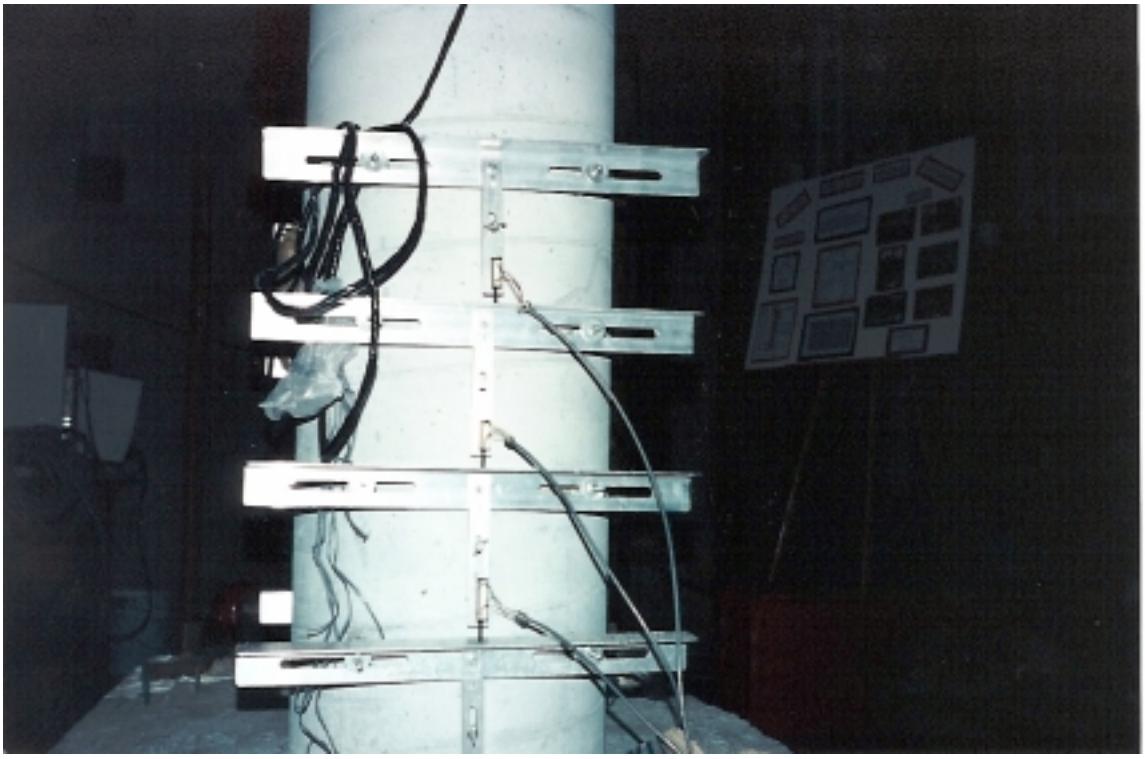

Figure 6.6 Picture of Linear Potentiometers Mounted on the South Face

The displacement of the linear potentiometer was recorded throughout the whole test. The average angle of rotation over each gage length θ_i was calculated using the following expression. Figure 6.7 illustrates how the rotation and curvature was found.

$$\theta_i = \frac{|XS_i| + |XN_i|}{D_i} \qquad (Eq.6.1)$$

θ_i = Average angle of rotation for i^{th} gage length

XS_i = South linear pot change in displacement

XNi = North linear pot change in displacement

Di = The horizontal distance between XNi and XSi

i = The gage length of consideration

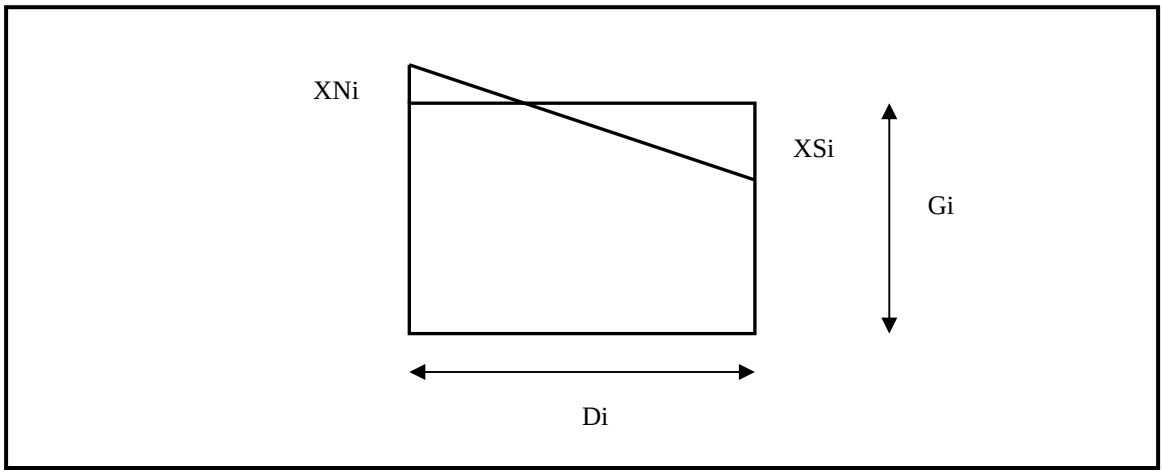

Figure 6.7 Calculation of Rotation and Curvature

The average curvature was calculated using the following expression. This curvature represents the average curvature over the gage length.

$$\phi_i = \frac{\theta_i}{G_i} \qquad (Eq.6.2)$$

ϕ_i = Average curvature over i^{th} gage length

G_i = Gage length i

The ultimate deflection of the column can be calculated from the average angle of rotation of each gage length. Calculating the deflection contributed by each gage length and summing up all of the individual deflections gives the total deflection. The following equations were used to calculate the total deflection.

$$\delta_i = \theta_i h_i \qquad (Eq.6.3)$$

$$\delta_T = \sum \delta_i \qquad (Eq.6.4)$$

h_i = The distance from the center of the gage length to the top of the column (see figure 6.8)

δ_T = Total Deflection

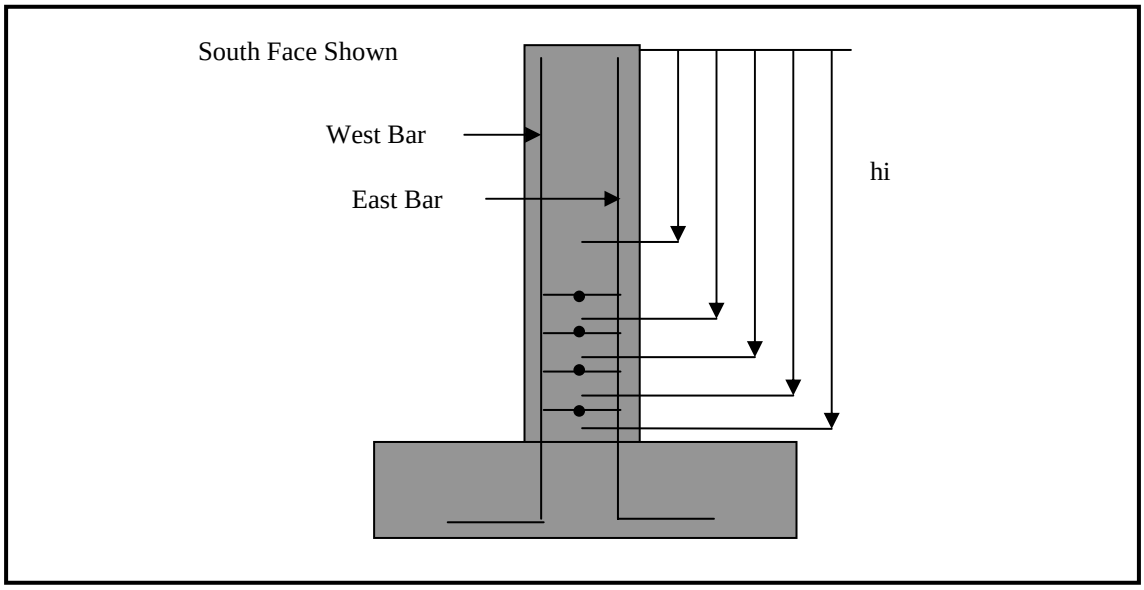

Figure 6.8 Heights used for Evaluation of Total Deflection

6.3 String Potentiometer

A string potentiometer with a 25-inch stroke was used to measure the horizontal deflection of the column. The string potentiometer was mounted to a rigid frame placed in front of the specimen. A leader line was used to connect the string potentiometer to the center of the cap. The string potentiometer was in line with the point in which the actuator was applying the load. The string potentiometer measured the displacement of the specimen independent of the actuator measurement of displacement.

6.4 Load Cells

Fifty kip load cells was used to measure the applied axial load. The load cells were placed in the basement between the 20-ton jack and the jack chair mounted to the basement ceiling.

7.0 Test Setup

After the columns had time to cure, they were setup for testing. The test setup was broken down into four steps. The steps were leveling and anchoring footing to the floor, axial load setup, mounting of actuator, and setting up the data acquisition system. The test setup was identical for all four columns.

The specimens were designed so that they could be fastened to floor. Cutouts were created in the specimens to accommodate the pattern of holes in the floor and actuator. There was a two-inch diameter hole in each corner of the footing for anchoring the footing to the floor and two slots on each side of the column to create room for applying the axial load through the floor. The cap stub had four holes designed to receive the actuator. Figure 7.1 shows how the cutouts were created in the footing of the specimens.

Figure 7.1 Footing Cutouts

7.1 Leveling and Anchoring Footing

A specimen covered six holes in the floor, each hole was three inches in diameter. For leveling the footing, fiber sheathing ½ inch thick was cut into one-foot squares with a three-inch hole drilled in the middle. A bead of silicone was place around the hole in the floor and the fiber sheathing was placed on top lining up the hole in the sheathing with the hole in the floor. The specimen was then placed on top of the sheathing with the holes in the specimen lining up with the holes in the floor and the fiber sheathing. After shimming if needed to level the specimen, there was about ½ inch gap between the specimen and the floor. A five-foot by nine-foot by two-inch tall form was placed around the base of the footing. A bead of silicone was placed in the corner between the formwork and the floor. After the silicone had dried, hydrocal was then mixed at a 1 to 1 volume ratio and poured into the form. The hydrocal filled up the void space between the footing and the floor ensuring that the entire footing was smoothly resting on the entire floor area beneath it. After the hydrocal had set up, the footing was secured to the floor. 1 3/8-inch dywidag bars were placed at each corner through the footing and the floor. Due to the rough surface on the top of the footing, the dywidag plates were placed and level on the footing and hydrocal was poured under the plate to create a uniform bond between the footing and the plate. With the rod extending a foot below the lab floor a plate and nut were placed on each rod. The rods were tensioned to 80 kips from the top of the footing using a 60-ton ram, securing the footing to the floor.

Figure 7.2 Securing Footing to Lab Floor

7.2 Axial Load Setup

By tensioning two rods on each side of the column and using a beam to distribute the loads across the cap stub, an axial load was supplied to the column. The load on the column was in the center of the column so that there is no initial P-Δ moment. To ensure that the beam was in the center of the column, the column was located and drawn on the top of the cap. The beam was placed on the cap, centering it with the column. With the beam in place, formwork was built and hydrocal was poured to fill in the low spots on the cap ensuring a constant bond between the beam and the cap. A 5/8″ diameter dywidag bar was extended threw the floor and secured to the beam. With three feet of rod extending into the basement a jack chair was placed on the rod and secured to the ceiling of the basement. A load cell was placed on each rod and then a 20-ton jack followed by a

3″ x 3″ x 1/2″ plate and then all of this was secured by a standard 5/8″-dywidag nut. The jacks were connected to a manifold, which was connected to a hand pump.

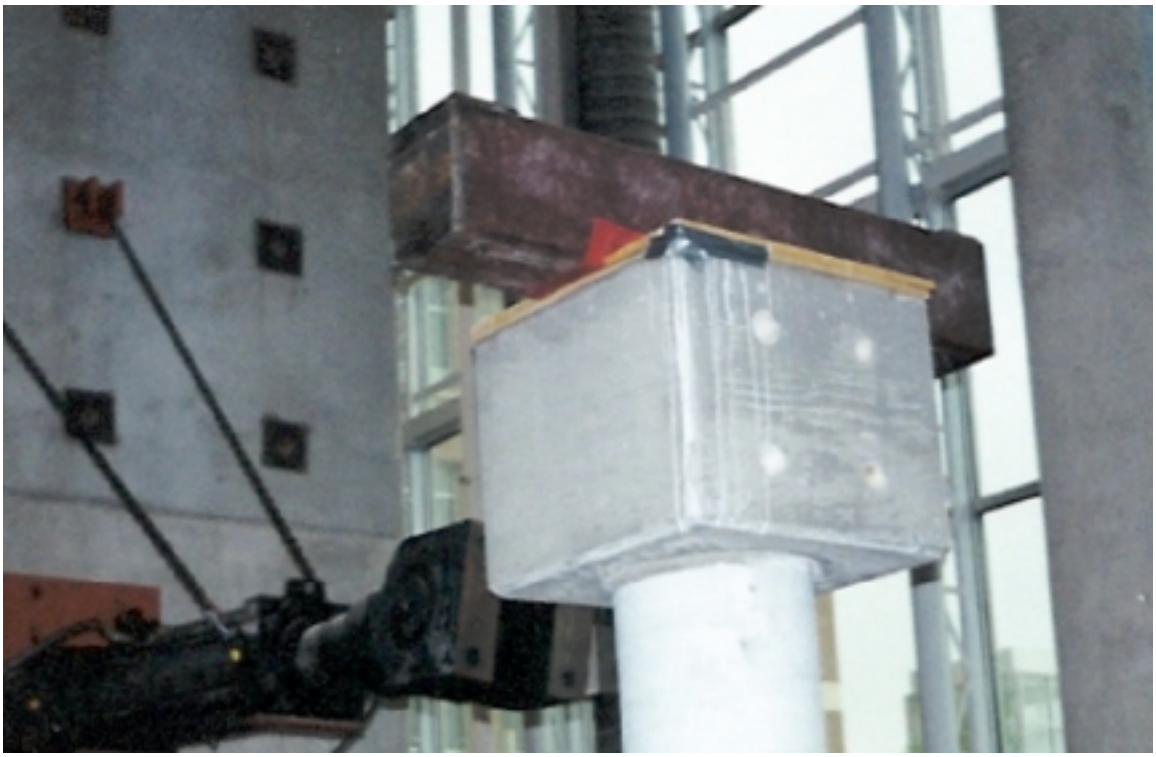

Figure 7.3 Cross Beam and Form Work on Top of Cap

7.3 Mounting the Actuator

A MTS 243.60T actuator with a 40-inch stroke and 220 kip load capacity was used to test the specimens. The holes in the cap were spaced so that they match the holes in the knuckle of the actuator with the resulting force in the center of the column. Four 1 ½ inch threaded rods were used to fasten the actuator to the north side of the specimen. Plates were used on south side of the specimen to distribute the force in the rods over the surface of the plate and into the cap. The rods were then tightened until the knuckle was flush with the face of the cap ensuring that the column was evenly loaded.

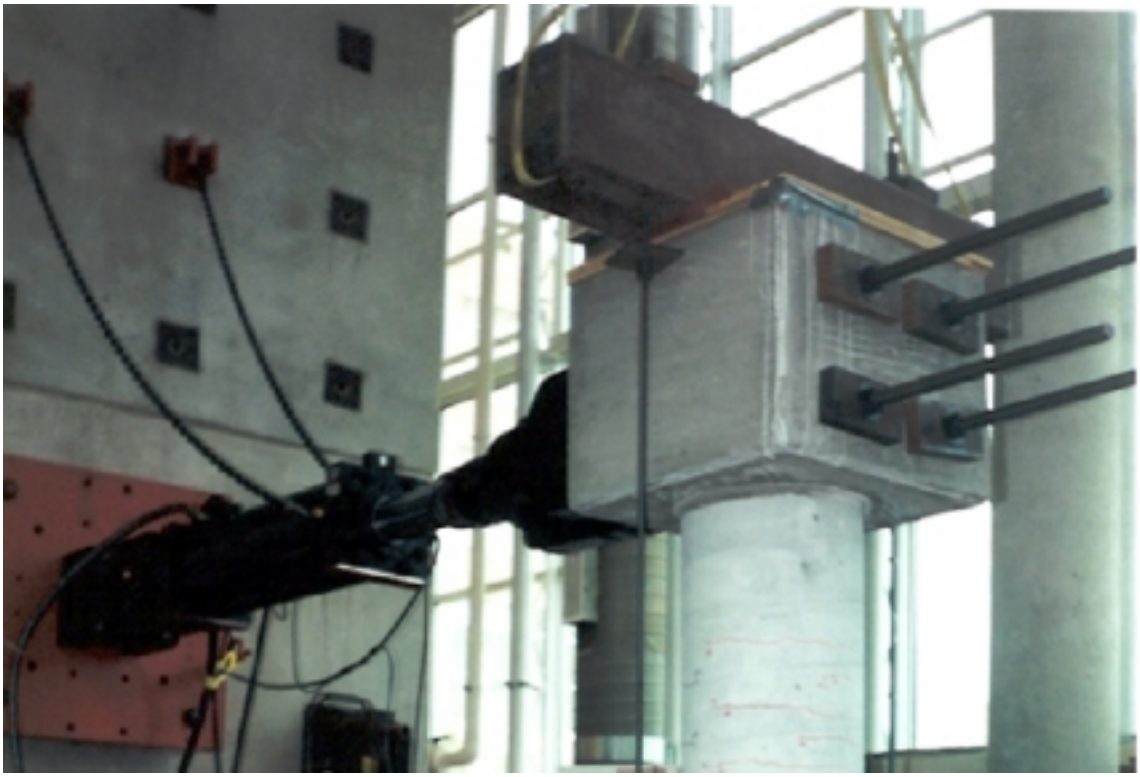

Figure 7.4 Mounting Actuator to Cap of Specimen

7.4 Data Acquisition

An Optim Megadac 3108AC Data Acquisition with a DOS based TCS program was used to collect the data for each specimen. All data was collected with respect to time: a reading was taken every two seconds. The strain gages were wired using a three wire half bridge. An 808QB card was used to read the transverse steel gages on the north side by applying an excitation amperage of 10 miliamps. The rest of the strain gages were read using 808FB card with an excitation voltage of 5 volts. The linear pots, string pots, and load cells were wired using a full bridge. These gages were wired into an 808FB card using an excitation voltage of 10 volts. The Actuator was wired into 682SH card with an excitation voltage of 10 volts. An X-Y recorder was connected to the load and displacement readings of the actuator.

8.0 Test Specimen 1

This is the first of the four test specimens tested in this project. This specimen was the our control specimen. Information learned in this test was used to determine the loading history for the next test.

This chapter will discuss all the aspects involved in testing the first specimen. This chapter will be broken into five parts; loading of specimen, estimation of maximum tension strain, observations made during the test, test results, and determination of how to load the next specimen.

The information gathered during the test will only be presented. Some preliminary observations and conclusions will be made but the main analysis of the data will be covered in chapter 12. Appendix A-2 contains graphs of column curvature and individual linear pot histories.

8.1 Loading of Specimen

From moment curvature analysis the first yield force and displacement have been calculated. The test specimen was loaded in force control up to yield as shown in figure 8.1. Once this point was reached the yield displacement was validated, by reading the string potentiometer, and then the equivalent yield displacement was calculated. From this point, the specimen was load in increments of displacement ductility as shown in figure 8.2.

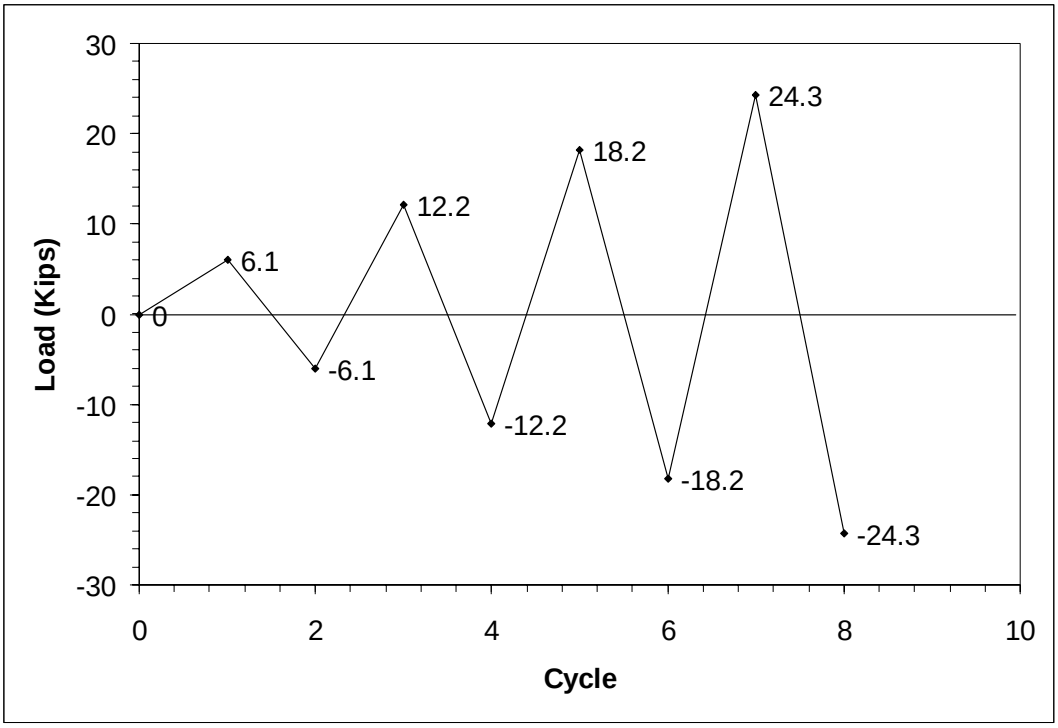

Figure 8.1 Force Control Loading of Specimen 1

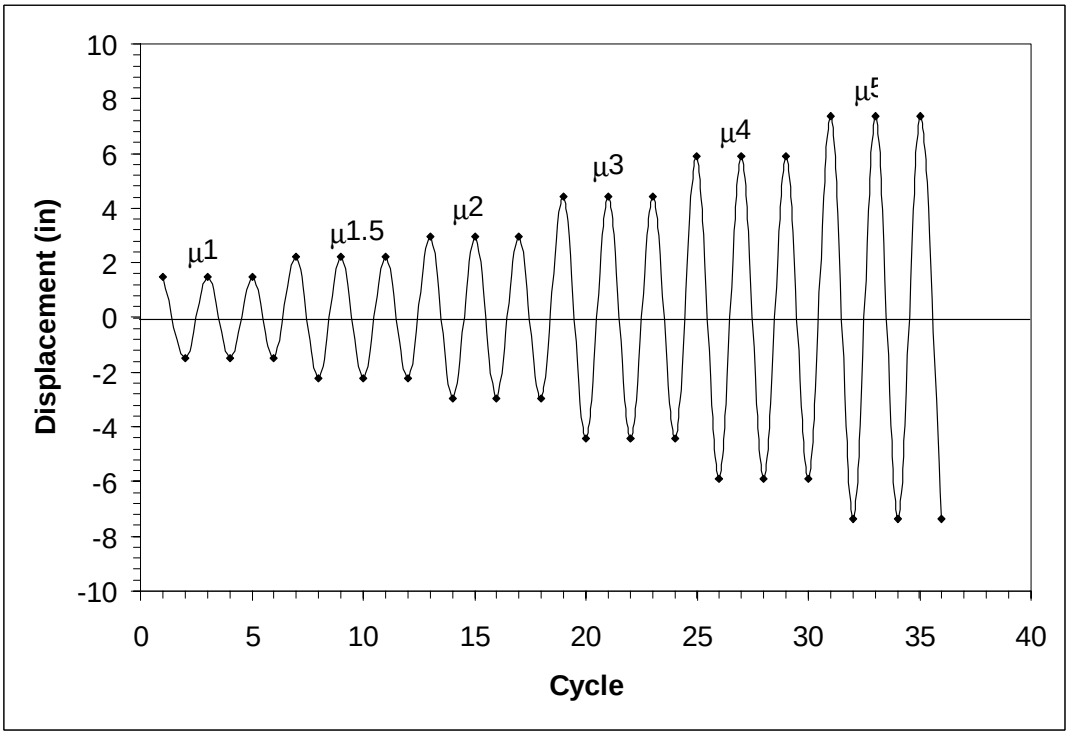

Figure 8.2 Displacement Control Loading of Specimen 1

8.2 Estimation of Maximum Tension Strain

There are no models to predict buckling based on tension strain capacity of longitudinal reinforcement. It should be noted that no buckling model was used to determine this range of maximum deflection for this specimen. The estimated deflection was based solely on the observation of previous test that had experienced a buckling failure. In these previous tests the ultimate deflection of the column was determined using the energy balance approach suggested by Mander (12). This approach focuses on evaluating failure by the maximum concrete strain.

In chapter four the maximum tension strain of the test specimens was determined. Also from chapter four it is noted that there were 5 previous tests that had about the same transverse steel ratio and axial load ratio. Table 8.1 gives a brief description of these columns for more detail about each specimen refer to Table 4.1.

Table 8.1 Test used to Estimate the Maximum Tension Strain

Reference	Column	Axial load Ratio	Transverse Steel Ratio	Steel Tension Strain
Hose	TU1	0.18	0.9	0.0575
Lehman	328	0.09	0.9	0.0755
Lehman	828	0.09	0.9	0.0793
Lehman	1028	0.09	0.9	0.0784
Smith	1	0.184	0.89	0.0601

From this information the maximum tension strain of the column was estimated. Once the maximum tension strain was estimated, the maximum deflection of the column was determined. The following equations were used in calculating the maximum deflection.

$$\phi_u = \frac{\varepsilon_s}{d - c} \qquad (Eq.8.1)$$

$$\phi_p = \phi_u - \phi_y \qquad (Eq.8.2)$$

$$\Delta_u = \Delta_p + \Delta_y \qquad (Eq.8.3)$$

$$\Delta_p = \phi_p \left(L_{eff}\right) L_p \qquad (Eq.8.7)$$

$$L_{eff} = L + 0.15\left(f_y\right) d_{bl} \qquad (Eq.8.4)$$

$$L_p = 0.08L + 0.15\left(f_y\right) d_{bl} \qquad (Eq.8.5)$$

$$\Delta_y = \frac{\left(\phi_y\right) L_{eff}^{\ 2}}{3} \qquad (Eq.8.6)$$

For this test specimen, the estimated maximum tension strain from the information given in Table 8.1 was in the range of 5.75% to 7.93%. This resulted in a maximum deflection of 6.4 inches to 8.7 inches and a maximum displacement ductility capacity of 5 to 6.

8.3 Observations

The following is a step by step account of the column response during the test. Each cycle will consist of the negative and positive direction of force or displacement loading. Each step will focus on cracks size and location on the column. Also things such as crushing of concrete or exposure of reinforcing steel will be discussed. The visual account will allow for a correlation between visual inspection and test results.

8.3.1 Force loading

The first cycle in force control was to 6 kips (25% of theoretical yield). No cracks were observed in the column.

The next cycle of force loading was to 12.2 kips (50% of theoretical yield). Cracks have formed 54'' up the column spaced at 4'' to 5'' intervals. The cracks extend from the east side to the west side of the column. The x-y recorder also showed a change in column stiffness at about 7 kips on the x-y recorder.

The next cycle of force loading was to 18.2 kips (75% of theoretical yield). The cracks that formed during the last cycle were extended during this cycle. Some new cracks also formed. The largest flexural crack width measured 0.002''.

The final force loading cycle was too theoretical yield at 24 kips. The LNP04 strain gage read 0.0028-tension strain, which is yield for the longitudinal bars indicating an agreement between analysis and experimental. The LNSP04 strain gage read 0.0017 compression strain, which is less than the yield strain. There were further crack extensions with the largest flexural crack width measuring to 0.007'' to 0.009''.

8.3.2 Displacement Loading

From the loading cycle at first yield the average deflection of the push and pull deflection was 0.975'', with the theoretical prediction being very accurate at 0.9706''. With this information, the equivalent yield point and the displacement was found for each level of ductility. The following equation was used to determine the equivalent yield point.

$$\Delta_y = \Delta_y' \left(\frac{F_i}{F_y'} \right) = .975'' \left(\frac{36.7k}{24.3k} \right) = 1.47'' \qquad (Eq.8.8)$$

The first cycle in displacement control was ductility 1, which is equivalent to a displacement of 1.47 inches. Four-inch long Shear cracks began to form in the column.

Some new flexural cracks formed in the column but mostly growth of old cracks. The tension strain in the column measured 0.0040. Cracks also started to form in the footing.

The next displacement level on the column was to a ductility of 1.5, which is equivalent to a deflection of 2.2 inches. A large flexural crack measuring 0.05'' in width formed at six inches up the column on the north side. On the south side of the column where a crack was closing, some minor crushing occurred. The strain gage on the longitudinal bar at the location of crushing read a strain of 0.0035.

The next displacement level on the column was to a ductility of 2, which is equivalent to a deflection of 2.9 inches. More shear cracks formed on the east and west faces of the column. The largest flexural crack width on the north side increased to 0.06'' at six inches above the footing. On the south side of the column minor spalling of the cover concrete occurred.

The next displacement level on the column was to a ductility of 3, which is equivalent to a deflection of 4.4 inches. More shear cracks formed on the east and west faces of the column. The transverse steel began to be exposed on the north and south sides. The spalling of concrete continued in the plastic hinge region. Due to the growth in length of the column, the axial load was reduced by 10 kips to bring it down closer to the original axial load of 51 kips. The extreme south longitudinal bar was exposed at 4 inches up the column.

The next displacement level on the column was to a ductility of 4, which is equivalent to a deflection of 5.9 inches. The extent of spalling increased to eight inches on the south side and nine inches on the north side. Longitudinal bars were exposed on the north and south sides of the column. During the second cycle in the pull direction,

the north side longitudinal bar began to buckle between the second and third spiral. When loading back in the other direction for the third cycle at this ductility, the south bar began to buckle between the second and third spiral. With the last pull of this cycle, the transverse steel on the north side had visible deformation. The column reinforcement buckled and the column was considered to be at failure. The column was then loaded to the next ductility to see if there is substantial degradation in strength.

The final displacement load on the column was to a ductility of 5, which is equivalent to a deflection of 7.35 inches. Further spalling occurred in the plastic hinge region with the north side measuring 10'' and the south side measuring 12''. During the first cycle of pull, the south bar ruptured causing a substantial lost in strength ultimately ending the test.

Figure 8.3 South Side of Specimen at Yield

Figure 8.4 North Side of Specimen at Ductility 1 Cycle 3

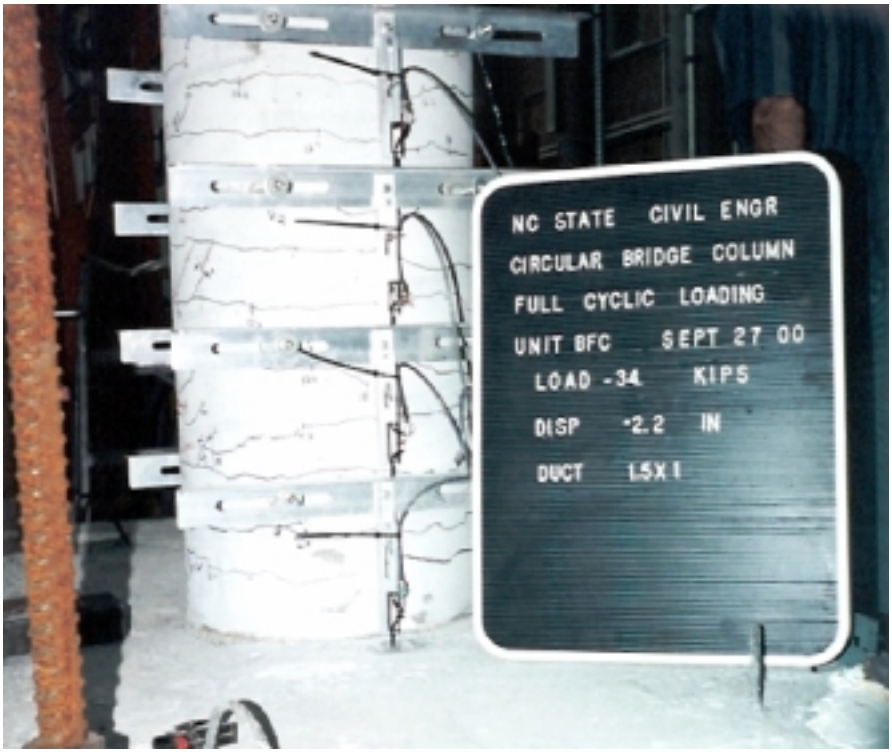

Figure 8.5 North Side of Specimen at Ductility 1.5 Cycle 1

Figure 8.6 North Side of Specimen at Ductility 2 Cycle 3

Figure 8.7 North Side of Specimen at Ductility 3 Cycle 3

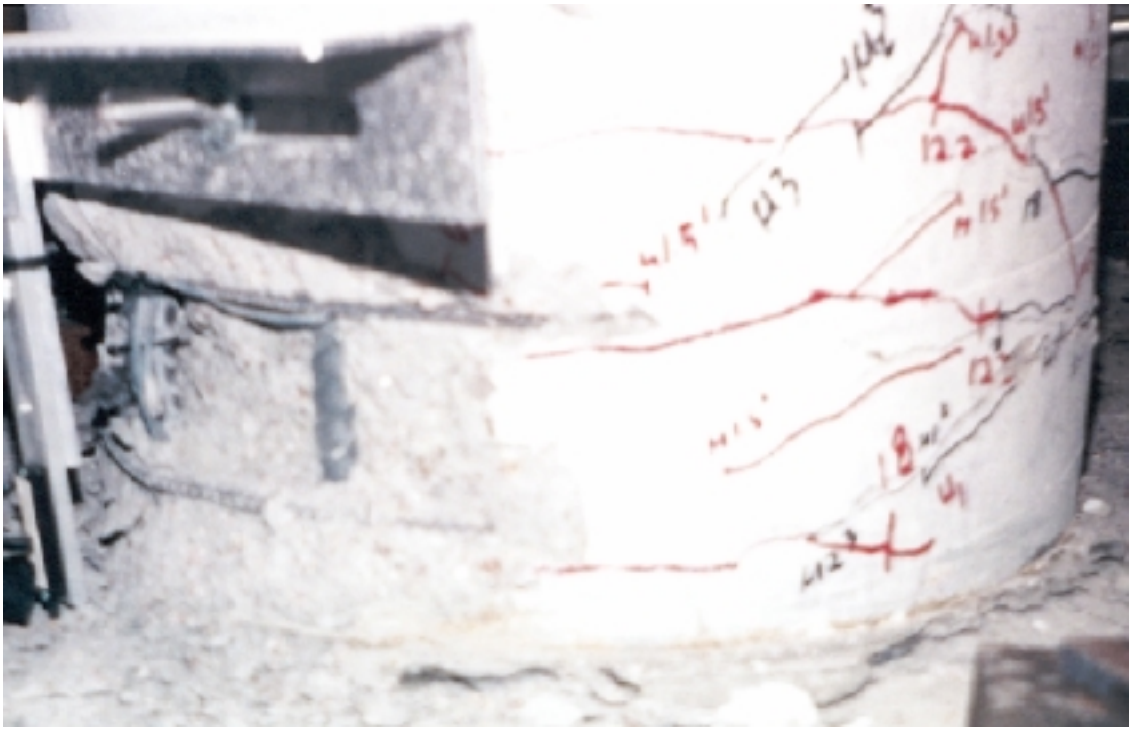

Figure 8.8 South Side of Specimen at Ductility 4

Figure 8.9 Buckling of Reinforcement South Side of Specimen at Ductility 4

Figure 8.10 South Side of Specimen after Test

8.4 Test Results

With the data obtained from the gages on or in the specimen, values can be associated with the observed response of the section. Figure 8.11 shows the force versus displacement response of the specimen. Also plotted on the same graph is the first yield force, ultimate force, and first yield displacement along with the response from moment curvature analysis. The response curve takes into account the P-Δ moment due to the axial load. Buckling began to occur in the bar at the location marked by X placed on the force versus displacement response curve.

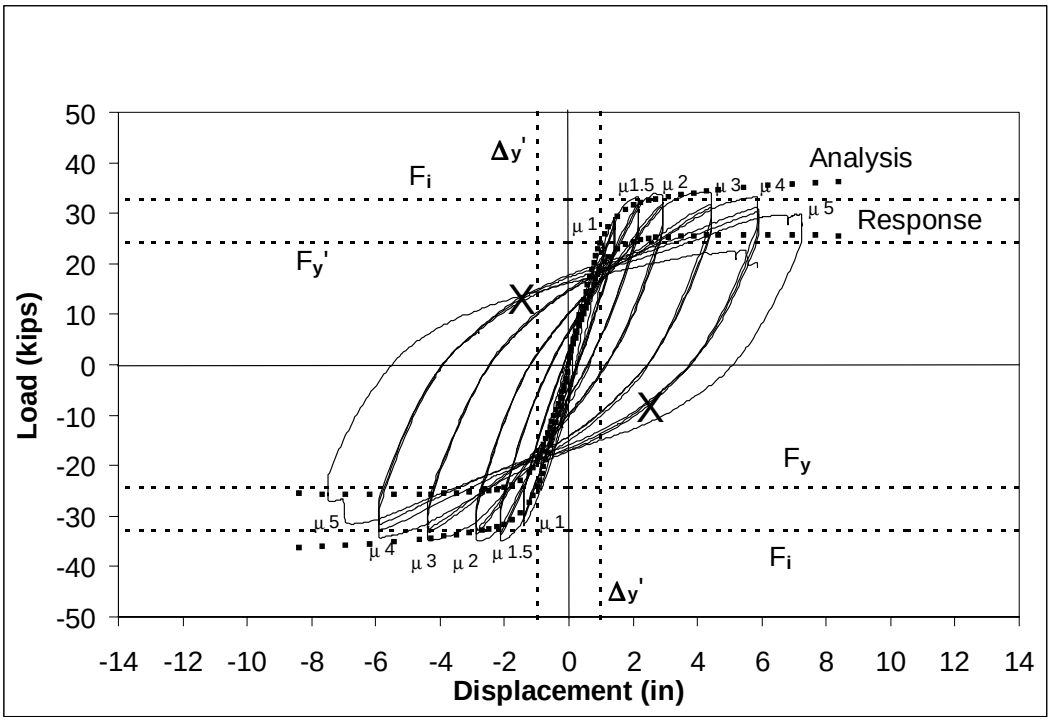

Figure 8.11 Force versus Displacement Response for Specimen 1

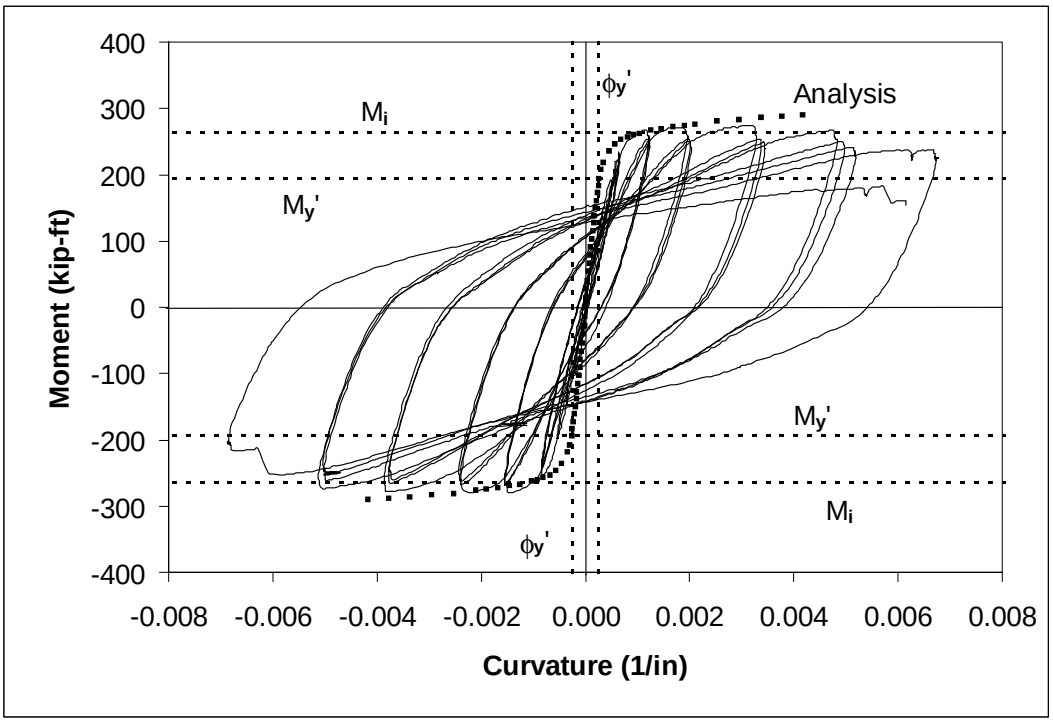

Figure 8.12 Moment versus Curvature for Specimen 1

The moment curvature graph was generated by multiplying the applied force by the column height and plotting the results against the curvature calculated from the

bottom gage length of the column, which has the largest curvature. The other three gage lengths also were used to measure the curvature of the column. Figure 8.13 shows the curvature profile of the column with the curvature being assumed linear after a column height of 28 inches. Using the equations in chapter 6, the ultimate deflection of the column can also be calculated from the curvature.

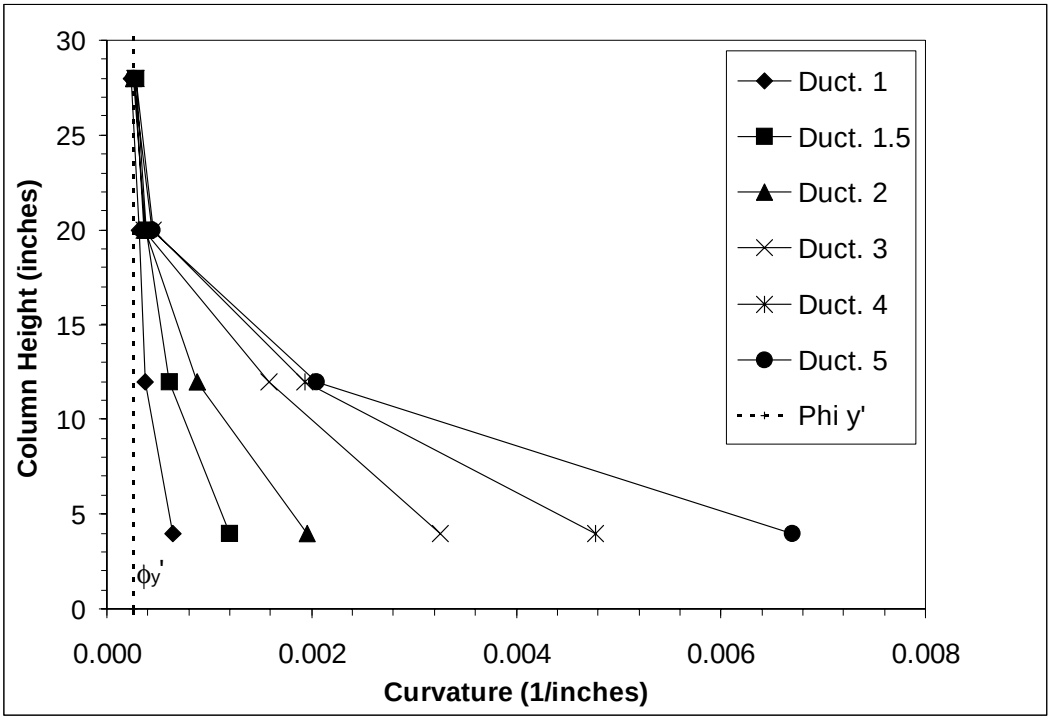

Figure 8.13 Curvature Profile of the Column at Different Levels of Ductility

The strain gages on the north and south sides of the column provide a profile of the strain in the longitudinal steel. The strain profile starts at four inches below the footing and extended 24 inches above the footing. At high levels of ductility some strain gages exceeded their capacity, this data is included in the figures shown below. A discussion will be given on the validity of these gage readings.

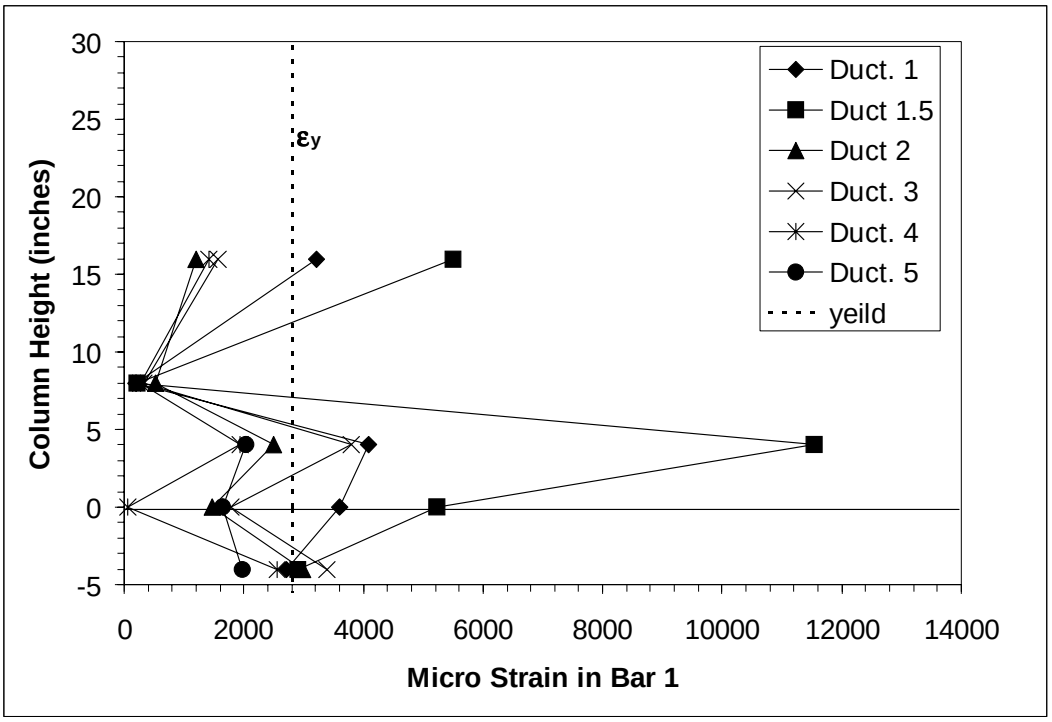

Figure 8.14 Strain Profile of the Longitudinal Steel on the North Side

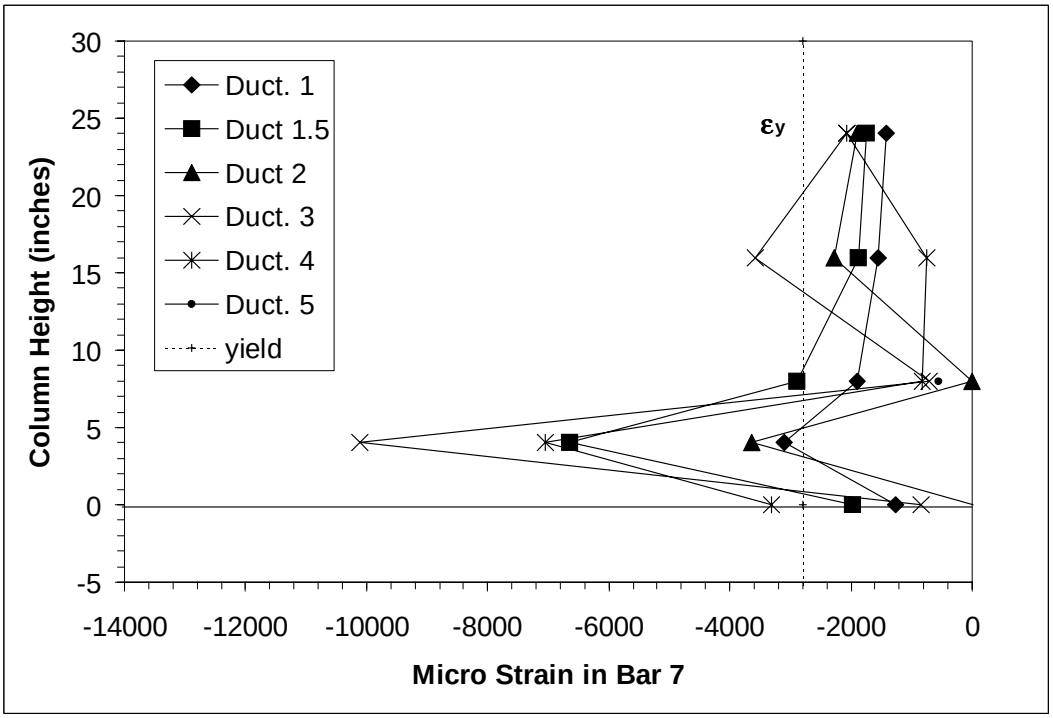

Figure 8.15 Strain Profile of the Longitudinal Steel on the South Side

The strain profiles of these figures show the strain to be highest at four inches above the top of the footing. Buckling of the longitudinal reinforcement occurred at this

location on the north and south side of the column. On the north side of the column the strain gage exceeded its capacity at a displacement ductility of 1.5 at four inches up the column. On the south side of the column the gage exceeded its capacity at a displacement ductility of 3 at four inches up the column. Since buckling took placed at 4 inches above the footing the strain gage hysteresis at this point is important. The cyclic action has created residual strain in the longitudinal bar, which can be seen in the strain gage hysteresis shown in figure 8.16 and 8.17 below.

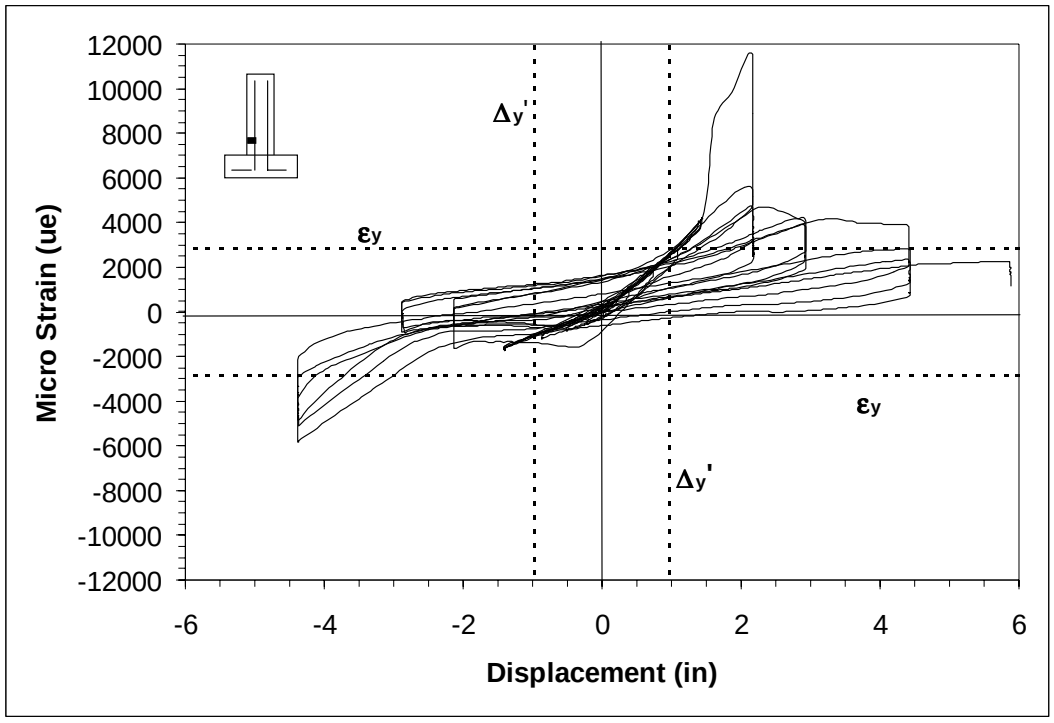

Figure 8.16 Longitudinal North at Positive 4 inches Strain Gage Hysteresis

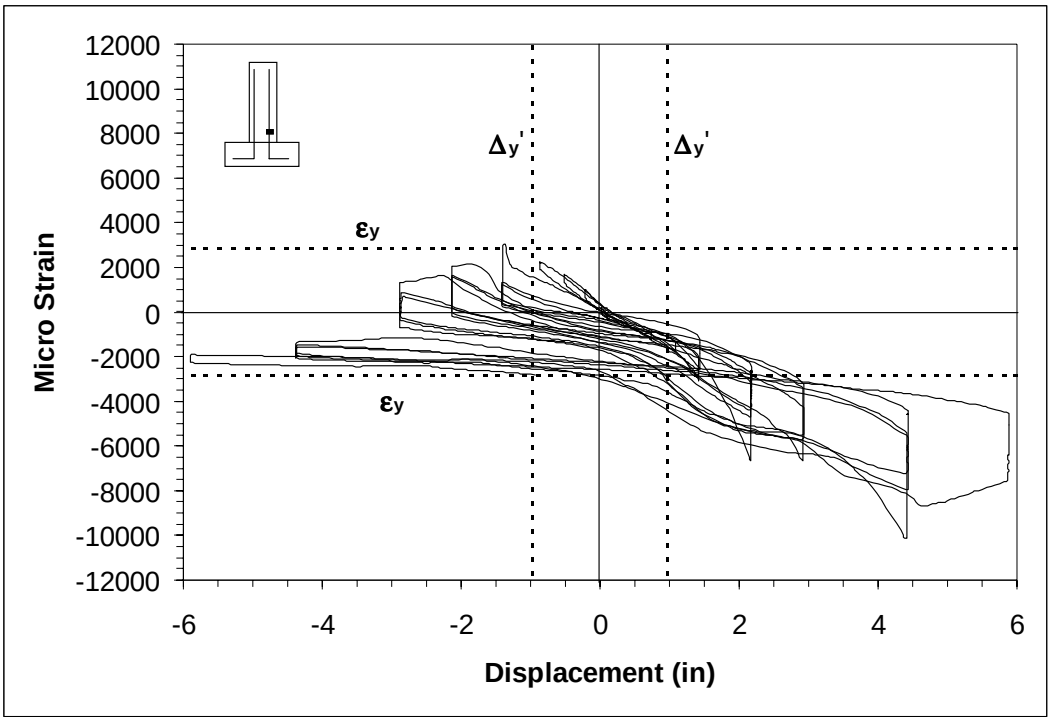

Figure 8.17 Longitudinal South at Positive 4 inches Strain Gage Hysteresis

With the strain gages on the transverse steel, strain profiles were generated for each side of the column. The transverse steel strain profiles for the column start at 6'' above the top of the footing and extends up the column to a height of 24''. Figure 8.18 and 8.19 display the strain profiles for each ductility level.

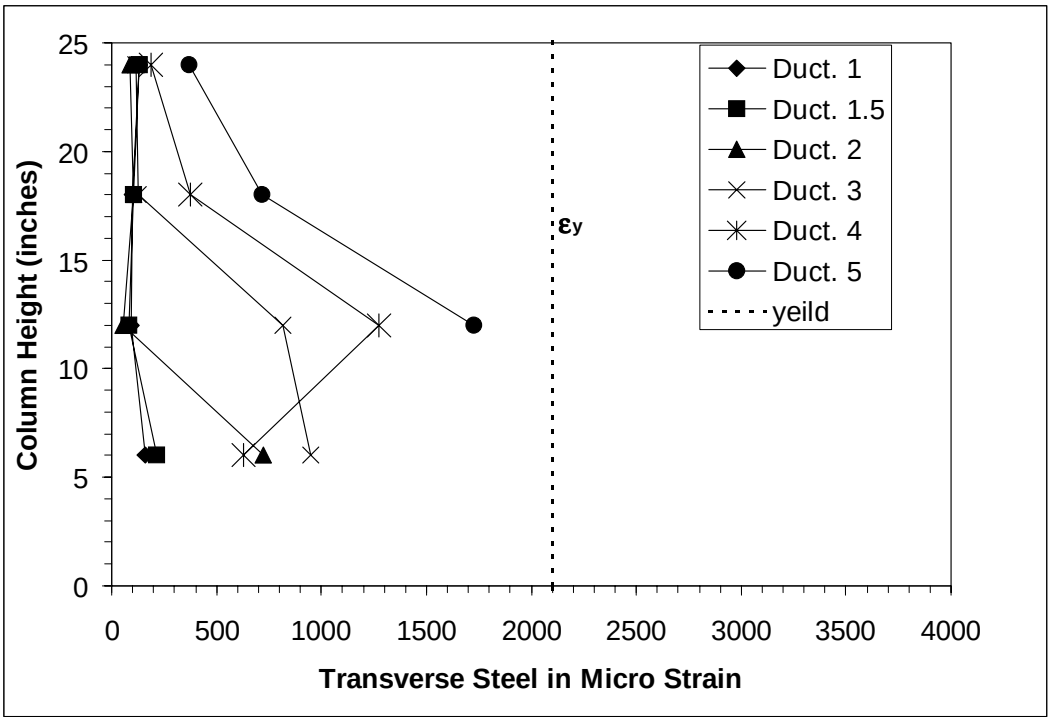

Figure 8.18 Transverse Steel Strain Profiles for the North Side

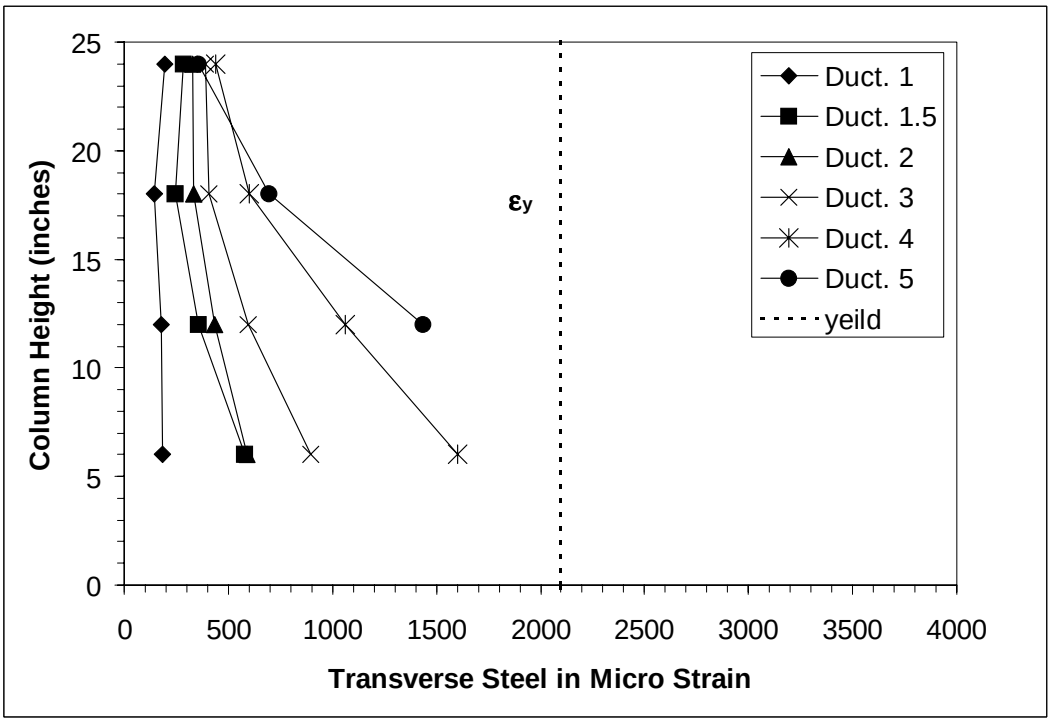

Figure 8.19 Transverse Steel Strain Profiles for the South Side

From Figures 8.18 and 8.19 it can be seen that the strain in the transverse steel was highest where buckling occurred. This is expected due to the fact that the

longitudinal bar was trying to push outwards and the transverse steel was resisting this motion. The transverse steel strain hysteresis is shown in the figures below.

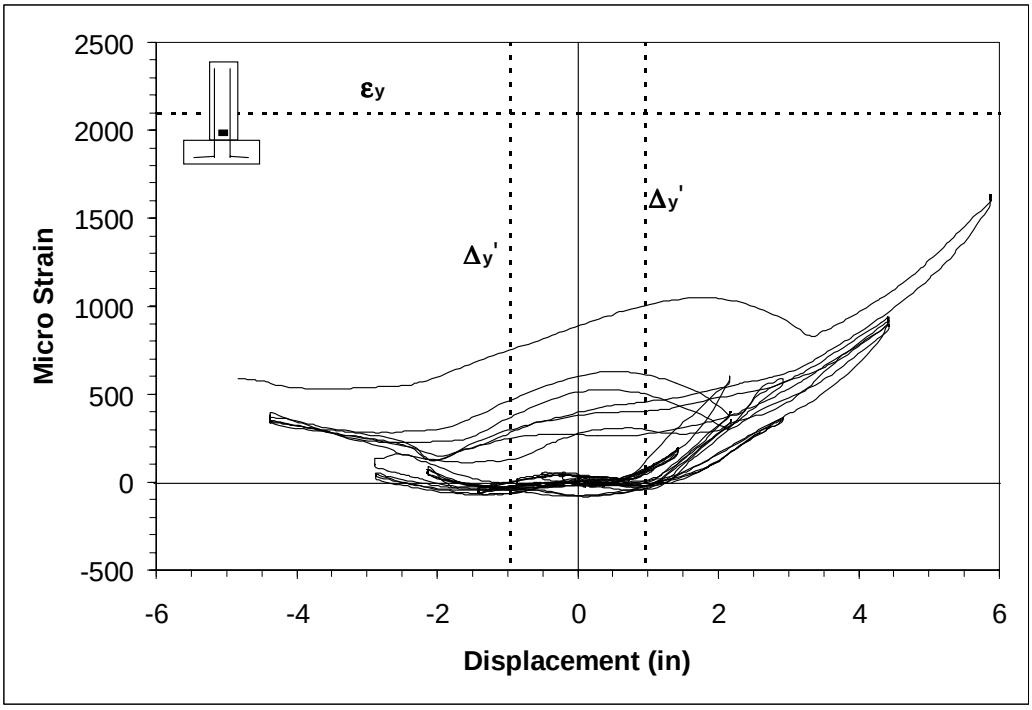

Figure 8.20 Transverse South at 6 inches Strain Gage Hysteresis

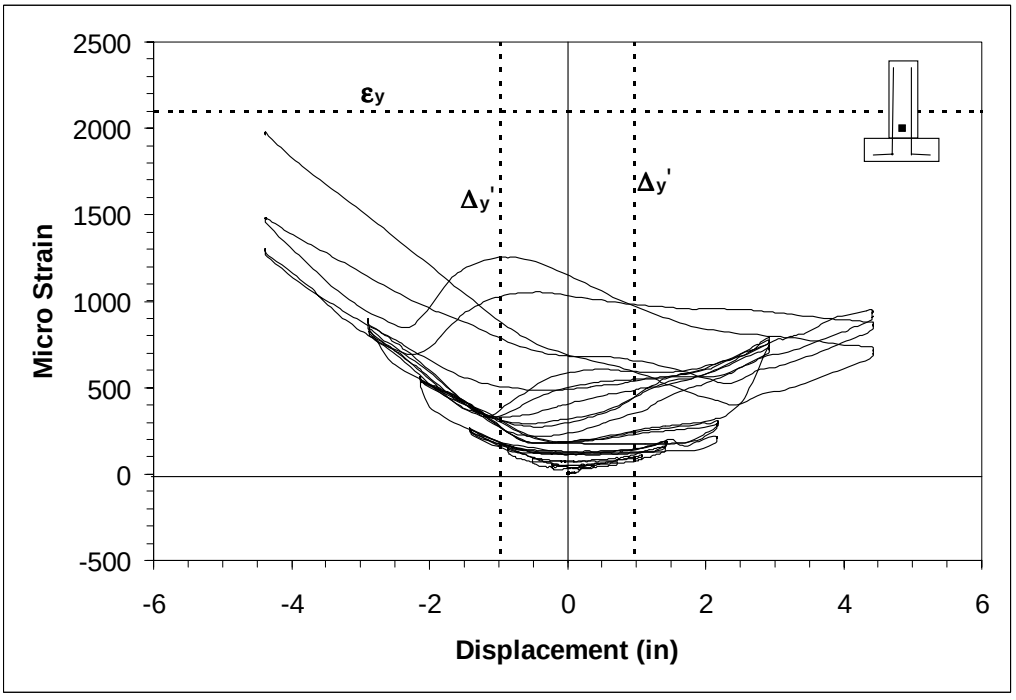

Figure 8.21 Transverse North at 6 inches Strain Gage Hysteresis

Since the strain gages did not work throughout the whole test, the strains at higher levels of ductility were not known. Using moment curvature analysis to determine Δ_y, and ϕ_y, the flexural tension strain was determined by the displacement of the column. Using the following equations the flexural tension strain was calculated for higher levels of ductility.

$$\Delta_p = \Delta_u - \Delta_y \qquad (Eq.8.9)$$

$$\phi_p = \frac{\Delta_p}{L_{eff}(L_p)} \qquad (Eq.8.10)$$

$$\phi_u = \phi_p + \phi_y \qquad (Eq.8.11)$$

$$\varepsilon_s' = \phi_u(c - d') \qquad (Eq.8.12)$$

$$\varepsilon_s = \phi_u(d - c) \qquad (Eq.8.13)$$

$$\varepsilon_c = \phi_u(c) \qquad (Eq.8.14)$$

The peak flexural tension strain in the push direction was 4.5% and 4.5% in the pull direction. Also note that the maximum compression strain that the extreme bars were subject to was 1.5%. At a ductility of 4, the extreme concrete compression strain was calculated to be 1.9%.

8.5 Observations for Next Test

During this test, the extreme bars on the north and south side buckled at the same displacement ductility. The bars experienced a peak flexural tension strain around 4.5% and compression strain of 1.5%. The column performed the same on both sides, as expected. To help determine if flexural tension strain was a contributing factor in

buckling of reinforcing steel, the second specimen will be loaded in a seismic manner where one side of the column is subjected to the yield tension strain, while the other is cycled in the usual manner. This will be discussed further in the next chapter.

9.0 Test Specimen 2

This chapter will discuss all the aspects involved in testing the second specimen. This chapter will be broken into five parts; loading of specimen, prediction of response, observations made during the test, test results, and determination of how to load the next specimen.

The information gathered during the test will only be presented. Some preliminary observations and conclusions will be made but the main analysis of the data will be covered in chapter 12. Appendix A-3 contains graphs of column curvature and individual linear pot histories.

9.1 Loading of Specimen

From moment curvature analysis the first yield force and displacement have been calculated. The test specimen was loaded in force control up to yield as shown in figure 9.1. Once this point was reached the yield displacement was validated, by reading the string potentiometer, and then the equivalent yield displacement was calculated. From this point, the specimen was load in increments of displacement ductility as shown in figure 9.2.

The cyclic loading in increments of displacement ductility was in the push direction only. On the return cycle, the column was brought back to yield in the pull direction for each cycle of loading. This exposes the extreme south bar to a maximum flexural tension strain of yield. In doing this, it is expected that buckling of the bars upon reversal would be delayed considerable due to the low level of tension strain they were subjected to.

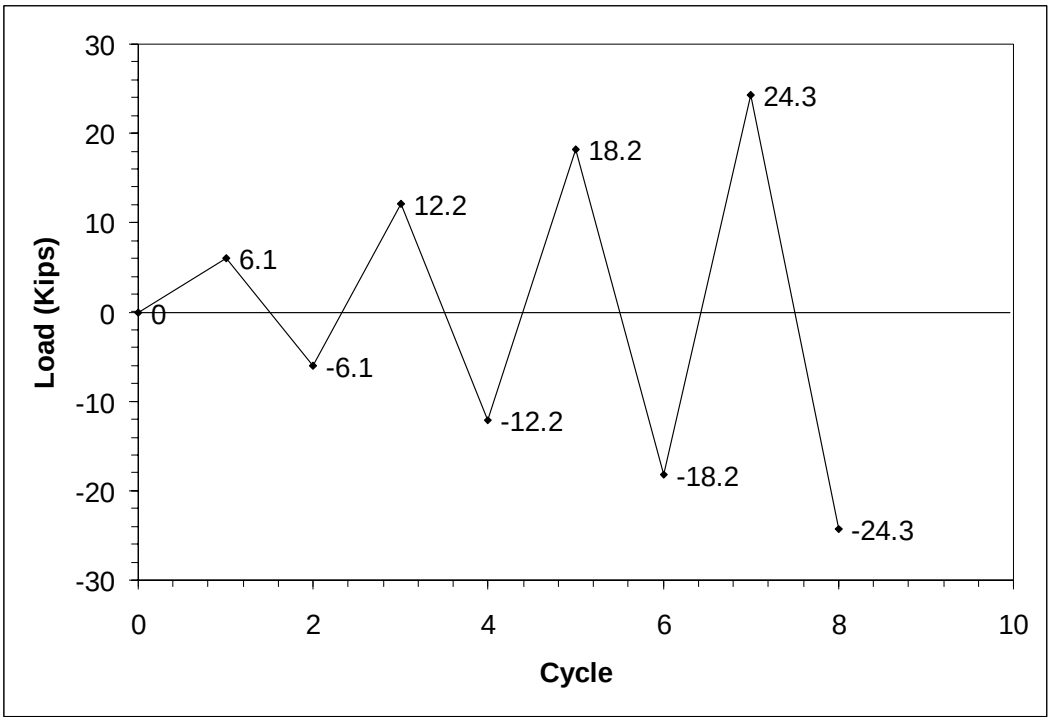

Figure 9.1 Force Control Loading of Specimen 2

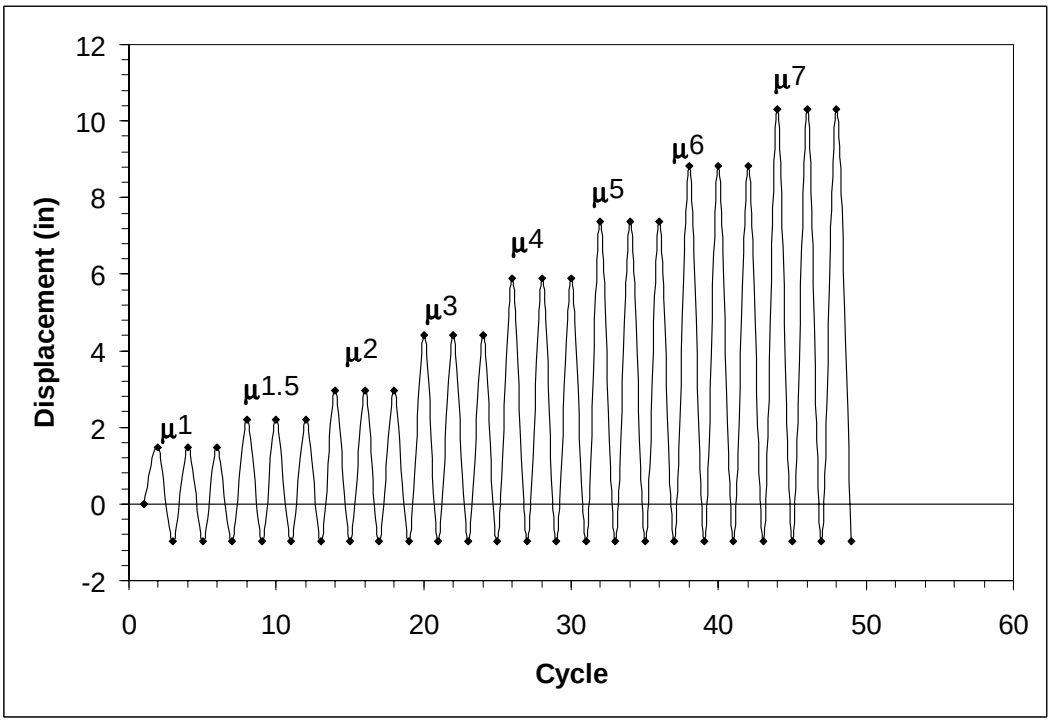

Figure 9.2 Displacement Control Loading of Specimen 2

9.2 Prediction of Response

There are no tests in the database to help predict what will happen under this loading history. The specimen was loaded to higher and higher levels of displacement ductility until buckling occurred. By using this type of loading history, the maximum tension strain that causes buckling can be determined. This loading history will provide information about the effect of tension strain on buckling.

9.3 Observations

The following is a step by step account of the column response during the test. Each cycle will consist of the positive and negative direction of force or displacement loading. Each step will focus on cracks size and location on the column. Also aspects such as crushing of concrete or exposure of reinforcing steel will be discussed. The visual account will allow for a correlation between visual inspection and test results.

9.3.1 Force loading

The first cycle in force control was to 6 kips (25% of theoretical yield). No cracks were observed in the column.

The next cycle of force loading was to 12.2 kips (50% of theoretical yield). Cracks have formed 45'' up the column spaced at 6'' intervals. The cracks extend from the east side to the west side about ¼ to ½ way around the column. The x-y recorder also showed a change in column stiffness at about 7 kips on the x-y recorder.

The next cycle of force loading was to 18.2 kips (75% of theoretical yield). The cracks that occurred during the last cycle were extended during this cycle. Cracks have

formed 67'' up the column spaced at 4'' intervals. Some new cracks also formed with the largest flexural crack width measuring 0.002''.

The final force loading cycle was too theoretical yield at 24 kips. The LNP04 strain gage read 0.0028 tension strain, which is yield for the longitudinal bars indicating an agreement between analytical and experimental. The LNSP04 strain gage read 0.0017 compression strain, which is less than the yield strain. There were further crack extensions with the largest flexural crack width increasing to 0.005''.

9.3.2 Displacement Loading

The equivalent yield displacement was determined during the first test and will be used in this test also. The equivalent yield displacement was 1.47 inches.

The first cycle in displacement control was ductility 1, which is equivalent to a displacement of 1.47 inches. Shear cracks began to form in the column. The largest flexural crack width increased to 0.007'' at seven inches above the footing. Some new cracks formed in the column but mostly growth of old cracks. The axial load was reduced by 2.4 kips to bring the load back to the original 51 kips.

The next displacement level on the column was to a ductility of 1.5, which is equivalent to a deflection of 2.2 inches. More flexural and shear cracks have formed in the column. There was also some crack extensions of flexural and shear cracks that already exist. The largest flexural crack width increased to 0.03'' at seven inches above the footing. Some incipient spalling of concrete began to occur on the south side of the column.

The next displacement level on the column was to a ductility of 2, which is equivalent to a deflection of 2.9 inches. The largest flexural crack width on the north side

increased to 0.03’’ at seven inches above the footing. On the south side of the column minor spalling of the cover concrete was still occurring.

The next displacement level on the column was to a ductility of 3, which is equivalent to a deflection of 4.4 inches. The largest flexural crack on the north side increased to 0.10’’ at seven inches above the footing. More shear cracks were forming on the east and west faces of the column. The transverse steel began to be exposed on the south side. On the south side there was crushing of concrete in the plastic hinge region. The extreme south longitudinal bar was exposed at 4 inches up the column.

The next displacement level on the column was to a ductility of 4, which is equivalent to a deflection of 5.9 inches. The flexural crack width on the north side seven inches above the footing increased to 1/8 inch wide. There were some shear cracks extension on the east and west faces. On the south side of the column some new crushing of the concrete occurred. In the last test buckling occurred at this level of ductility, but there were no signs of buckling.

The next displacement level on the column was to a ductility of 5, which is equivalent to a deflection of 7.35 inches. There were three longitudinal bars exposed on the south side of the column and still no signs of buckling. The flexural crack width on the north side at seven inches above the footing increased to 3/16 of an inch. Small cracks began to form in the footing along the east and west faces. There was extension of old shear cracks and formation of new shear cracks. Some minor spalling began on the north side of the column.

The next displacement level on the column was to a ductility of 6, which is equivalent to a deflection of 8.84 inches. The largest flexural crack seven inches above

the footing on the north side increased to $^{3}/_{16}$ to ¼ inches in width. More spalling occurred on the north side of the column. The extent of spalling increased to 14'' on the south side of the column.

The next displacement level on the column was to a ductility of 7, which is equivalent to a deflection of 10.3 inches. The three outer most bars on the north side of the column buckled at the location of the largest flexural crack. The extent of spalling increased to 15 inches on the north side. It is significant to note the north side buckled after being exposed to large tension strain and rather low compression strains. The south side of the column experienced large compression strain but rather low-tension strains and did not buckle. This will be discussed further in chapter 12.

The next displacement load on the column was to a ductility of 8, which is equivalent to a deflection of 11.8 inches. The extreme longitudinal bar on the north side ruptured before the column reached a ductility of 8. With this failure the test was stopped and the column was brought back to zero displacement.

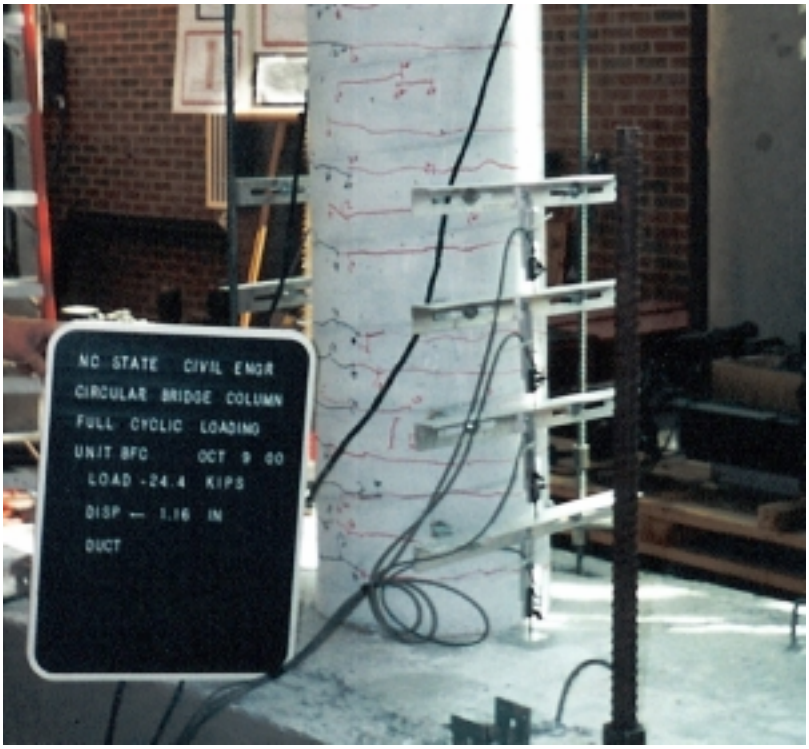

Figure 9.3 South Side of Specimen at Yield

Figure 9.4 South Side of Specimen at Ductility 1 Cycle 3

Figure 9.5 South Side of Specimen at Ductility 1.5 Cycle 3

Figure 9.6 South Side of Specimen at Ductility 2 Cycle 3

Figure 9.7 North Side of Specimen at Ductility 3 Cycle 1

Figure 9.8 South Side of Specimen at Ductility 4 Cycle 3

Figure 9.9 South Side of Specimen at Ductility 5 Cycle 1

Figure 9.10 South Side of Specimen at Ductility 6 Cycle 3

Figure 9.11 North Side of Specimen at Ductility 6 Cycle 3

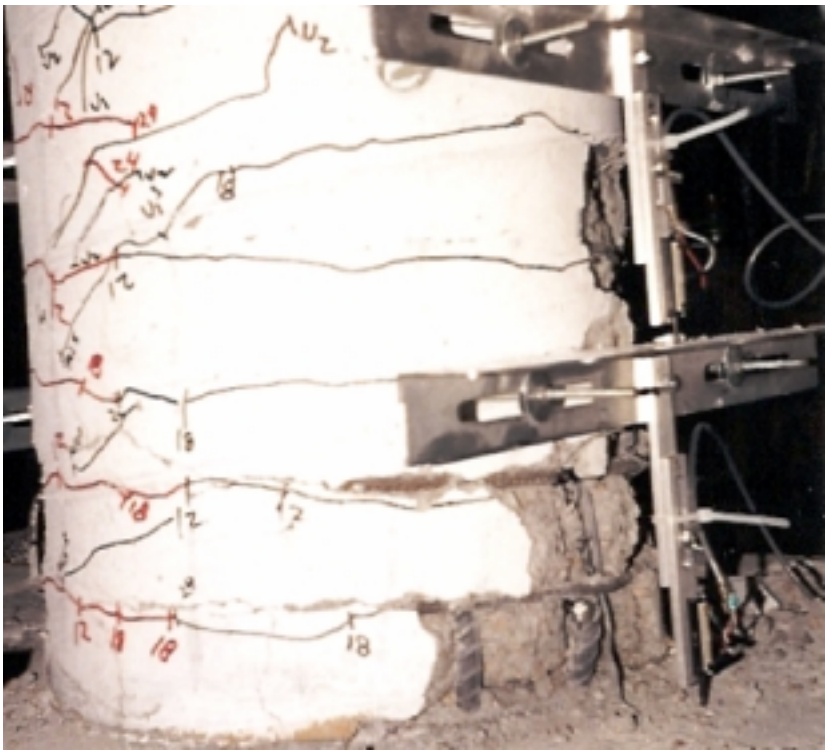
Figure 9.12 Buckling of Reinforcement North Side of Specimen at Ductility 7

Figure 9.13 Rupture of Reinforcement North Side of Specimen at Ductility 7

9.4 Test Results

With the data obtained from the gages on or in the specimen, values can be associated with the observed response of the section. Figure 9.14 shows the force versus displacement response of the specimen. Also plotted on the same graph is the first yield force, ultimate force, and first yield displacement along with the response from moment curvature analysis. The Response curve takes into account the P-Δ moment due to the axial load. Buckling began to occur in the bar at the location marked by X on the force versus displacement response curve.

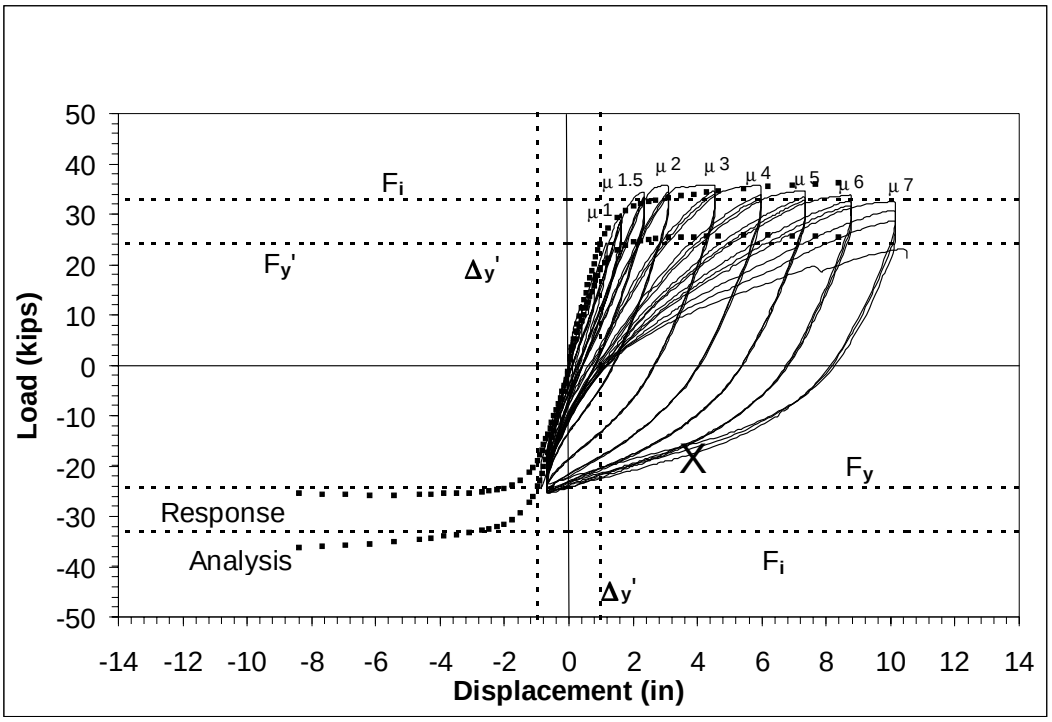

Figure 9.14 Force versus Displacement Response for Specimen 2

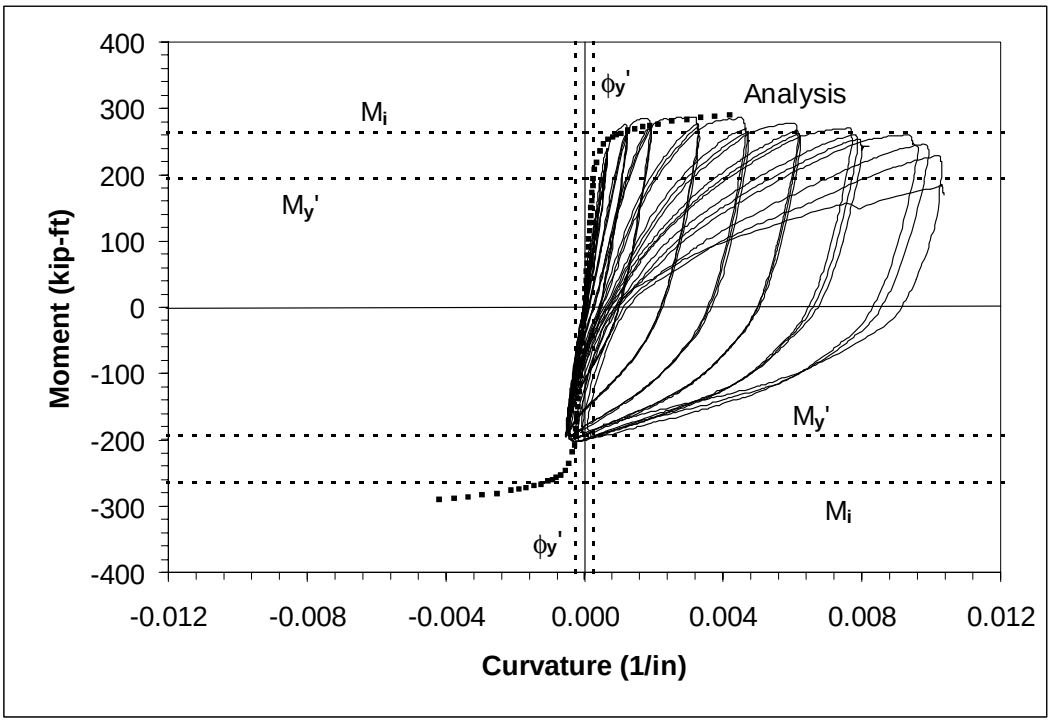

Figure 9.15 Moment versus Curvature for Specimen 2

The moment curvature graph was generated by multiplying the applied force by the column height and plotting the results against the curvature calculated at the bottom

gage length of the column, which has the largest curvature. The other three gage lengths also were used to measure the curvature of the column. Figure 9.16 shows the curvature profile of the column with the curvature being assumed linear after a column height of 28 inches. Using the equations in chapter 6, the ultimate deflection of the column can also be calculated from the curvature.

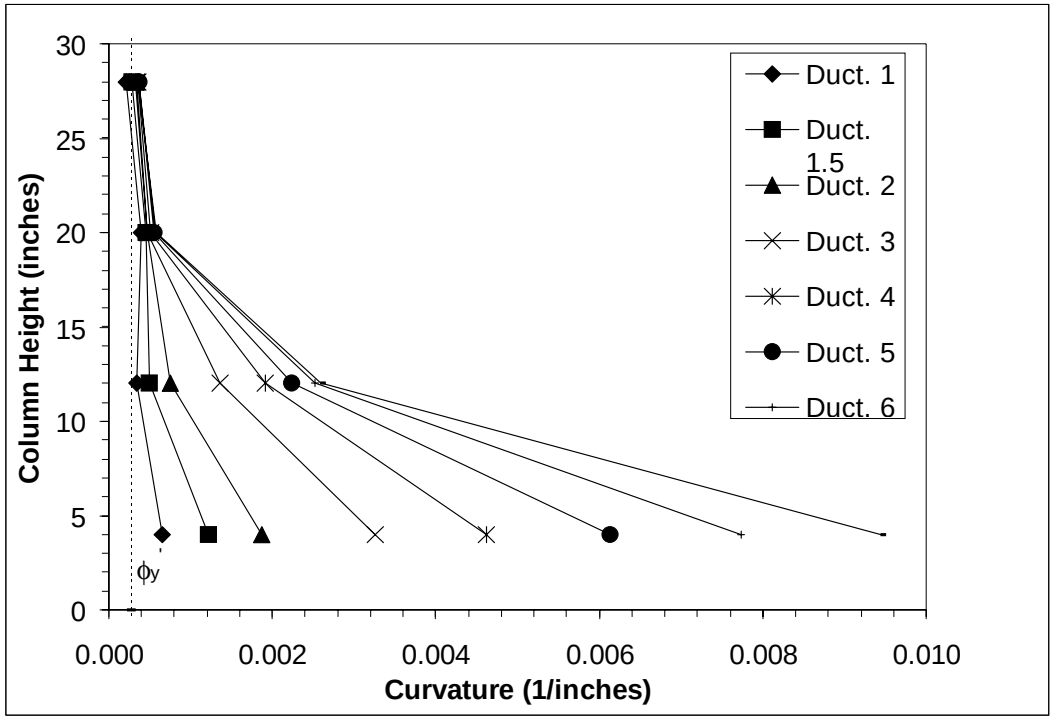

Figure 9.16 Curvature Profile of the Column at Different Levels of Ductility

The strain gages on the north and south sides of the column provide a profile of the strain in the longitudinal steel. The strain profile starts at four inches below the footing and extends 24 inches above the footing. At high levels of ductility some strain gages exceeded their capacity, this data is included in the figures shown below. A discussion will be given on the validity of these gage readings.

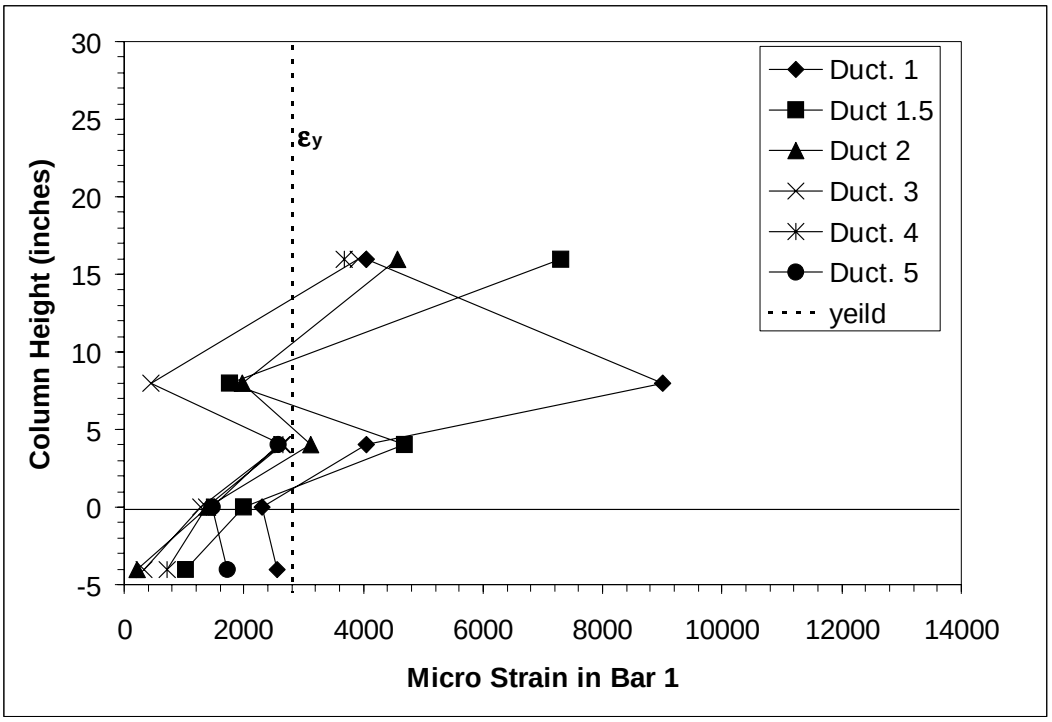

Figure 9.17 Strain Profile of the Longitudinal Steel on the North Side

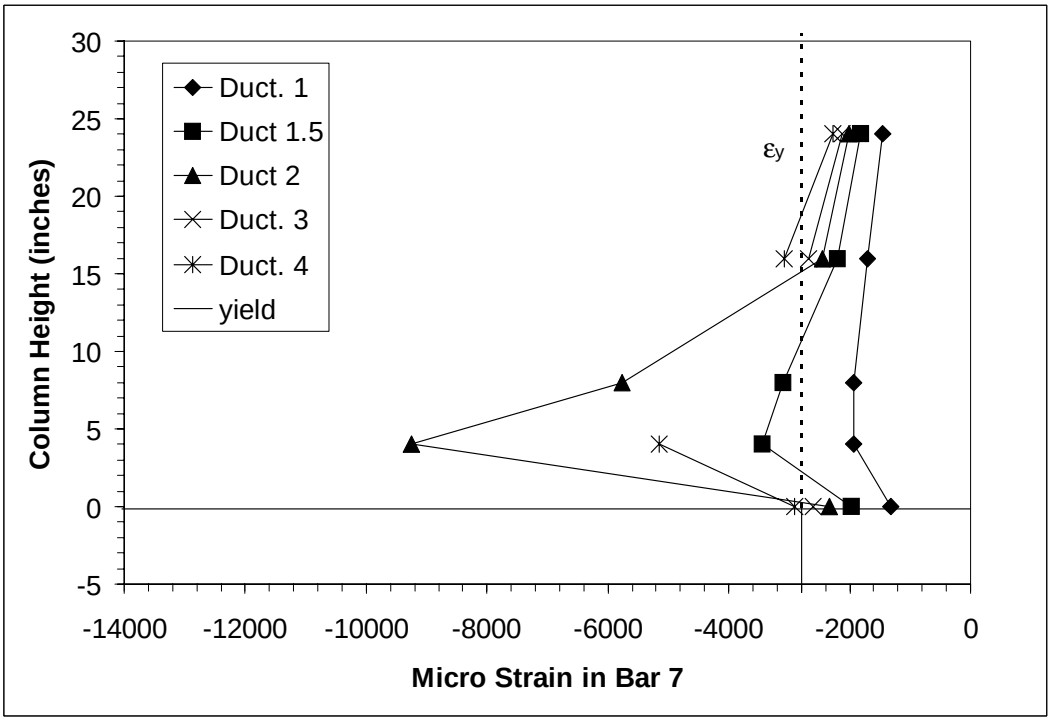

Figure 9.18 Strain Profile of the Longitudinal Steel on the South Side

The strain profiles of these graphs show the strain to be highest at four inches above the top of the footing. Note the strain gages exceeded their capacity in the region

where buckling occurred. The strain gages exceeded their capacity at a displacement ductility of 1.5 for figure 9.17 and ductility 2 for figure 9.18. Buckling of the longitudinal reinforcement occurred at the location of the largest crack on the north side of the column. The strain hysteresis of the LNP04 gage is shown in the figure below. As can be seen in figure 9.19 the strain gage exceeded its capacity at yield. Even though the strain gage did no last long, some of the residual strain can be seen in the figure below.

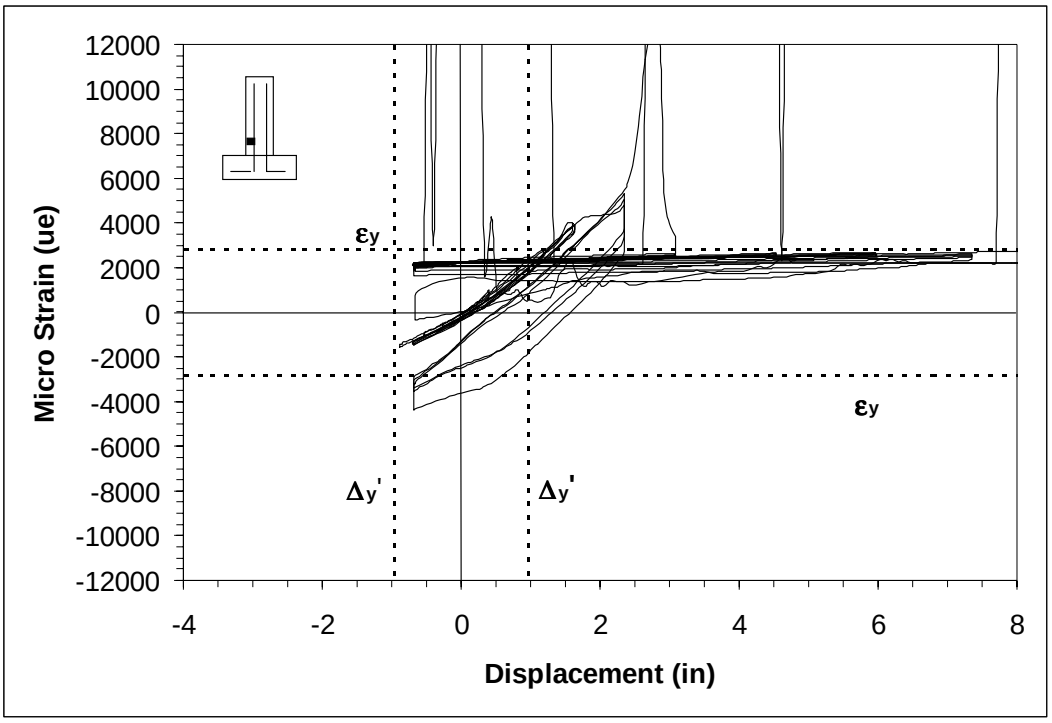

Figure 9.19 Longitudinal North at Positive 4 inches Strain Gage Hysteresis

With the strain gages on the transverse steel, strain profiles were generated for each side of the column. The transverse steel strain profiles for the column start at 6'' above the top of the footing and extends up the column to a height of 24''. Figure 9.21 and 9.22 display the strain profiles for each ductility level. The strain hysteresis of the transverse steel for six inches above the footing closet to where buckling occurred is shown below.

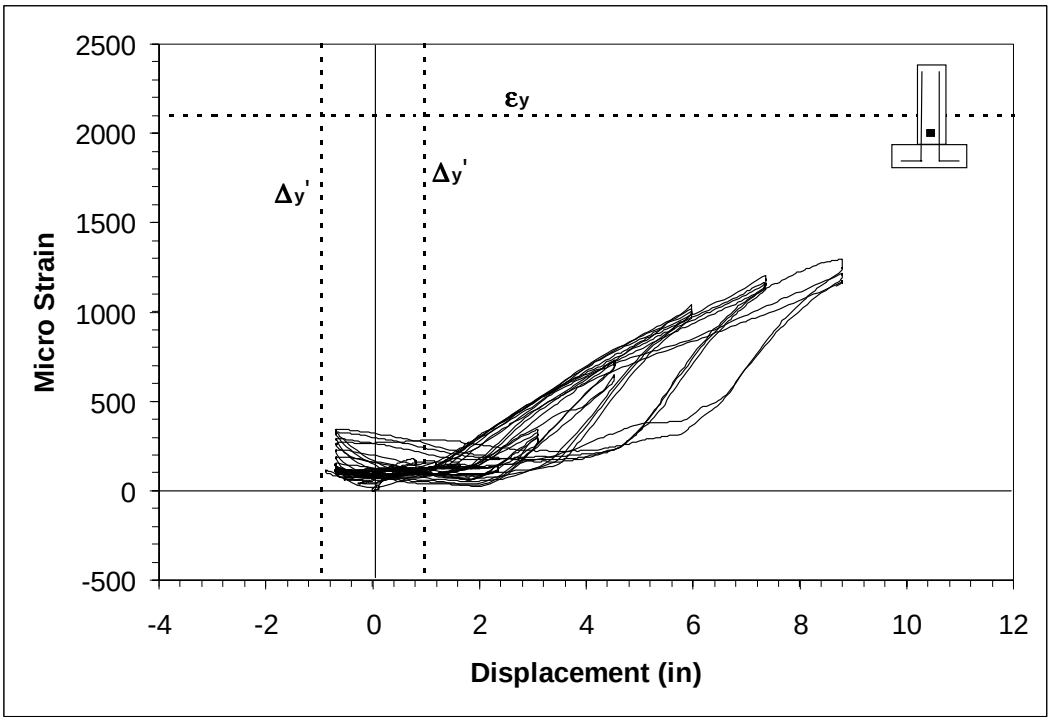

Figure 9.20 Transverse North at 12 inches Strain Gage Hysteresis

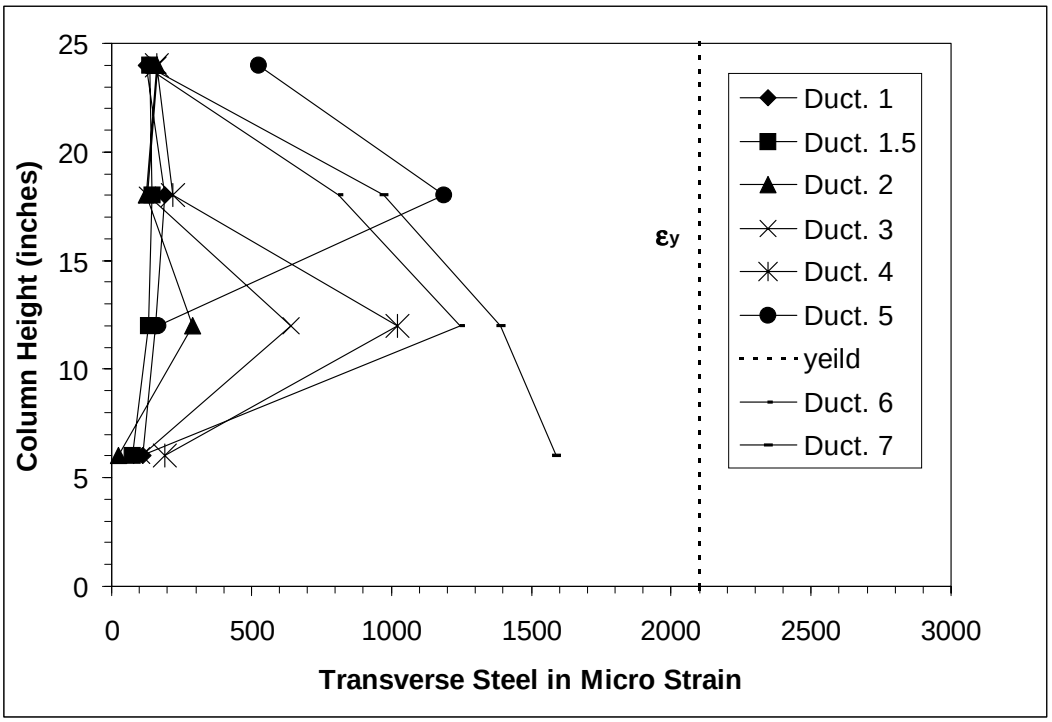

Figure 9.21 Transverse Steel Strain Profiles for the North Side

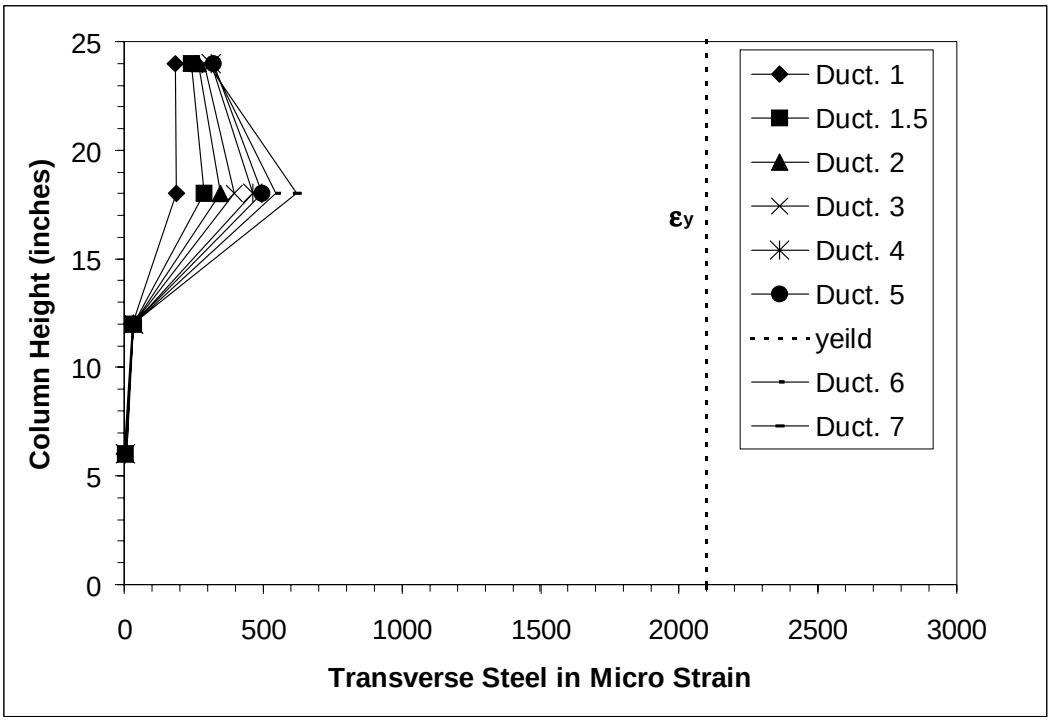

Figure 9.22 Transverse Steel Strain Profiles for the South Side

The strain gage on the transverse steel worked good up to failure. Notice that the transverse steel strains were well below yield. From Figures 9.21 it can be seen that the strain in the transverse steel was highest where buckling occurred. This is expected due to the fact that the longitudinal bar was trying to push outwards and the transverse steel was resisting this motion.

Since the strain gages do not work throughout the whole test, the strain at higher levels of ductility were not known. Using moment curvature analysis the flexural tension strain in the longitudinal steel was calculated from the displacement of the column. Using equations 8.9 through 8.14, the maximum flexural tension strain and compression strain were calculated for this test.

These equations show that the maximum flexural tension strain in the push direction was 8.3%. At a displacement ductility of 7 the extreme concrete compression

strain was calculated to be 3.4%. Also note that the maximum compression strain that the extreme bars was subjected to was 2.7%.

9.5 Observations for Next Test

During this test, the extreme bars on the north side buckled at a displacement ductility of 7. The bars experienced a flexural tension strain of 8.3% and a growth strain of 3.2%. The object of this test was to see if the south bars would buckle before the north bars after being exposed to low levels of tension strains and high levels of compression strains. This did not happen, supporting the idea that tension strain is an important factor in buckling of reinforcing. With this notion of tension strain being a factor in buckling, then maybe the growth of the column is also a contributing factor. For the next test the column will be load in one cycle to a displacement ductility of 7. If growth strain is not a factor, then the longitudinal steel should buckle during the reverse loading cycle before crack closure.

10.0 Test Specimen 3

This chapter will discuss all the aspects involved in testing the third specimen. This chapter will be broken into five parts; loading of specimen, prediction of response, observations made during the test, test results, and determination of how to load the next specimen.

The information gathered during the test will only be presented. Some preliminary observations and conclusions will be made but the main analysis of the data will be covered in chapter 12. Appendix A-4 contains graphs of column curvature and individual linear pot histories.

10.1 Loading of Specimen

From moment curvature analysis the first yield force and displacement have been calculated. The test specimen was loaded in force control up to yield as shown in figure 10.1. Once this point was reached the yield displacement was validated, by reading the string potentiometer, and then the equivalent yield displacement was calculated. From this point, the specimen was load in increments of displacement ductility as shown in figure 10.2.

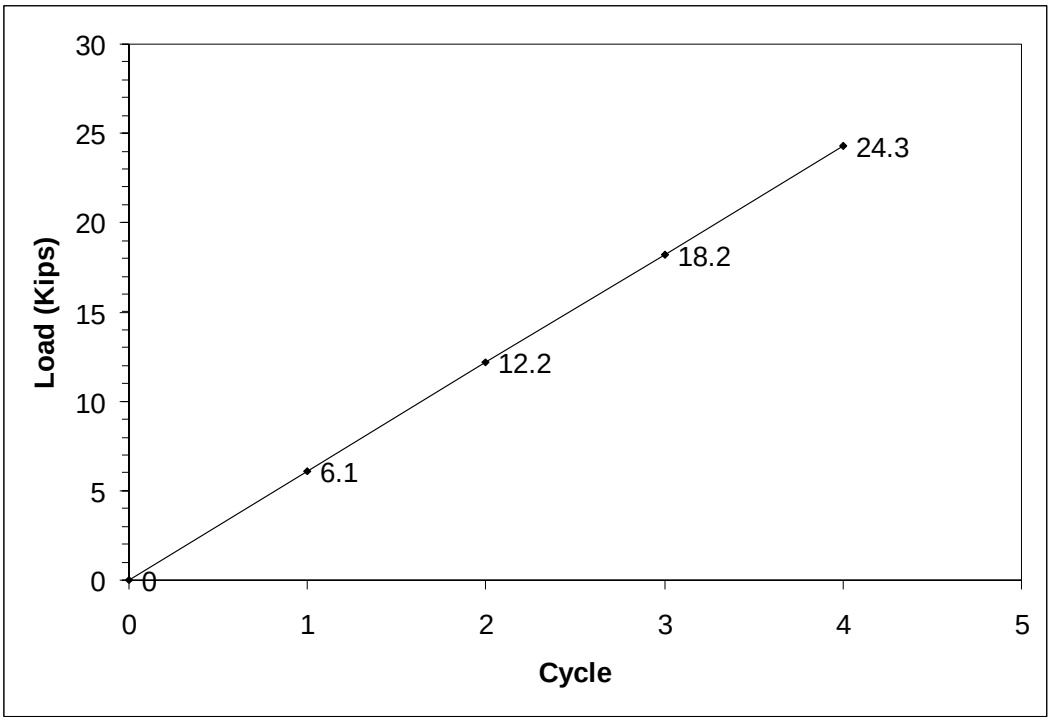

Figure 10.1 Force Control Loading of Specimen 3

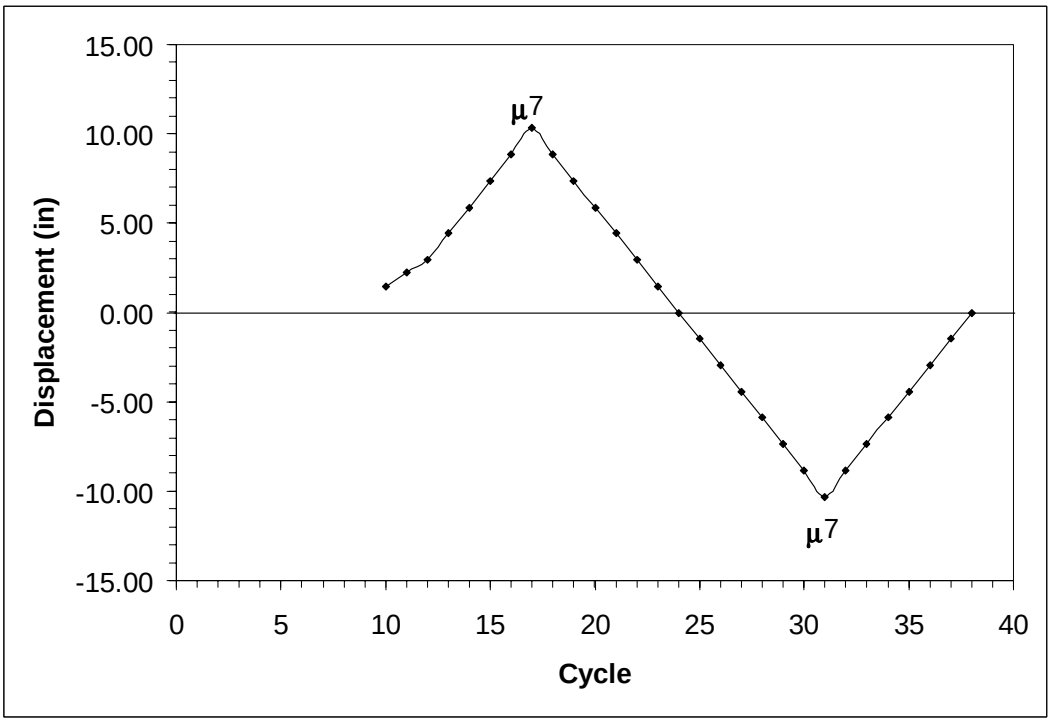

Figure 10.2 Displacement Control Loading of Specimen 3

10.2 Prediction of Response

The last test column was loaded cyclically placing the north side in tension. This test will load the column monotonically placing the north side in tension to a displacement ductility of 7. During the reversal cycle, the longitudinal steel should buckle on the north side before crack closure. The information gathered during this test can help determine if cyclic loading of the previous test was important factor in the onset of buckling.

10.3 Observations

The following is a step by step account of the column response during the test. Each step will focus on cracks size and location on the column. Also things such as crushing of concrete or exposure of reinforcing steel will be discussed. The visual account will allow for a correlation between visual inspection and test results.

10.3.1 Force loading

The first cycle in force control was to 6 kips (25% of theoretical yield). No cracks were observed in the column.

The next cycle of force loading was to 12.2 kips (50% of theoretical yield). Cracks have formed 53'' up the column spaced at 6'' intervals. The cracks extend from the east side to the west side of the column. The x-y recorder also showed a change in column stiffness at about 7 kips on the x-y recorder.

The next cycle of force loading was to 18.2 kips (75% of theoretical yield). The cracks that occurred during the last cycle were extended during this cycle. Some new cracks also formed.

The final force loading cycle was too theoretical yield at 24 kips. The LNP04 strain gage read 0.0028-tension strain, which is yield for the longitudinal bars indicating an agreement between analytical and experimental. The LNSP04 strain gage read 0.0017 compression strain, which is less than the yield strain. Flexural cracks have formed the full height of the column. There were further crack extensions with the spacing between cracks in the plastic being 3 inches.

10.3.2 Displacement Loading

The equivalent yield displacement was determined during the first test and will be used in this test also. The equivalent yield displacement was 1.47 inches.

The first cycle in displacement control was ductility 1, which is equivalent to a displacement of 1.47 inches. Shear cracks began to form in the column. Some new cracks formed in the column but mostly growth of old cracks.

The next displacement level on the column was to a ductility of 1.5, which is equivalent to a deflection of 2.2 inches. More shear cracks formed on the east and west faces of the column. There were shear and flexural crack extensions.

The next displacement level on the column was to a ductility of 2, which is equivalent to a deflection of 2.9 inches. First signs of crushing occurred on the south side of the column. There were also some crack extensions.

The next displacement level on the column was to a ductility of 3, which is equivalent to a deflection of 4.4 inches. More shear cracks formed on the east and west faces of the column. The largest flexural crack width increased to 0.06’’ located at six inches above the footing.

The next displacement level on the column was to a ductility of 4, which is equivalent to a deflection of 5.9 inches. The plastic hinge increased to 12 inches on the south side of the column. Some new shear cracks formed on the east and west faces of the column.

The next displacement level on the column was to a ductility of 5, which is equivalent to a deflection of 7.35 inches. The extreme longitudinal bar on the south side of the column was exposed. The largest flexural crack width increased to 3/32'' located at six inches above the footing.

The next displacement level on the column was to a ductility of 6, which is equivalent to a deflection of 8.84 inches. There was further crushing of the concrete on the south side of the column. The largest flexural crack width increased to 1/8'' located at six inches above the footing.

The next displacement level on the column was to a ductility of 7, which is equivalent to a deflection of 10.31 inches. The largest flexural crack width increased to 3/16'' located at six inches above the footing. There were no signs of buckling on the south side of the column. The specimen was then loaded in the opposite direction.

The next displacement level of notable consideration was to a ductility of 2 in the pull direction, which is equivalent to a deflection of –2.93 inches. The cracks on the north side of the column closed. There was no evidence of buckling of the longitudinal steel on this side of the column.

The next displacement level of notable consideration was to a ductility of 7 in the pull direction, which is equivalent to a deflection of –10.31 inches. Further spalling

occurred in the plastic hinge region on the north side. The bars on the north side have not buckled. The specimen was then loaded back to zero displacement.

As the column reached zero displacement the longitudinal bars on the south side of the column began to buckle. The three outer most bars buckled between the 2 and 3 spiral. Failure of the column had been reached but the column was loaded out to ductility 7 in the push direction to measure the lost in strength.

When the column reached a ductility of 4, the spiral on the south side of the column ruptured. The rupture occurred where the longitudinal bars were pushing against the spiral. At this point, the test was stopped and the column was brought back to zero deflection.

Figure 10.3 North Side of Specimen at Yield

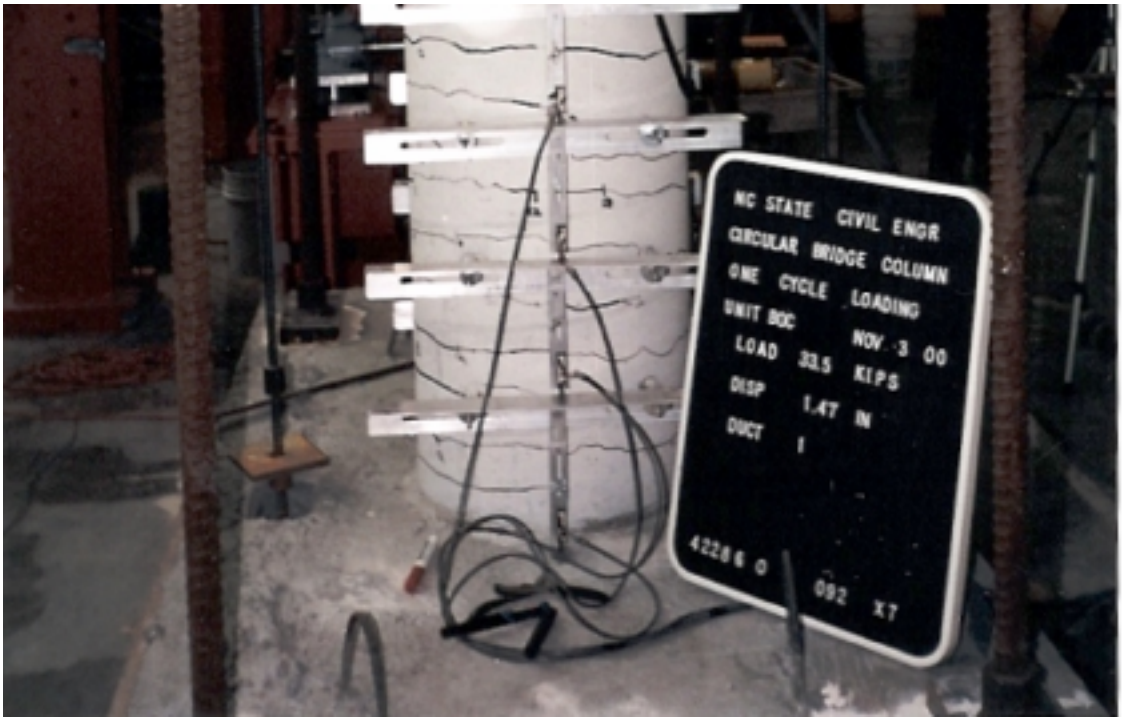

Figure 10.4 North Side of Specimen at Ductility 1

Figure 10.5 North Side of Specimen at Ductility 1.5

Figure 10.6 North Side of Specimen at Ductility 2

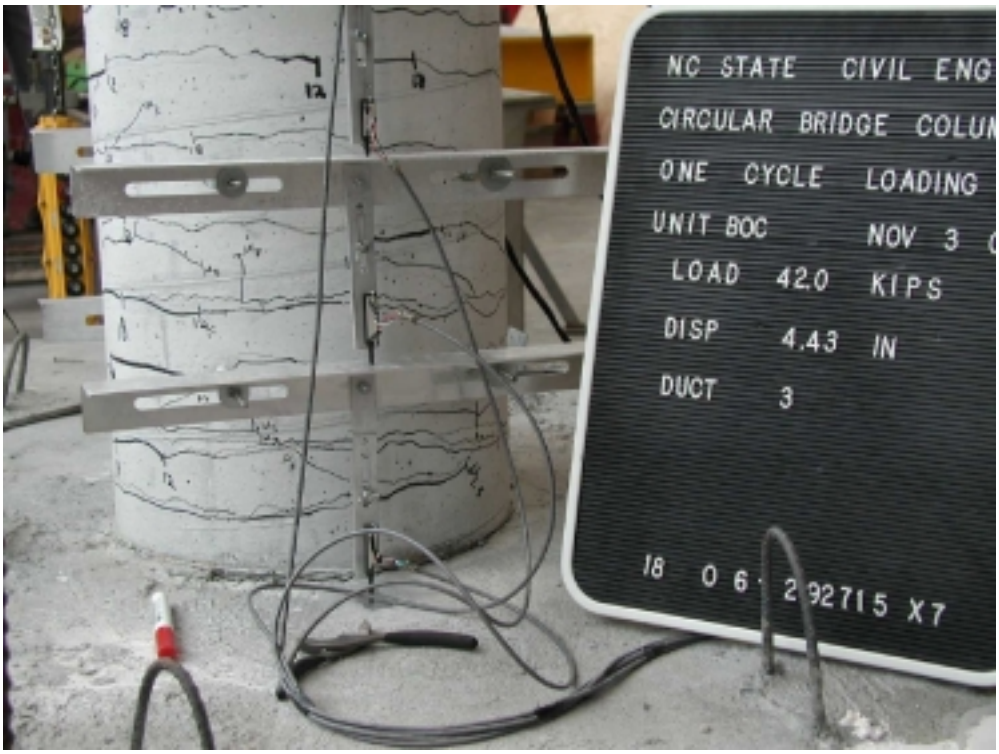

Figure 10.7 North Side of Specimen at Ductility 3

Figure 10.8 South Side of Specimen at Ductility 3

Figure 10.9 East Side of Specimen at Ductility 4

Figure 10.10 North Side of Specimen at Ductility 5


Figure 10.11 South Side of Specimen at Ductility 5

Figure 10.12 South Side of Specimen at Ductility 6

Figure 10.13 South Side of Specimen at Ductility 7

Figure 10.14 West Side of Specimen at Ductility 7

Figure 10.15 North Side of Specimen at Ductility 7 (in the pull direction)

Figure 10.16 South Side of Specimen at Ductility 7 (in the pull direction)


Figure 10.17 South Side of Specimen at Failure

10.4 Test Results

With the data obtained from the gages on or in the specimen, values can be associated with the observed response of the section. Figure 10.18 shows the force versus displacement response of the specimen also plotted on the same graph is the first yield force, ultimate force, and first yield displacement along with the response from moment curvature analysis. The response curve takes into account the P-Δ moment of the axial load. Buckling began to occur in the bar at the location marked by X on the force versus displacement response curve.

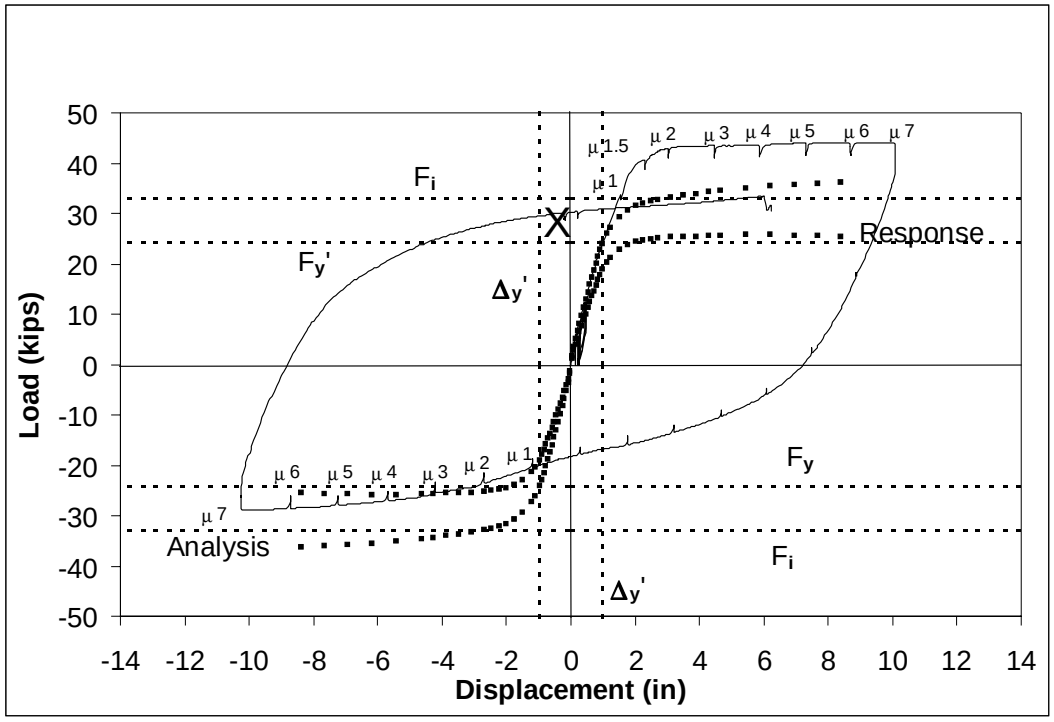

Figure 10.18 Force versus Displacement Response for Specimen 3

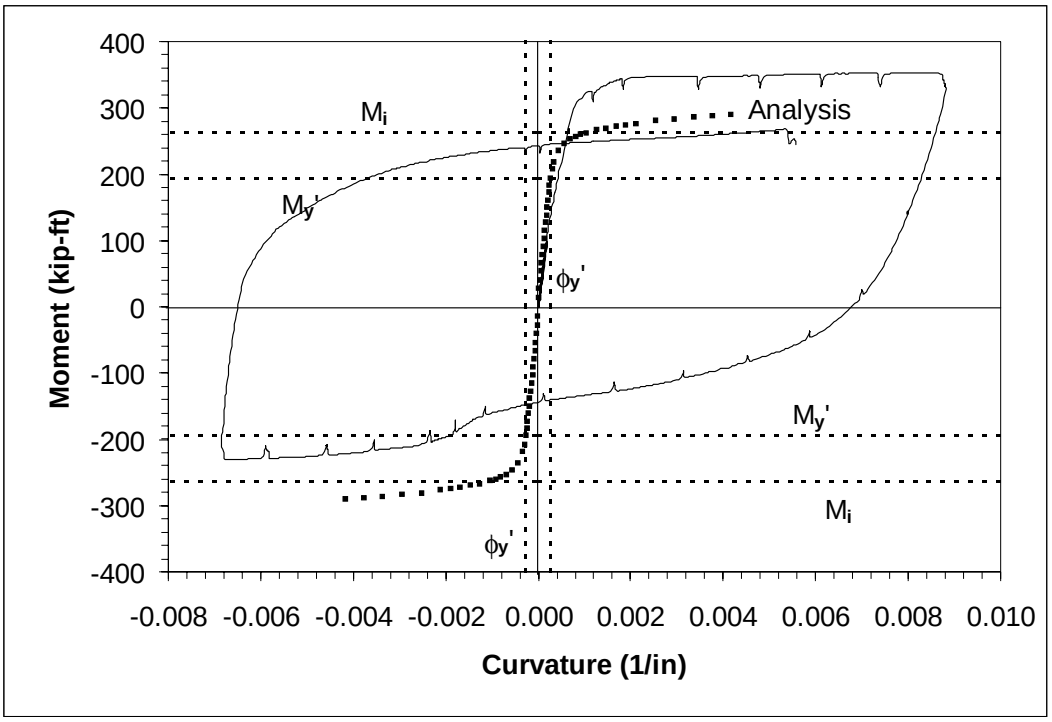

Figure 10.19 Moment versus Curvature for Specimen 3

The moment curvature graph was generated by multiplying the applied force by the column height and plotting the results against the curvature calculated at the bottom gage length of the column, which has the largest curvature. The other three gage lengths also were used to measure the curvature of the column. Figure 10.20 shows the curvature profile of the column with the curvature being assumed linear after a column height of 28 inches. Using the equations in chapter 6, the ultimate deflection of the column can also be calculated from the curvature.

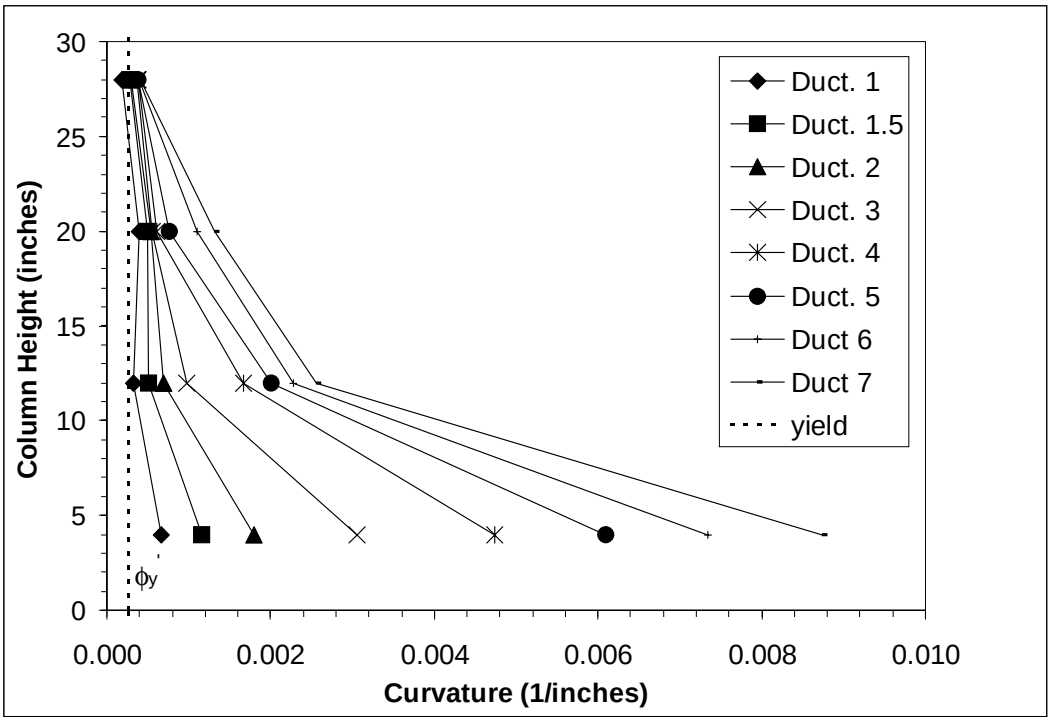

Figure 10.20 Curvature Profile of the Column at Different Levels of Ductility

The strain gages on the north and south sides of the column provide a profile of the strain in the longitudinal steel. The strain profile starts at four inches below the footing and extends 24 inches above the footing. At high levels of ductility some strain gages exceeded their capacity, this data is included in the figures shown below. A discussion will be given on the validity of the gage readings.

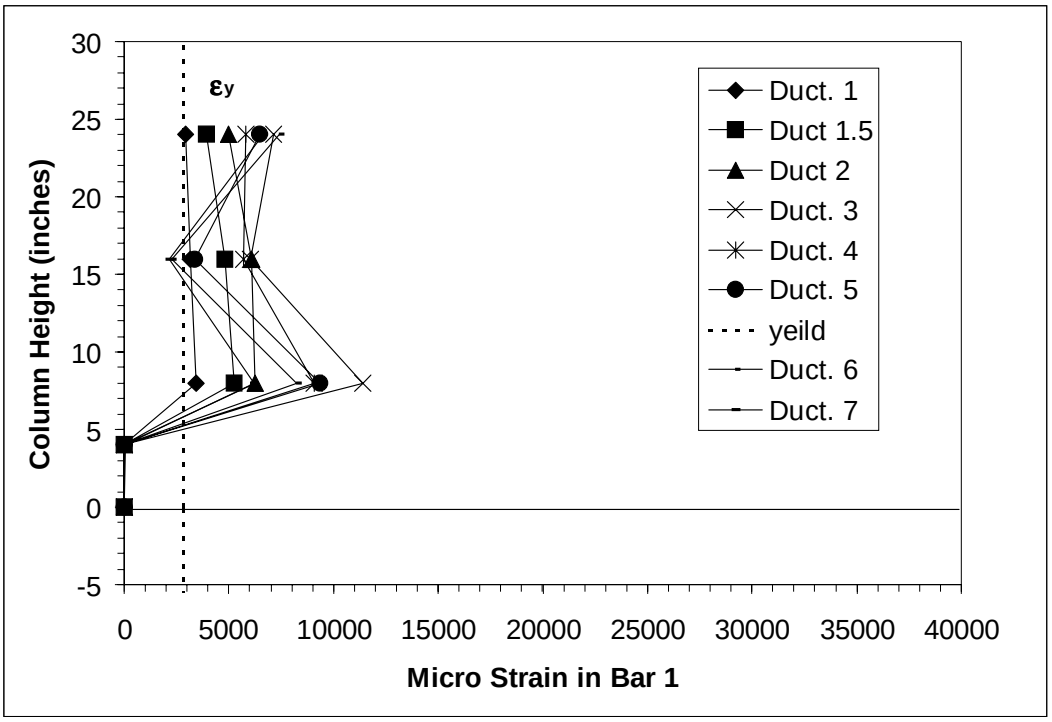

Figure 10.21 Strain Profile of the Longitudinal Steel on the North Side

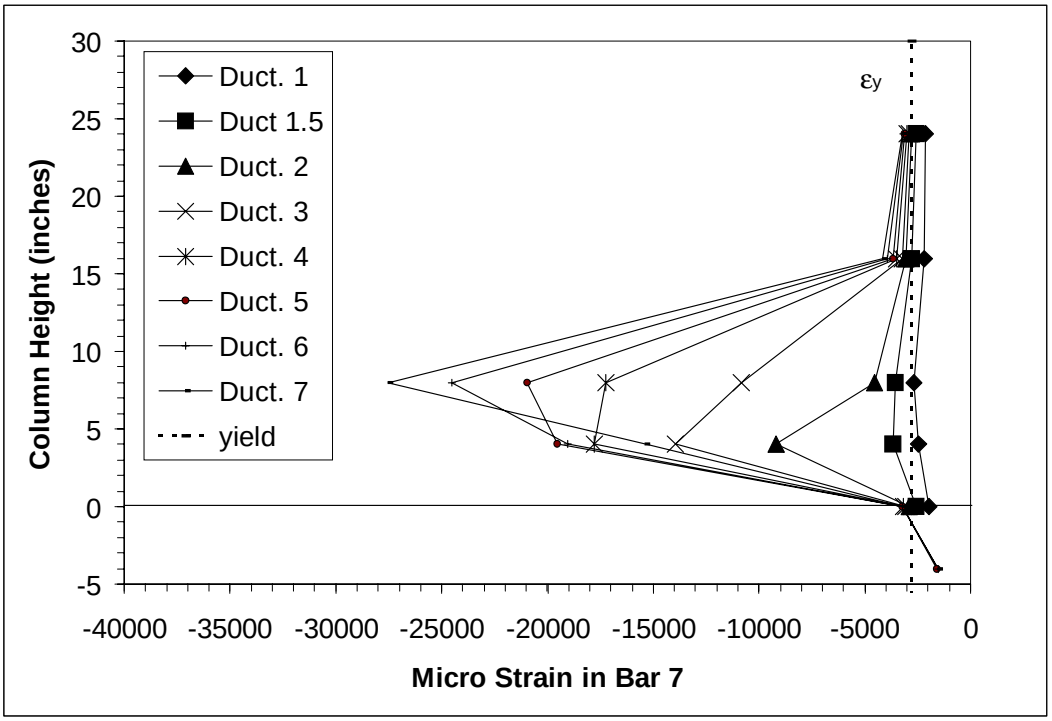

Figure 10.22 Strain Profile of the Longitudinal Steel on the South Side

The strain profiles of these figures show the strain to be highest at eight inches above the top of the footing. Buckling of the longitudinal reinforcement accrued at five

inches above the top of the footing on the south side of the column. The strain gages exceeded their capacity by the time the south bar reached a ductility of 7 in the pull direction. As far as the north side, the strain gages exceeded their capacity at a displacement ductility of 3.

With the strain gages on the transverse steel, strain profiles were generated for each side of the column. The transverse steel strain profiles for the column start at 6'' above the top of the footing and extends up the column to a height of 24''. Figure 10.23 and 10.24 display the strain profiles for each ductility level.

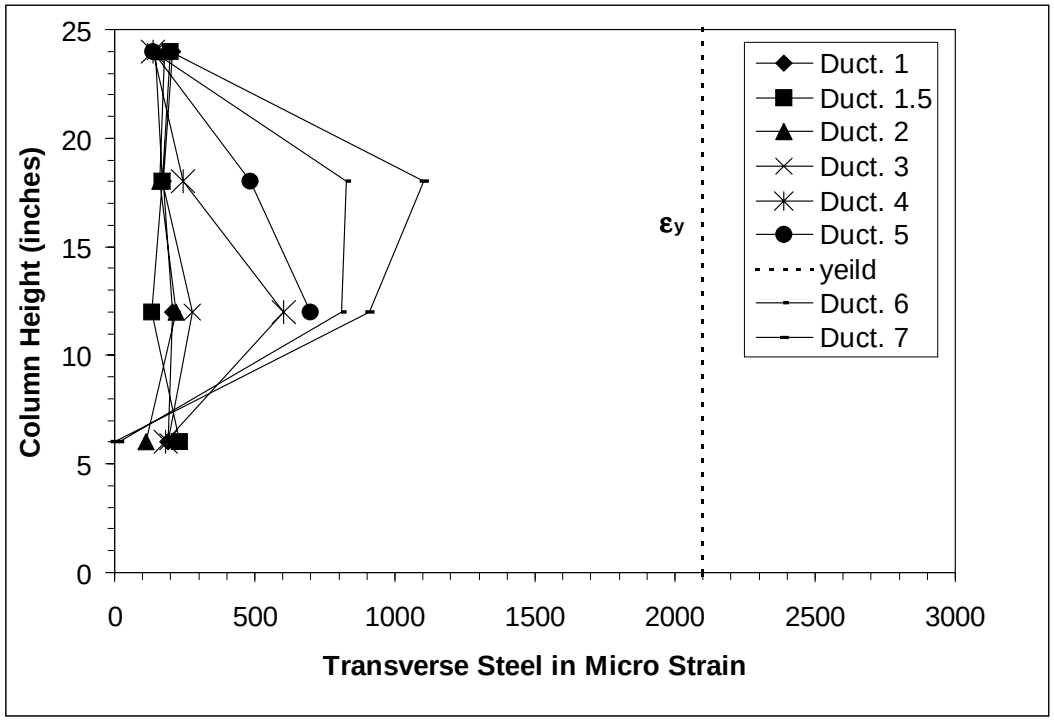

Figure 10.23 Transverse Steel Strain Profiles for the North Side

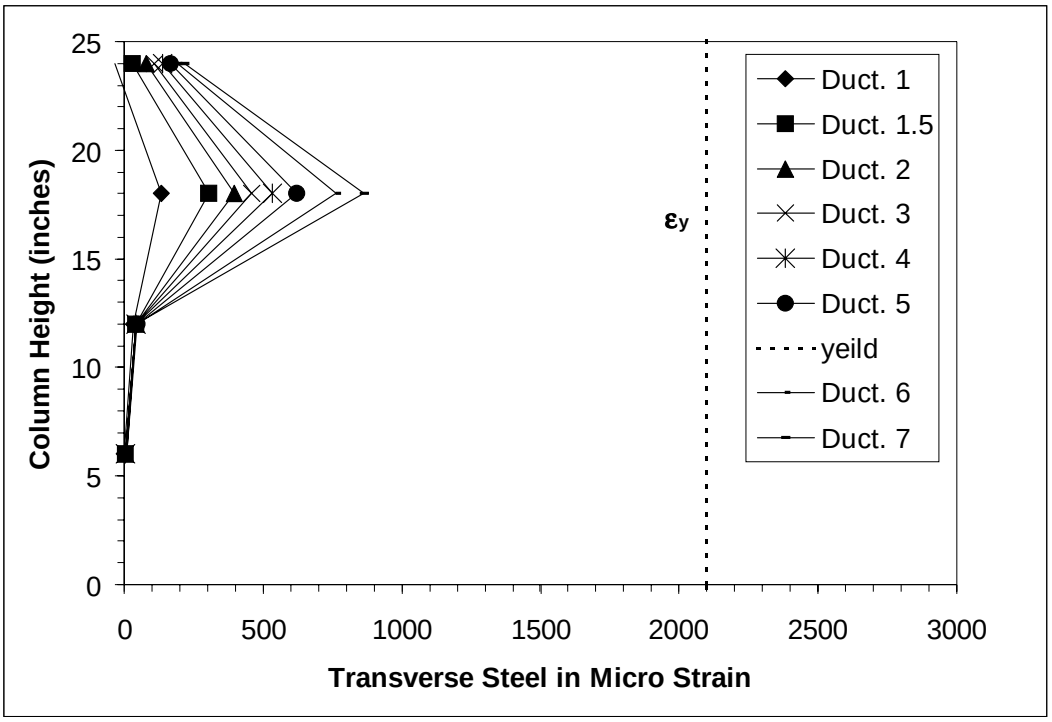

Figure 10.24 Transverse Steel Strain Profiles for the South Side

From Figures 10.23 and 10.24 it can be seen that the strain gages on the south side of the transverse steel did not work where buckling occurred. The closest strain gage on the transverse steel that was working properly was at 18 inches above the footing. The strain hysteresis of this gage is shown in Figure 10.25.

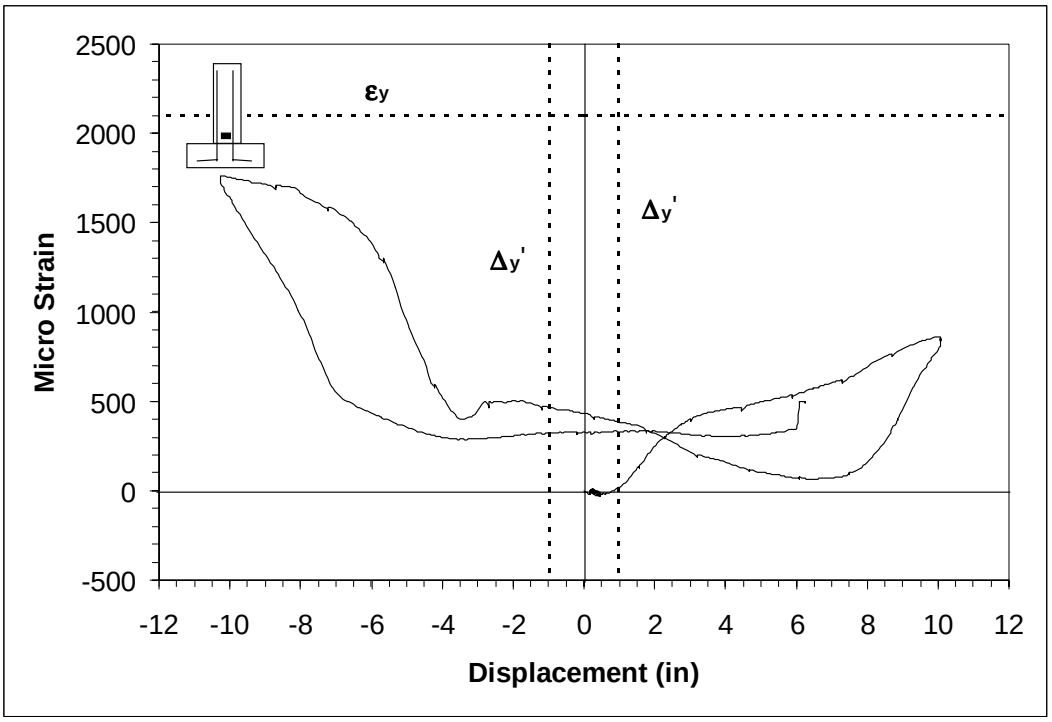

Figure 10.25 Transverse South 18 inches Strain Gage Hysteresis

Since the strain gages do not work throughout the whole test the strain at higher levels of ductility were not known. Using moment curvature analysis, the flexural tension strain in the longitudinal steel was calculated from the displacement of the column. Using the equations in chapter 8, the tension strain was calculated for key points during the test.

The maximum flexural tension strain in the push direction was 8.3%. At a ductility of 7 the extreme concrete compression strain was calculated to be 3.5%. Also note that the maximum compression strain that the extreme bar was subjected to was 2.7%.

10.5 Observations for Next Test

During the test, the north bar did not buckle as predicted. Supporting the idea that residual strain is also an important factor in predicting buckling. The south bar

experienced a maximum flexural tension strain of 8.3% and a growth strain of .4% before buckling. For the last test, the column could be loaded in the same manner but pushed to a higher displacement ductility before loading in the opposite direction.

11.0 Test Specimen 4

This chapter will discuss all the aspects involved in testing the fourth specimen. This chapter will be broken into four parts; loading of specimen, prediction of response, observations made during the test, test results, and observations.

The information gathered during the test will only be presented. Some preliminary observations and conclusions will be made but the main analysis of the data will be covered in chapter 12. Appendix A-5 contains graphs of column curvature and individual linear pot histories.

11.1 Loading of Specimen

From moment curvature analysis the first yield force and displacement have been calculated. The test specimen was loaded in force control up to yield as shown in figure 11.1. Once this point was reached the yield displacement was validated, by reading the string potentiometer, and then the equivalent yield displacement was calculated. From this point the specimen was load in increments of displacement ductility as shown in figure 11.2.

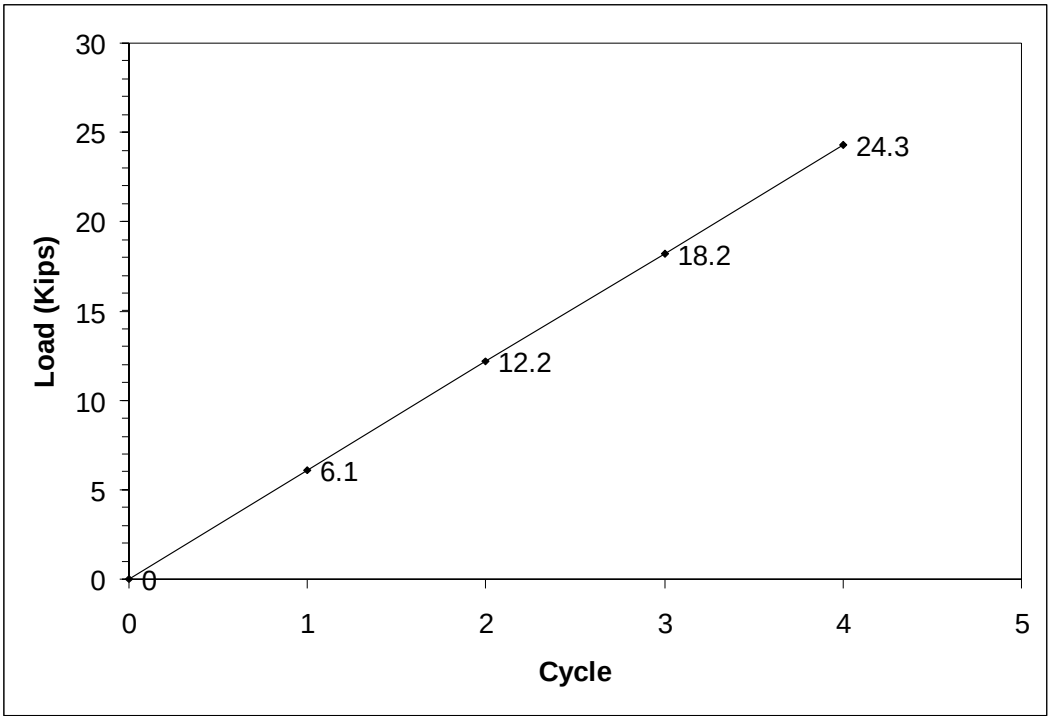

Figure 11.1 Force Control Loading of Specimen 4

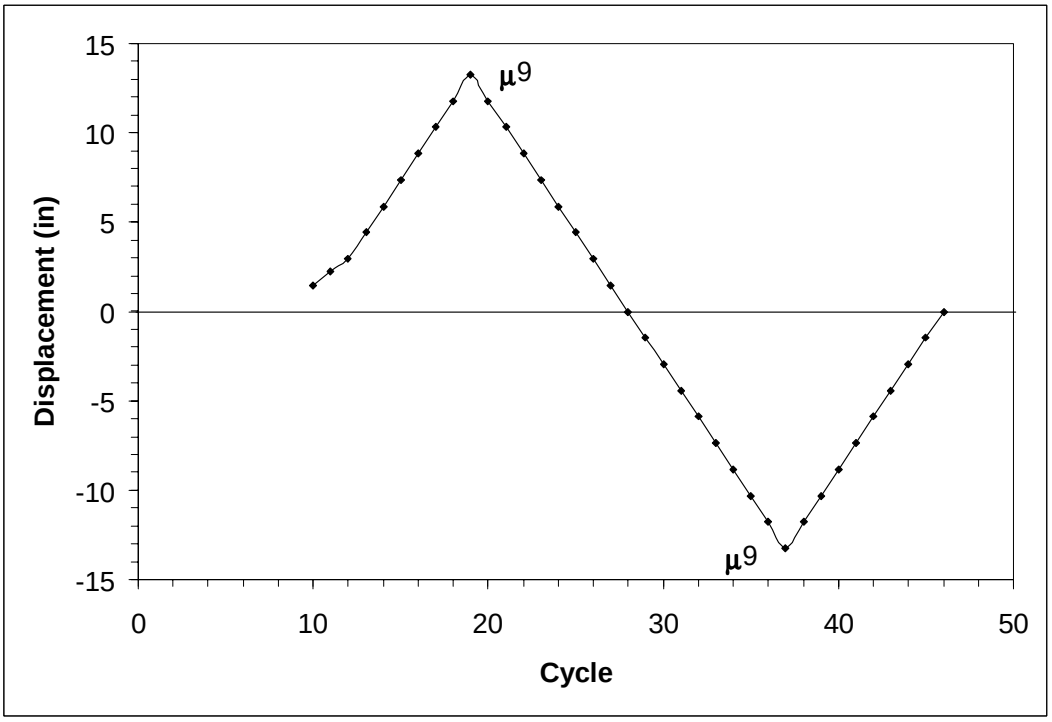

Figure 11.2 Displacement Control Loading of Specimen 4

11.2 Prediction of Response

In the test three, the column was pushed to a displacement ductility of 7 creating a peak flexural tension strain of 8.3%. The column was then loaded to a displacement ductility of 7 in the opposite direction. During the reverse loading from this direction, the south bar buckled just before the column reached a zero deflection. The total tension strain in the south reinforcement was calculated by adding the peak flexural tension strain and the growth strain the bar was exposed to. When the column was load to a displacement ductility of 7 in the pull direction, the south bar had been exposed to a total tension strain of 8.7%. For test four, the column needed to be loaded to a peak flexural tension strain greater than 8.7% in the push direction so that buckling would occur. A displacement ductility of 9 will create the needed flexural tension strain in the bar.

This column will be loaded to a displacement ductility of 9 in the push direction in one cycle. This will place the north side of the column in tension and the south side in compression. During the reversal cycle, the longitudinal steel should buckle on the north side before crack closure.

11.3 Observations During the Test

The following is a step by step account of the column response during the test. Each step will focus on cracks size and location on the column. Also things such as crushing of concrete or exposure of reinforcing steel will be discussed. The visual account will allow for a correlation between visual inspection and test results.

11.3.1 Force loading

The first cycle in force control was to 6 kips (25% of theoretical yield). No cracks were observed in the column.

The next cycle of force loading was to 12.2 kips (50% of theoretical yield). The cracks extended from the east side to the west side of the column. The x-y recorder also showed a change in column stiffness at about 7 kips on the x-y recorder.

The next cycle of force loading was to 18.2 kips (75% of theoretical yield). Cracks have formed 45'' up the column spaced at 8'' intervals. The cracks that occurred during the last cycle were extended during this cycle. Some new cracks also formed in the column.

The final force loading cycle was too theoretical yield at 24 kips. The LNP04 strain gage read 0.0028-tension strain, which is yield for the longitudinal bars indicating an agreement between analytical and experimental. The LNSP04 strain gage read 0.0017 compression strain, which is less than the yield strain. Flexural cracks have formed the full height of the column. The largest flexural crack width on the north side of the column measured 0.002'' at five inches up the column.

11.3.2 Displacement Loading

The equivalent yield displacement was determined during the first test and will be used in this test also. The equivalent yield displacement was 1.47 inches.

The first cycle in displacement control was ductility 1, which is equivalent to a displacement of 1.47 inches. Shear cracks began to form in the column. Some new flexural cracks formed in the column but mostly growth of old cracks. The largest

flexural crack width on the north side of the column increased to 0.007'' at five inches up the column.

The next displacement level on the column was to a ductility of 1.5, which is equivalent to a deflection of 2.2 inches. More shear cracks formed on the east and west faces of the column. There were also shear and flexural crack extensions. The largest flexural crack width on the north side of the column increased to 0.03'' at five inches up the column.

The next displacement level on the column was to a ductility of 2, which is equivalent to a deflection of 2.9 inches. First signs of crushing occurred on the south side of the column. There were also some extensions of old cracks. Some inclined flexural cracks also formed on the north side of the column. The largest flexural crack width on the north side of the column increased to 0.045'' at five inches up the column.

The next displacement level on the column was to a ductility of 3, which is equivalent to a deflection of 4.4 inches. More shear cracks formed on the east and west faces of the column.

The next displacement level on the column was to a ductility of 4, which is equivalent to a deflection of 5.9 inches. New shear cracks formed on the east and west faces of the column. The largest flexural crack width on the north side of the column increased to 0.125'' at five inches up the column.

The next displacement level on the column was to a ductility of 5, which is equivalent to a deflection of 7.35 inches. There were new notable changes in the column.

The next displacement level on the column was to a ductility of 6, which is equivalent to a deflection of 8.84 inches. There was further crushing of the concrete on

the south side of the column with the plastic hinge region measuring 20 inches. The largest flexural crack width on the north side of the column increased to 7/32'' located at five inches above the footing.

The next displacement level on the column was to a ductility of 7, which is equivalent to a deflection of 10.31 inches. The largest flexural crack width on the north side of the column increased to 1/4'' located at five inches above the footing. There were two longitudinal bars exposed on the south side of the column at three inches above the footing. There were no signs of buckling on the south side of the column.

The next displacement level on the column was to a ductility of 8, which is equivalent to a deflection of 11.7 inches. The largest flexural crack width on the north side of the column increased to 9/32'' located at five inches above the footing. There were still no signs of buckling on the south side of the column.

The next displacement level on the column was to a ductility of 9, which is equivalent to a deflection of 13.2 inches. The largest flexural crack width on the north side of the column increased to 5/16'' located at five inches above the footing. There were still no signs of buckling on the south side of the column. The column was then loaded in the other direction.

The next displacement level of notable consideration was to a ductility of 3 in the push direction, which is equivalent to a deflection of 4.34 inches. The cracks on the north side of the column were still open and some minor crushing has taken place. The north side longitudinal bar began to buckle.

The next displacement level of notable consideration was to a ductility of 7 in the pull direction, which is equivalent to a deflection of –10.3 inches. Further spalling

occurred in the plastic hinge region on the north side. The bars on the north side have fully buckled. The specimen was then loaded back to zero displacement.

As the column reaches zero displacement, the longitudinal bars on the south side of the column began to buckle. Three of the outer most bars on the south side buckled between the 2 and 3 spiral.

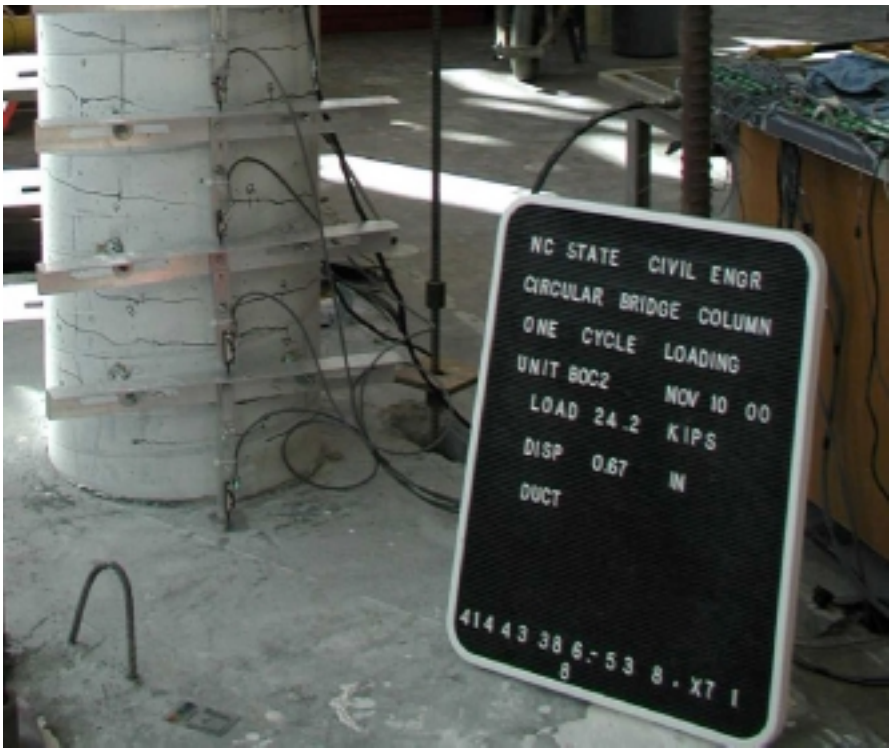

Figure 11.3 North Side of Specimen at Yield

Figure 11.4 North Side of Specimen at Ductility 1

Figure 11.5 North Side of Specimen at Ductility 1.5

Figure 11.6 North Side of Specimen at Ductility 2

Figure 11.7 South Side of Specimen at Ductility 3

Figure 11.8 South Side of Specimen at Ductility 4

Figure 11.9 North Side of Specimen at Ductility 5

Figure 11.10 South Side of Specimen at Ductility 6


Figure 11.11 North Side of Specimen at Ductility 7

Figure 11.12 South Side of Specimen at Ductility 8

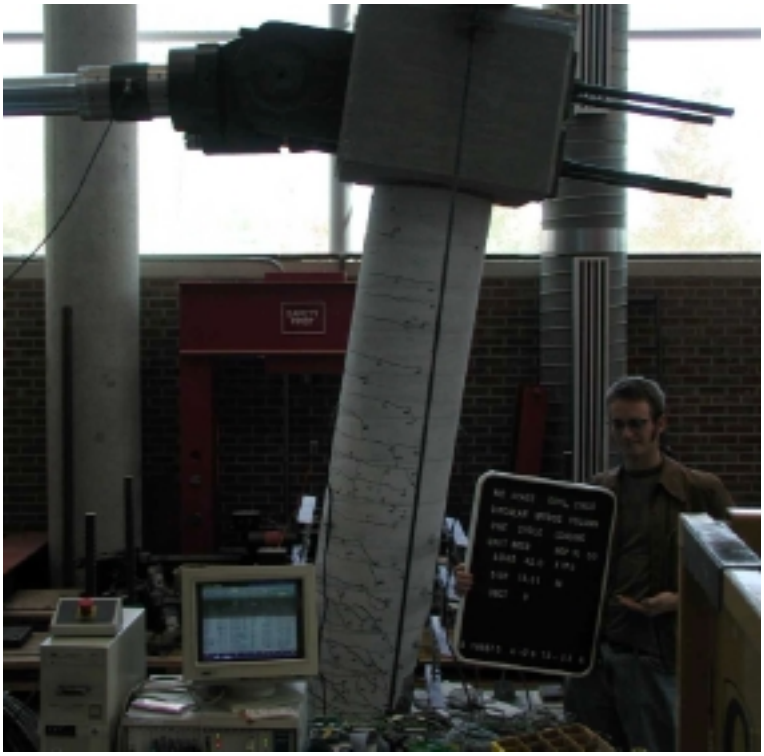
Figure 11.13 West Side of Specimen at Ductility 9

Figure 11.14 North Side of Specimen at 2.9 inches

Figure 11.15 North Side of Specimen Buckling


Figure 11.16 North Side of Specimen at Failure

11.4 Test Results

With the data obtained from the gages on or in the specimen, values can be associated with the observed response of the section. Figure 11.17 shows the force versus displacement response of the specimen also plotted on the same graph is the first yield force, ultimate force, and first yield displacement along with the response from moment curvature analysis. The response curve takes into account the P-Δ moment due to the axial load. Buckling began to occur in the bar at the location marked by X on the force versus displacement response curve.

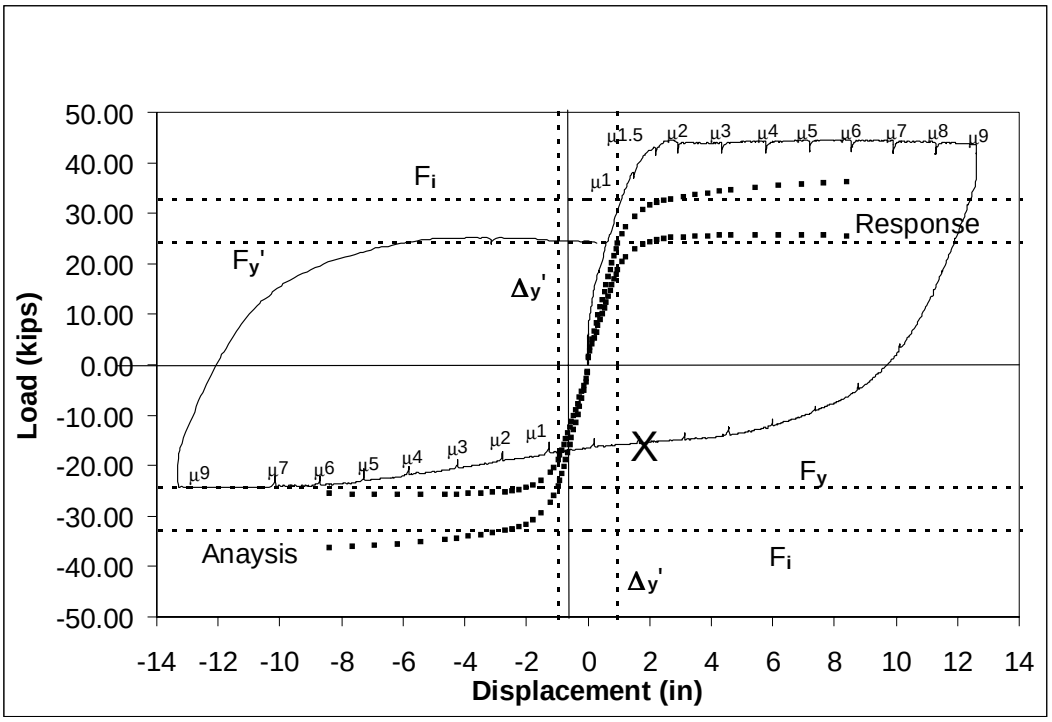

Figure 11.17 Force versus Displacement Response for Specimen 4

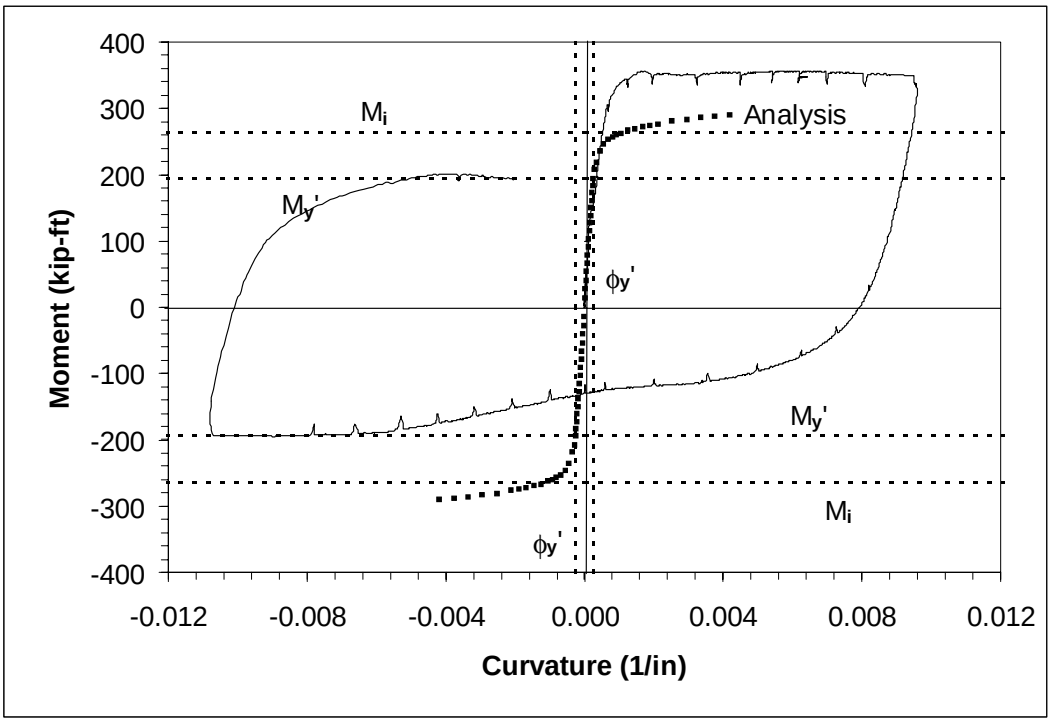

Figure 11.18 Moment versus Curvature for Specimen 4

The moment curvature graph was generated by multiplying the applied force by the column height and plotting the results against the curvature calculated at the bottom

gage length of the column, which has the largest curvature. The other three gage lengths also were used to measure the curvature of the column. Figure 11.19 shows the curvature profile of the column with the curvature being assumed linear after a column height of 28 inches. Using the equations in chapter 6, the ultimate deflection of the column can also be calculated from the curvature.

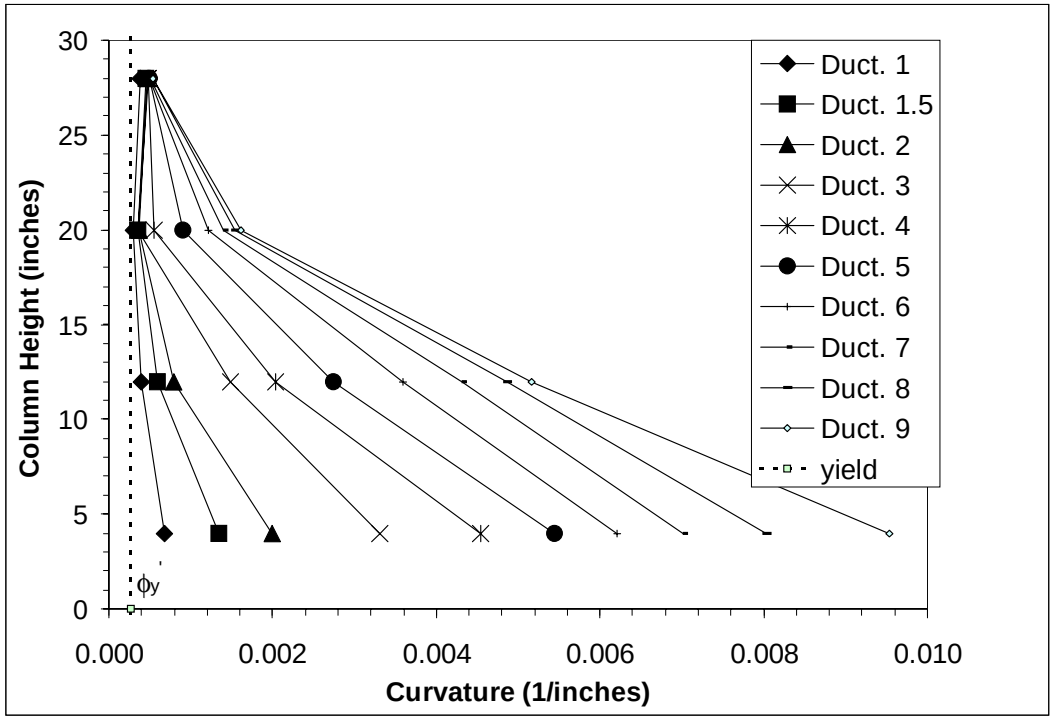

Figure 11.19 Curvature Profile of the Column at Different Levels of Ductility

The strain gages on the north and south sides of the column provide a profile of the strain in the longitudinal steel. The strain profile starts at four inches below the footing and extends 24 inches above the footing. At high levels of ductility some strain gages exceeded their capacity, this data is included in the figures shown below. A discussion will be given on the validity of these gage readings.

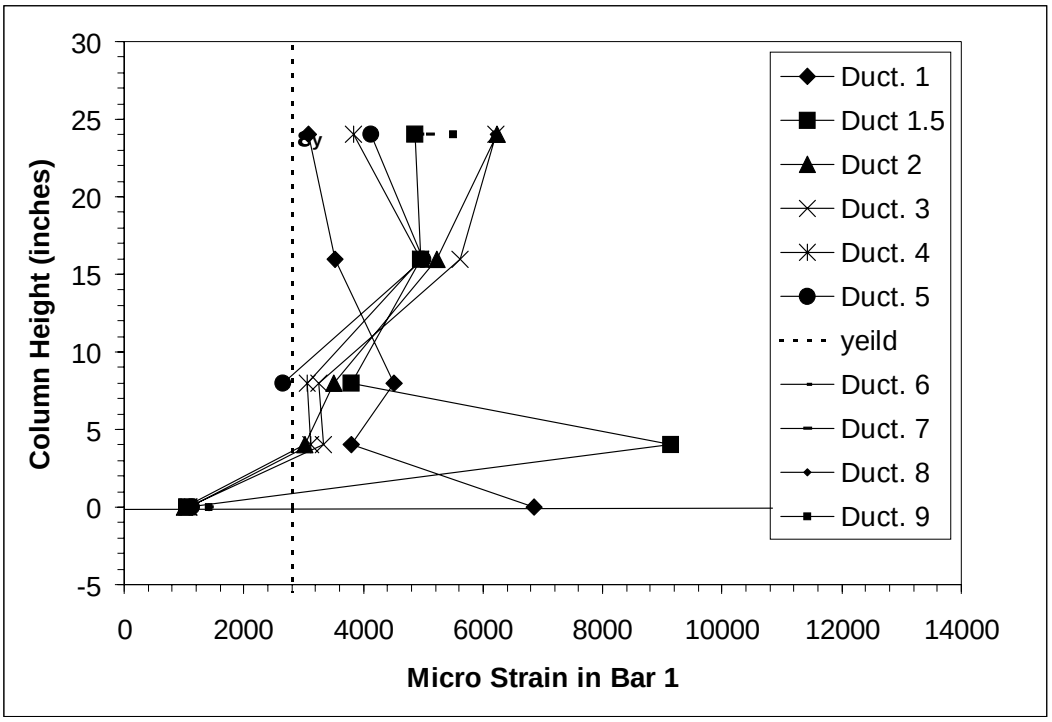

Figure 11.20 Strain Profile of the Longitudinal Steel on the North Side

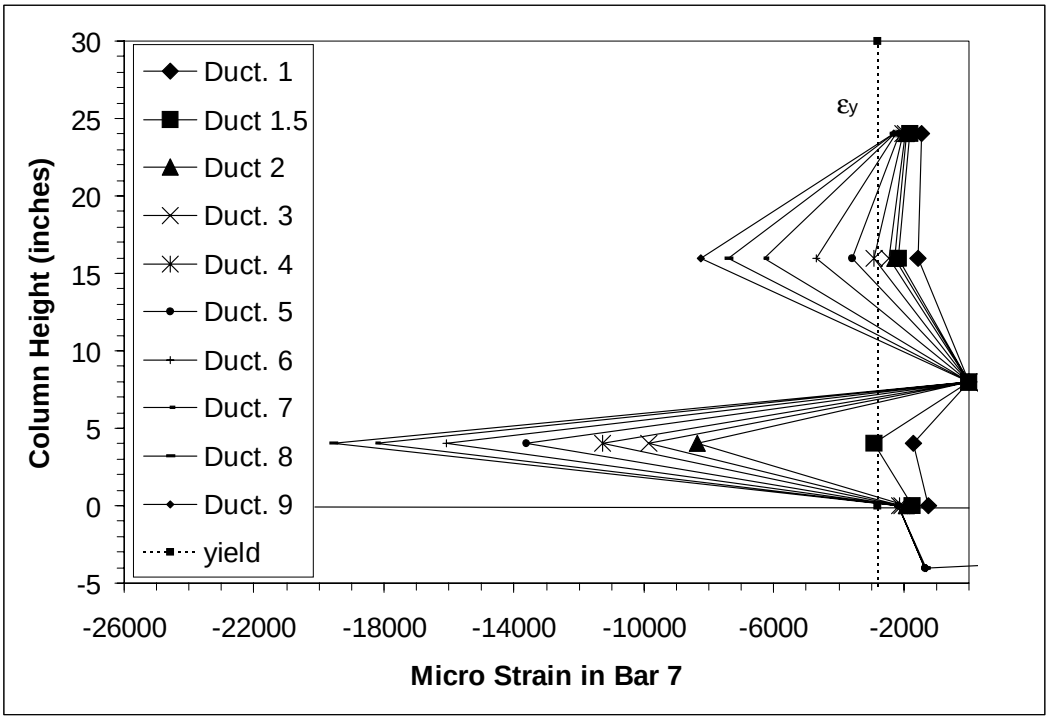

Figure 11.21 Strain Profile of the Longitudinal Steel on the South Side

The strain profiles of these graphs show the strain to be highest at four inches above the top of the footing. Buckling of the longitudinal reinforcement accrued at five

inches above the top of the footing on the north side of the column. The north side strain gage at 4 inches above the footing exceeded its capacity at a displacement ductility of 1.5 on the south side the strain gage in the same location worked until a displacement ductility of 9. The south gage did not last long after the south side of the column was placed into tension. Since the strain gage on the north side of the column did not last long, there is no real significant strain hysteresis to show

With the strain gages on the transverse steel, strain profiles were generated for each side of the column. The transverse steel strain profiles for the column start at 6'' above the top of the footing and extends up the column to a height of 24''. Figure 11.22 and 11.23 display the strain profiles for each ductility level.

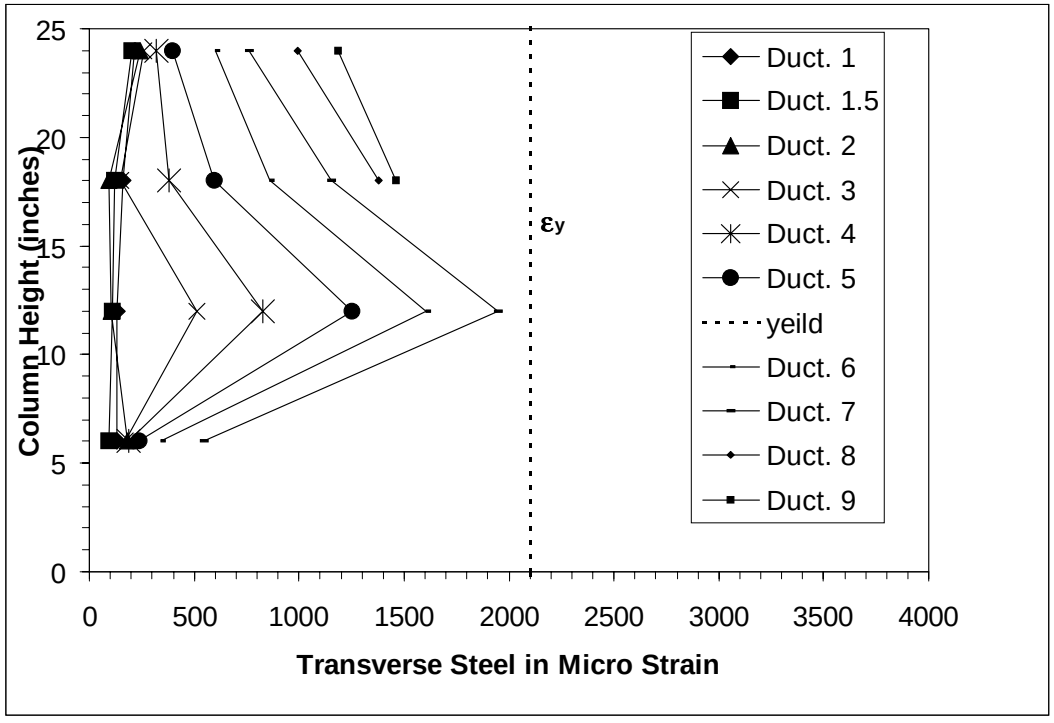

Figure 11.22 Transverse Steel Strain Profiles for the North Side

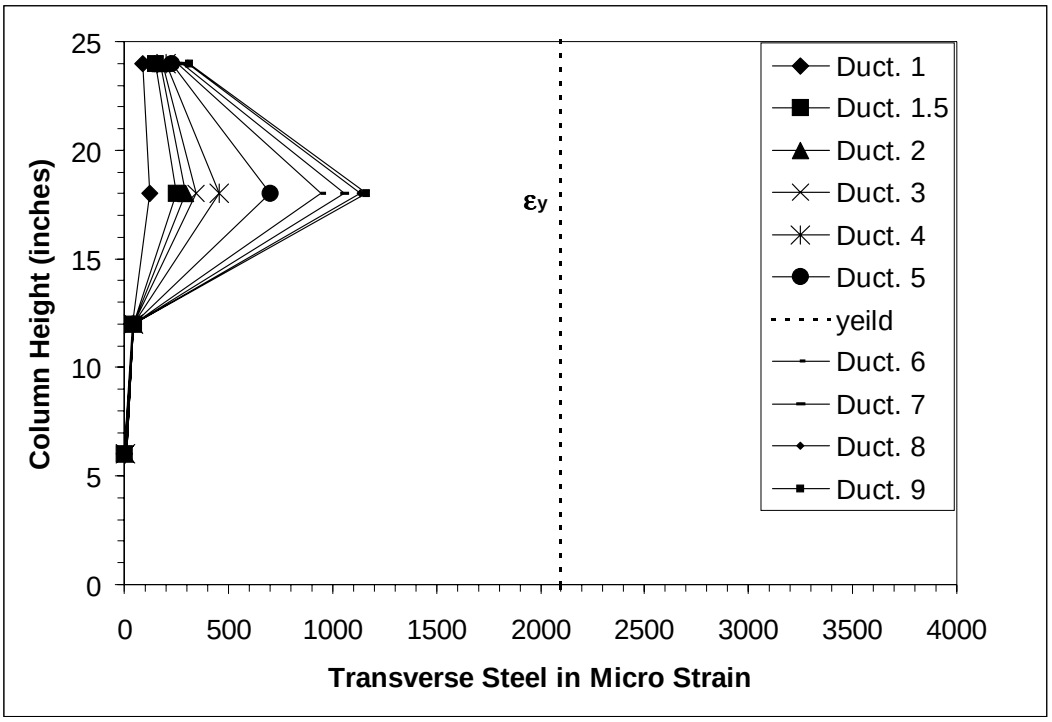

Figure 11.23 Transverse Steel Strain Profiles for the South Side

From Figures 11.22 and 11.23 it can be seen that the strain in the transverse steel was highest at 12 inches above the footing. This is expected due to the fact that the longitudinal bar was trying to push outwards and the transverse steel was resisting this motion. The strain gage at six inches above the footing exceeded its capacity early in the test. The figure below shows the strain hysteresis for the transverse strain gage 12 inches above the footing.

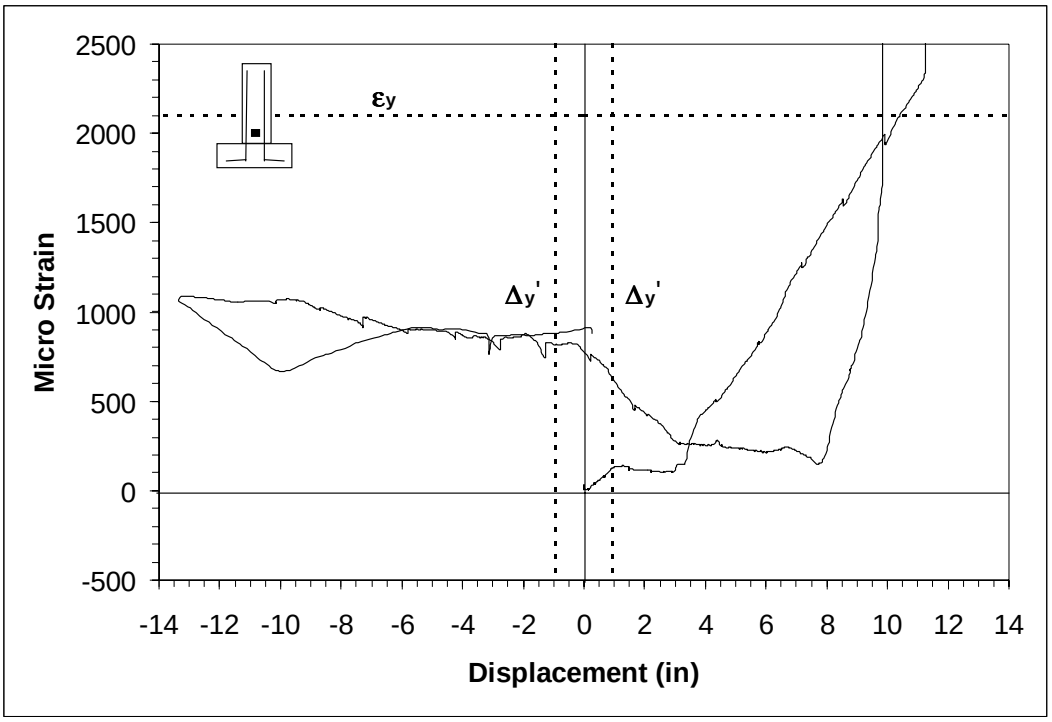

Figure 11.24 Transverse North at 12 inches Strain Gage Hysteresis

Since the strain gages do not work throughout the whole test the strain at higher levels of ductility were not known. Using moment curvature analysis, the tension strain in the longitudinal steel was calculated from the displacement of the column. Using equations 8.9 through 8.14, the maximum tension and compression strains were calculated for key points.

At a displacement ductility of 9, the flexural steel tension strain in the push direction was 10.8% and the extreme steel compression strain was 3.5%. Also note that the maximum concrete compression strain was 4.5%.

11.5 Observations

The column did perform as predicted early in this chapter. The cracks on the north side of the column were still open when buckling started to occur on the north side

of the column. Buckling did occur rather early during the reverse cycle at a displacement of 4.43 inches in the push direction.

12.0 Analysis of Test Data

This chapter will focus on the analysis of the test data. Each test specimen will be evaluated separately at first, then a correlation will be drawn among all of the specimens. With the information gathered from the test specimens a method of analysis will be presented. A characteristic compression strain will be found for the columns tested in this report. The characteristic compression strain is a function of the axial load ratio and transverse steel ratio. By knowing the characteristic compression strain of a column, the ultimate deflection of the column can be determined using the procedure described in this chapter.

It is useful to be able to analyze a column that is already in use but it is also useful to design a column for a target displacement and know that the longitudinal reinforcement in the column will not buckle before the column reaches the target displacement. A method to design a column to reach a target displacement without buckling of reinforcement will be presented. The axial load ratio will be given and transverse steel ratio will be determined based on the required characteristic compression strain needed to reach the target displacement.

12.1 Analysis of Each Test Specimen

The analysis of the test specimens begins with test specimen 2. From this specimen, the importance of tension strain on buckling was presented. Test specimens 3 and 4 will give some insight on the characteristic compression strain of these test columns. All the information gathered from these three test will be put together to

explain the results of test specimen 1. The table below shows the peak flexural tension strain, compression strain, and growth strain for all of the columns tested.

Table 12.1 Strains in Percent Based on Deflection

Column	North Side		South Side		Growth Strain North	Growth Strain South
	ε_s	ε_s'	ε_s	ε_s'	ε_{gr}	ε_{gr}
Specimen 1	4.5	1.5	4.5	1.5	2.1	1.9
Specimen 2	8.3	0.2	0.2	2.7	3.2	1.8
Specimen 3	8.3	2.7	8.3	2.7	N/A	0.4
Specimen 4	10.8			3.5	N/A	N/A

Table 12.2 Strains in Percent Based on Curvature

Column	Curvature	North Side		South Side		Growth Strain North	Growth Strain South
	Φ_u	ε_s	ε_s'	ε_s	ε_s'	ε_{gr}	ε_{gr}
Specimen 1	0.004779	5.68	1.85	5.68	1.85	2.1	1.9
Specimen 2	0.009453	11.23	3.66	0.2	3.66	3.2	1.8
Specimen 3	0.008745	10.38	3.39	10.38	3.39	N/A	0.4
Specimen 4	0.009534	11.32			3.69	N/A	N/A

Test 2 was conducted by loading one side of the column cyclically while only placing the other side of the column in yield tension. The reinforcement buckled on the north side of the column, this side of the column was exposed to a rather small compression strains and large tension strains.

The peak flexural tension strain that the north side of the column was subjected to was 8.3% before buckling under a compression strain of .2%. From this test it was shown that if a bar is tensioned far enough then it takes very little compression strain to buckle the bar. Buckling occurred because the modulus of the bar at the location of maximum strain had been reduced to zero.

Test specimens 3 and 4 were attempts to determine the characteristic compression strain of the column experimentally. For test specimen 3 the column was loaded in one cycle to a displacement ductility of 7 in the push direction. Then during the reverse cycle

the column reinforcement should have buckled on the north side before crack closure. The longitudinal steel did not buckle during the reverse loading to a displacement ductility of 7 in the pull direction. The column was then reload to a displacement ductility of 7 in the push direction. As the column reached zero deflection the longitudinal steel on the south side of the column buckled. The south bar had experienced a peak flexural tension strain of 8.3% before the bar buckled and a growth strain of .4%. The bar on the south side of the column experienced an 8.7% total tension strain before failure. For the fourth specimen the column was loaded to a displacement that created a strain greater than 8.7% in the tension steel.

Test specimen 4 was load to displacement ductility of 9 in one cycle that created a flexural tension strain of 10.8% on the north side of the column. During the reverse cycle the column reinforcement buckled at a displacement of 2.8 inches. This information along with test 3, shows that the characteristic compression strain for these test specimens to be greater than 8.7% but less than 10.8%. This characteristic compression strain defined here is only valid for columns tested in this project.

A range for the characteristic compression strain that has been determined by specimens 3 and 4 can be accounted for by two components. These components are peak tension strain and growth strain of a specimen. The peak flexural tension strain is the maximum flexural tension strain induced in the bar before it buckles in compression. The peak growth strain is the maximum growth strain of the column before the onset of buckling. The equation below illustrates how these strains are used to determine the characteristic compression strain capacity for the specimen. Note that equation 12.1

represents the criteria for buckling, namely, when the total applied tension strain (ε_{stt}) equal the characteristic compression strain (ε_{sch}), buckling is expected to occur.

$$\varepsilon_{stt} = \varepsilon_{sch} = \varepsilon_{stp} + \varepsilon_{sgr} \qquad (Eq.12.1)$$

ε_{sch} = Characteristic Compression Strain Capacity
ε_{stp} = Peak Flexural Tension Strain
ε_{sgr} = Growth Strain
ε_{stt} = Total Steel Tension Strain

The peak flexural tension strain is calculated using equation 4.11 from chapter 4. The peak growth strain can be calculated from the growth of the linear pots divided by the gage length. The peak growth strain can also be determined by conducting a fiber model or cyclic section analysis of the column.

12.2 Method of Analysis for an Existing Column

For columns that have already been design it is important to be able to evaluate the ultimate deflection before buckling. The procedure below will allow for the evaluation of any circular column given the material properties, axial load ratio, and corresponding characteristic compression strain. First perform moment curvature analysis of the column to determine the neutral axis depth (c) and equivalent yield curvature (ϕ_y).

$$\varepsilon_{sch} - \varepsilon_{sgr} = \varepsilon_{stp} \qquad (Eq.12.2)$$

$$\varepsilon_{sch} - \varepsilon_{sgr} = \phi_u (d - c) \qquad (Eq.12.3)$$

$$\phi_p = \phi_u - \phi_y \qquad (Eq.12.4)$$

$$\Delta_p = \phi_p \left(L_p\right) L_{eff} \qquad (Eq.12.5)$$

$$\Delta_y = \frac{\phi_y \left(L_{eff}\right)^2}{3} \qquad \textit{Single Bending} \qquad (Eq.12.6)$$

$$\Delta_u = \Delta_y + \Delta_p \qquad (Eq.12.7)$$

Equation 12.1 is solved for the peak flexural tension stain, producing equation 12.2. Taking equation 12.2 and substituting equations 4.11 to form equation 12.3 starts the procedure. The ultimate curvature (ϕ_u) can then be calculated from equation 12.3. Using equation 12.4 the plastic rotation (ϕ_p) can be calculated. The plastic deflection (Δ_p) and yield deflection (Δ_y) can be calculated using equations 12.5 and 12.6. Equation 12.7 determines the maximum deflection of the column at buckling.

12.3 Circular Column Design Process

The following is a procedure that allows a designer to design a column for a target displacement and ensure that buckling does not occur before this displacement is reached. To start the process the designer must assume or determine the following: longitudinal bar diameter, column diameter, longitudinal steel ratio, and target displacement.

$$\phi_y = \frac{2.45\left(\frac{f_y}{E}\right)}{Col.Dia.} \qquad (Eq.12.8)$$

$$L_{eff} = L_{col} + 0.044\left(f_y\right) dbl \qquad (Eq.12.9)$$

$$\Delta_y = \frac{\phi_y \left(L_{eff}\right)^2}{3} \qquad (Eq.12.10)$$

$$\Delta_p = \Delta_u - \Delta_y \qquad (Eq.12.11)$$

$$\phi_p = \frac{\Delta_p}{L_{col}(L_p)} \qquad (Eq.12.12)$$

$$\phi_u = \phi_p + \phi_y \qquad (Eq.12.13)$$

$$K = \phi_u(D) \qquad (Eq.12.14)$$

$$c = \frac{\in_c}{\phi_u} \qquad (Eq.12.15)$$

$$\varepsilon_{sch} - \varepsilon_{sgr} = \phi_u(d - c) \qquad (Eq.12.16)$$

Once the designer has chosen the parameters described in the previous paragraph the equivalent yield curvature (ϕ_y), equivalent yield displacement (Δ_y) and the plastic displacement (Δ_p) can be calculated. Equation 12.8 is used to approximate the yield curvature of a circular column. With the plastic displacement known, the plastic curvature (ϕ_p) can be calculated and then combined with the equivalent yield curvature (ϕ_y) to find the ultimate curvature (ϕ_u). The variable K can be calculate using equation 12.14 then using K with the figures 12.1 to 12.4 that corresponds with the appropriate longitudinal steel ratio the maximum concrete strain can be found (9). Using equation 12.15 the neutral axis depth (c) of the column can be found. All of this information is substituted into equation 12.16 and, as long as the sum of the peak flexural tension strain and growth strain is less than the characteristic compression strain, the column reinforcement will not buckle at the target deflection. If the required characteristic

compression strain exceeds what is practically attainable with regards to transverse reinforcement, then the target displacement or column diameter must be adjusted and the process repeated. Recall that the characteristic compression strain is a function of the transverse steel ratio and axial load ratio.

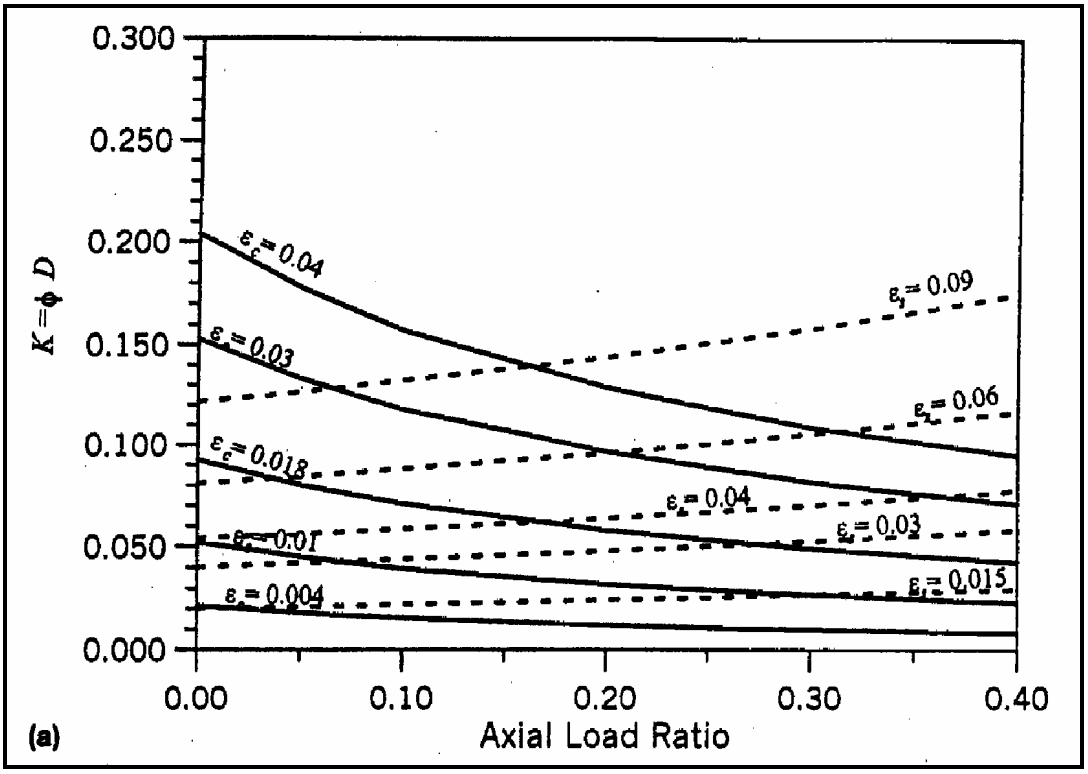

Figure 12.1 Longitudinal Steel Ratio 1% (9)

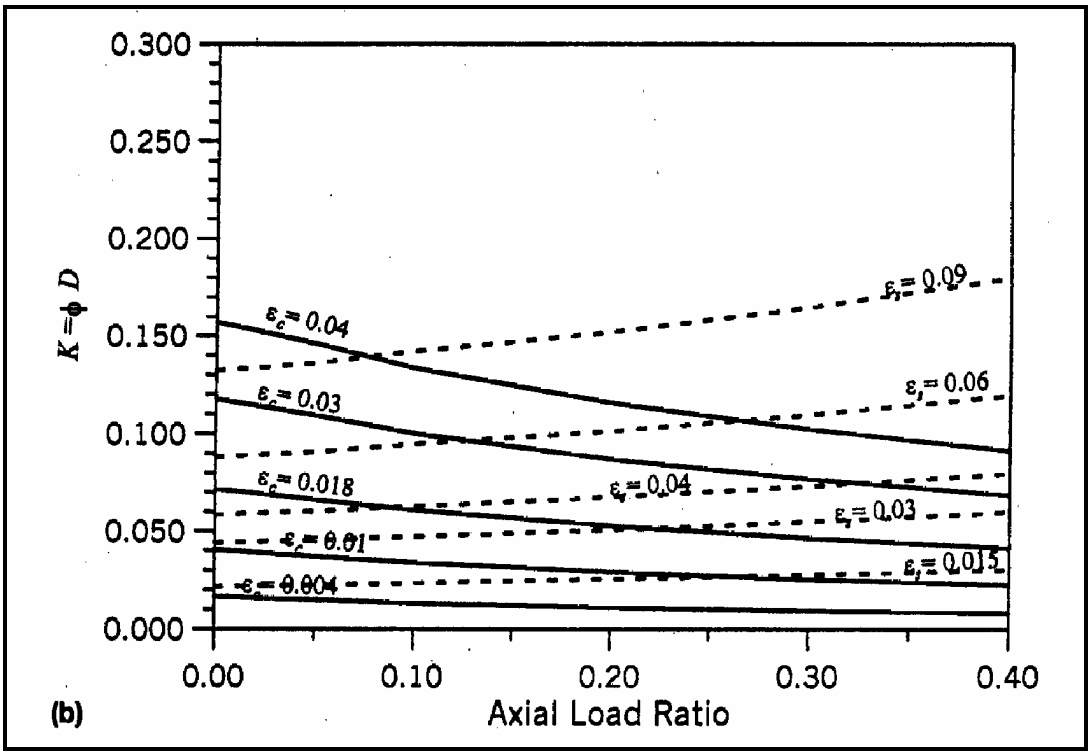

Figure 12.2 Longitudinal Steel Ratio 2% (9)

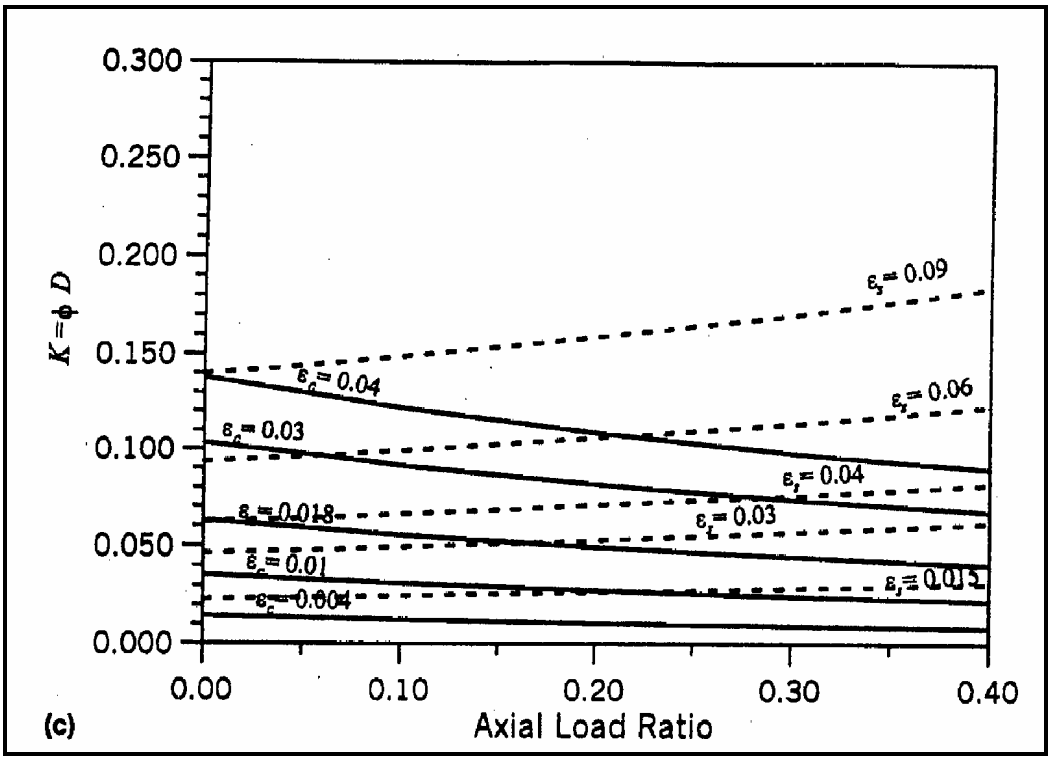

Figure 12.3 Longitudinal Steel Ratio 3% (9)

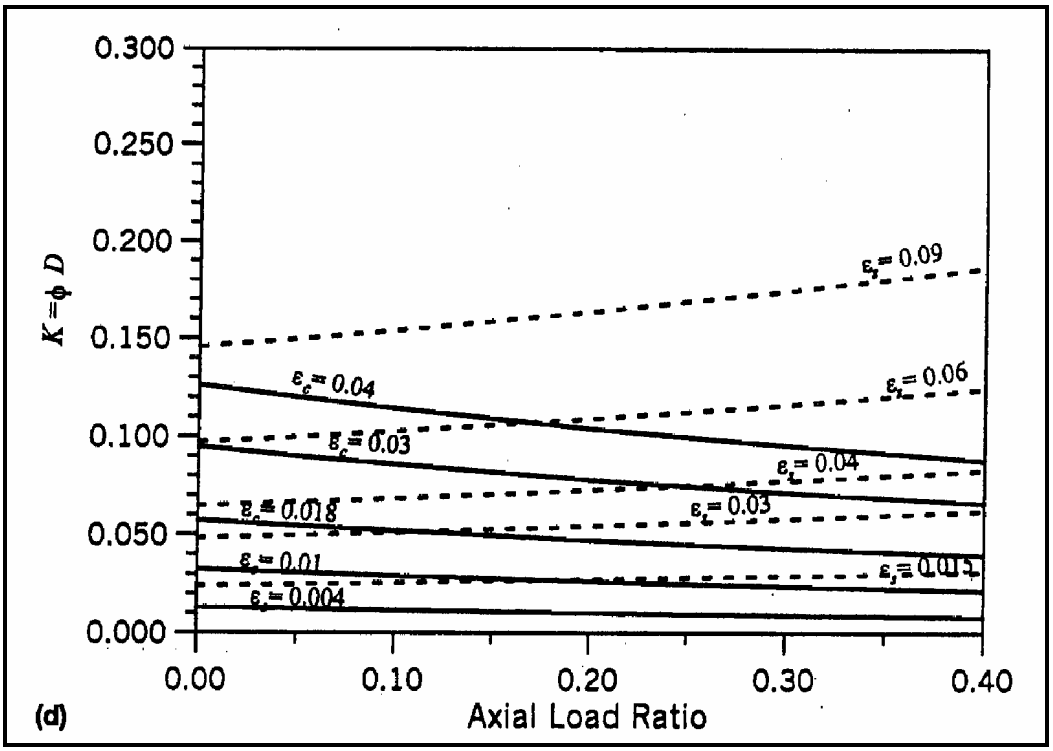

Figure 12.4 Longitudinal Steel Ratio 4% (9)

This report has proposed a procedure to design or evaluate the maximum displacement of a circular column before buckling of reinforcement. For the columns tested during this project a characteristic strain has been determined to be greater than 8.7% but less than 10.8%. The axial load and transverse steel ratio will effect the characteristic compression strain of the column. The database in chapter 4 consists of columns with different axial load ratio and transverse steel ratios in which the peak flexural tension strains have been calculated. The database is far from complete but trends show that an increase in axial load ratio decreases the characteristic compression strain. An increase in the transverse steel ratio will increase the characteristic compression strain.

13.0 Conclusions

Presented in this report are the results of a series of tests aimed at identifying the importance of tension strain on buckling of reinforcement in reinforced concrete columns. In the course of the study, it was identified that the propensity for buckling was tied directly to peak steel tension strain. The peak steel tension strain was shown to be comprised of two components: one due to flexure, and one due to column growth.

Calculation of flexural tension strain is straight forward, however evaluation of the growth strain is not and is a function of loading history and column details.

It is also noted that the compression strain capacity, for which there are several models, is an important variable. Future research must be focused on these aspects: 1) evaluation of growth strain, 2) evaluation of compression strain capacity.

13.1 Review of Proposed Model

As discussed in the previous chapter, the proposed buckling mechanism aims to identify the total steel tension strain that the reinforcing bars can be subjected to in a reinforced concrete column before buckling during the reverse cycle. This total steel tension strain, which was identified as ε_{stt}, was shown to be comprised of two components: one due to flexural tension strain ε_{stp}, and one due to "growth" or "residual" strain at zero column displacement ε_{sgr}, which is of course a function of the loading history. It was then postulated that reinforcing bars in reinforced concrete columns would not buckle during the reverse cycle as long as the total steel tension strain did not exceed the characteristic compression strain capacity ε_{scc} of the reinforcing bars.

The value of this mechanism was then illustrated in an assessment and a design approach. In the assessment approach, the steps are as follows.

1. Given the column geometry and reinforcing bar details, evaluate the characteristic compression strain capacity, ε_{scc} using existing double modulus models.
2. Equate the characteristic compression strain capacity to the total steel tension strain.
3. Determine the column growth based on a prescribed loading history.
4. Solve for the allowable flexural tension strain as shown in equation 13.1.
5. Utilize ε_{stp} to calculate the allowable maximum column displacement.

For the design approach, the steps are as follows.

1. Select a target displacement.
2. Evaluate the flexural tension strain based on the chosen target displacement.
3. Evaluate the column growth strain.
4. Evaluate the required total steel tension strain capacity.
5. Determine the required characteristic compression strain capacity by equating it to the required steel tension strain capacity.
6. Detail the tension reinforcement to sustain the required characteristic compression strain capacity.

$$\varepsilon_{stp} = \varepsilon_{scc} - \varepsilon_{sgr} \qquad (Eq.13.1)$$

In order to implement the above procedures, two aspects will require further investigation, namely: assessment of existing models for characteristic compression strain

capacity, and development of an analytical model for evaluation of the growth strain. Future work must concentrate on each of these areas. The subsequent sections will briefly describe how this may be approached.

13.2 Future Studies on Growth Strain

Before discussing future analytical studies on growth strain, a review of data obtained in this study is appropriate. Figures 13.1 and 13.2 represent the experimentally measured growth strain at zero column displacement verses column displacement ductility. For example, referring to figure 13.1, after cycling test unit one to μ_Δ=4, the residual strain upon return to zero displacement was approximately 1.9%. Although these graphs are specific to the loading history and test unit discussed in this report, the results are promising. As might be imagined, the goal of future analytical studies should be to develop a family of such curves for use in assessment design. This can only be accomplished through an extensive parametric study using cyclic section analysis where appropriate steel and concrete, and cyclic constitutive models are employed. Stress versus strain curves such as that proposed by Dodd look promising to achieve this objective.

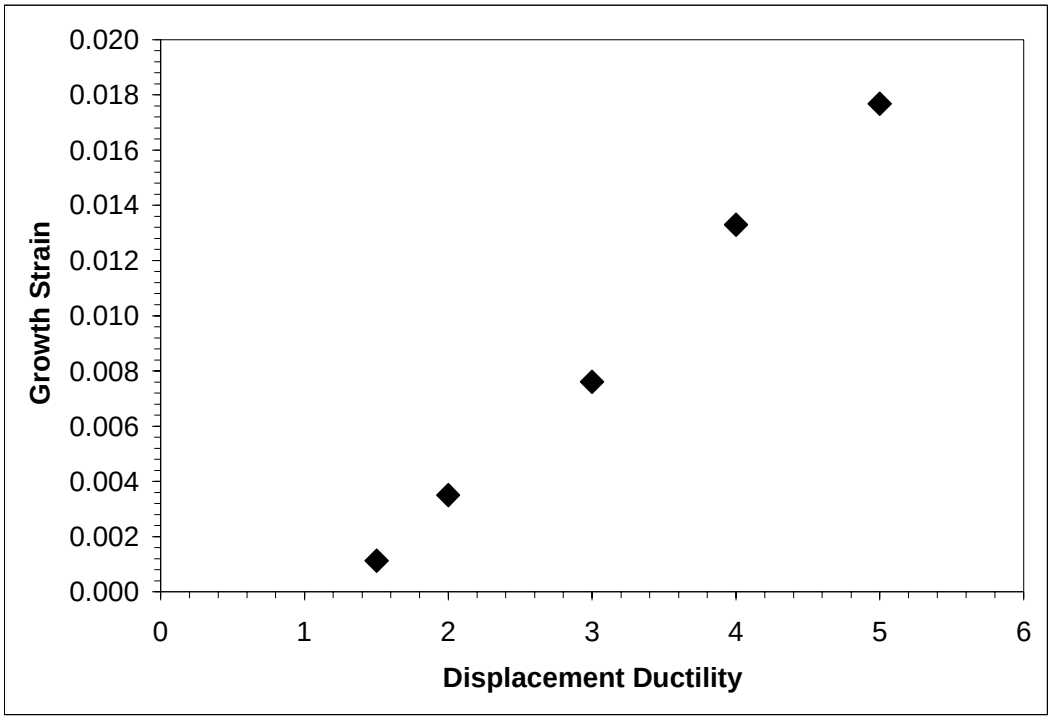

Figure 13.1 Growth Strain for Test Specimen 1

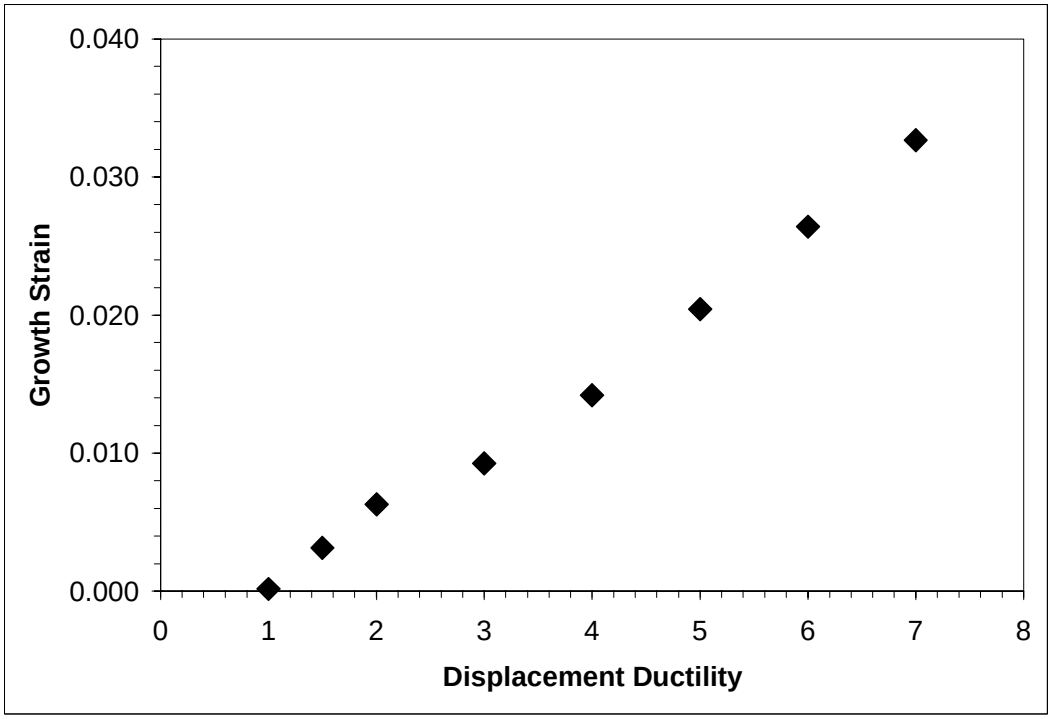

Figure 13.2 Growth Strain for Test Specimen 2

13.3 Future Studies on Characteristic Compression Strain

There has been extensive past research on models to predict the characteristic compression strain capacity, such as the double modulus approach. As part of the next phase of this research, such models will be reviewed to determine the most promising to be used in conjunction with the mechanism proposed in this research.

REFERENCES

1. Ang Beng Ghee, Priestley, M.J.N. and Paulay, T., *Seismic Shear Strength of Circular Bridge Piers*, Report 85-5, Department if Civil Engineering, University of Canterbury, Christchurch, New Zealand, July 1985.

2. Ang Beng Ghee, Priestley, M.J.N. and Park, R., *Ductility of Reinforced Concrete Bridge Piers Under Seismic Loading*, Report 81-3, Department if Civil Engineering, University of Canterbury, Christchurch, New Zealand, February 1981, 113 pages.

3. Chai, Y.H.; and Elayer, D.T., *Lateral Stability of Reinforced Concrete Columns Under Axial Reversed Cyclic Tension and Compression*, Department of Civil and Environmental Engineering U.C. Davis.

4. Dodd, L. L. and Restrepo-Posada, J.I., *Model for Predicting Cyclic Behavior of Reinforcing Steel,* ASCE Journal of Structural Engineering, Vol. 121, No. 3, March 1995.

5. Cheok, G.S.; and Stone, William C., *Behavior of 1/6-Scale Model Bridge Columns Subjected to Cyclic Inelastic Loading*, NBSIR 86-3494, Center for Building Technology, National Engineering Laboratory, National Institute of Standards and Technology, Gaithersburg, Maryland, 20899, November 1986, 291 pages.

6. Hose, Yael D.; Frieder Seible; M.J.N. Priestley; *Strategic Relocation of Plastic Hinges in Bridge Columns*, University of California at San Diego, September 1997, 195 pages.

7. King, D.J., Priestley, M.J.N., and Park, R. (1986). "Computer Programs for Concrete Column Design.*"*, *Research Report 86/12*, Department of Civil Engineering, University of Canterbury, New Zealand.

8. Kowalsky, Mervyn J.; and Priestley, M.J.N.; *Direct Displacement-Based Design of Multi-Span Reinforced Concrete Bridges,* University of California, San Diego, 1997.

9. Kowalsky, Mervyn J., *Deformation Limit States for Circular RC Bridge Columns*, ASCE Journal of Structural Engineering, August 2000 pages 869-878.

10. Kunnath, Sashi K.; El-Bahy, Ashraf; Stone, William C.; and Taylor, Andrew W., *Cumulative Seismic Damage of Circular Bridge Columns: Benchmark and Low-Cycle Fatigue Tests*, ACI Structural Journal, V. 96, No. 4, July-August 1999, pages 633-641.

11. Lehman, D.E.; Calderone, A.J.; and Moehle, J.P., *Behavior and Design of Slender Columns Subjected to Lateral Loading*, University of California, Berkeley, Department of Civil Engineering.

12. Mander, J.B., Priestley, M.J.N., and Park, R. (1988). "Theoretical Stress-Strain Model for Confined Concrete." *Journal of the Structural Division, ASCE*, 114(8), 1804-1825.

13. Papia, Maurizio and Russo, Gaetano, *Compressive Concrete Strain at Buckling of Longitudinal Reinforcement*, ASCE Journal of Structural Engineering, Vol. 115, No. 2 February 1989, pages 382-397.

14. Pantazopoulou, S.J., *Detailing For Reinforcement Stability in RC Members*, ASCE Journal of Structural Engineering, June 1998, 623-632.

15. Paulay, T. and Priestley, M.J.N., *Stability of Ductile Structural Walls*, ACI Structural Journal, Vol. 90, No. 4, July-August 1993.

16. Priestley, M.J.N.; and Seible, F., *Seismic Design and Retrofit of Bridges*, John Wiley & Sons, Inc., New York 1996, 686 pages.

17. Sanchez, A.; Seible, F.; and Priestley, N., *Seismic Performance of Flared Bridge Column*, University of California at San Diego, Report number SSRP-97/06, 1997

18. Scribner, Charles F., *Reinforcement Buckling on Reinforced Concrete Flexural Members*, ACI Structural Engineering, 83 (6), 966-973.

19. Stone, William C.; and Cheok, Geraldine S., *Inelastic Behavior of Full-Scale Bridge Columns Subjected to Cyclic Loading*, NIST BSS 166, Building Science Series, Center for Building Technology, National Engineering Laboratory, National Institute of Standards and Technology, Gaithersburg, Maryland, 20899, November 1986, 291 pages.

20. Wong, Y.L.; Paulay, T.; and Priestley, M.J.N., *Squat Circular Bridge Piers Under Multi-Directional Seismic Attack*, Report 90-4, Department of Civil Engineering, University of Canterbury, Christchurch, New Zealand, October 1990, 264 pages.

21. Zahn, F.A.; Park, R.; and Priestley, M.J.N., *Design of Reinforced Concrete Bridge Columns for Strength and Ductility*, Report 86-7, Department of Civil Engineering, University of Canterbury, Christchurch, New Zealand, March 1986, 380 pages.

APPENDIX

Appendix A-1

Example of Single Bending Analysis

- Given – c, d, $\phi_{y,}$ Δ_u

  d = 0.372 m
  c = 0.143 m
  ϕ_y = 0.014674 m^{-1}
  Δ_u = 0.042 m

- L_{col} = Length of the column

$$L_{col} = A.R.(Col.Dia)$$

$$L_{col} = 2.0(0.400m) = 0.80m$$

- L_{sp} = Length of strain penetration

$$L_{sp} = 0.022(f_y)dbl$$

$$L_{sp} = 0.022(423MPa)(0.016m) = 0.1489m$$

- L_{eff} = effective length of the column

$$L_{eff} = L_{col} + L_{sp}$$

$$L_{eff} = 0.80m + 0.1489m = 0.949m$$

- Δ_y = Yield displacement

$$\Delta_y = \frac{\phi_y (L_{eff})^2}{3}$$

$$\Delta_y = \frac{0.014674m^{-1}(0.949m)^2}{3} = 0.0044m$$

- Δ_p = Plastic Deformation

$$\Delta_p = \Delta_u - \Delta_y$$

$$\Delta_p = 0.042m - 0.0044m = 0.0376m$$

- L_p = Plastic Hinge Length, the great of the following equations

$$L_p = 0.08(L_{col}) + 0.022F_y dbl$$

$$L_p = 0.08(0.8m) + 0.022(423MPa)(0.016m) = 0.213m$$

$$L_p = 0.044F_y dbl$$

$$L_p = 0.044(423MPa)(0.016m) = 0.298m$$

- ϕ_p = Plastic Rotation

$$\phi_p = \frac{\Delta_p}{L_p L_{col}}$$

$$\phi_p = \frac{0.038m}{0.298m(0.80m)} = 0.1595m^{-1}$$

- ϕ_u = Ultimate Rotation

$$\phi_u = \phi_p + \phi_y$$

$$\phi_u = 0.1595m^{-1} + 0.014674m^{-1} = 0.17418m^{-1}$$

- $\in_{sm}$ = Strain at extreme tension fiber

$$\in_{sm} = \phi_u (d - c)$$

$$\in_{sm} = 0.17418m^{-1}(0.372m - 0.143m) = 0.0399$$

- $\in_{cu}$ = Strain at extreme compression fiber

$$\in_{cu} = \phi_u (c)$$

$$\in_{cu} = 0.17418m^{-1}(0.143m) = 0.0249$$

Example of Double Bending Analysis

- Given – c, d, $\phi_{y,}$ Δ_u

  d = 0.429 m
  c = 0.144 m
  $\phi_y = 0.012252\ m^{-1}$
  $\Delta_u = 0.050$ m

- L_{col} = Length of the column

$$L_{col} = A.R.(Col.Dia)(S/D)$$

$$L_{col} = 2.0(0.457m)(2) = 1.828m$$

- L_{sp} = Length of strain penetration

$$L_{sp} = 0.044(f_y)dbl$$

$$L_{sp} = 0.044(428MPa)(0.016m) = 0.3013m$$

- L_{eff} = effective length of the column

$$L_{eff} = L_{col} + L_{sp}$$

$$L_{eff} = 1.828m + 0.3013m = 2.13m$$

- Δ_y = Yield displacement

$$\Delta_y = \frac{\phi_y (L_{eff})^2}{3}$$

$$\Delta_y = \frac{0.012252m^{-1}(2.13m)^2}{6} = 0.00926m$$

- Δ_p = Plastic Deformation

$$\Delta_p = \Delta_u - \Delta_y$$

$$\Delta_p = 0.050m - 0.00926m = 0.0376m$$

- L_p = Plastic Hinge Length, the great of the following equations

$$L_p = 0.08(L_{col}) + 0.022F_y dbl$$

$$L_p = 0.08(0.91m) + 0.022(428MPa)(0.016m) = 0.224m$$

$$L_p = 0.044F_y dbl$$

$$L_p = 0.044(428MPa)(0.016m) = 0.3013m$$

- ϕ_p = Plastic Rotation

$$\phi_p = \frac{\Delta_p}{L_p L_{col}}$$

$$\phi_p = \frac{0.04074m}{0.3013m(1.828m)} = 0.07397m^{-1}$$

- ϕ_u = Ultimate Rotation

$$\phi_u = \phi_p + \phi_y$$

$$\phi_u = 0.07397m^{-1} + 0.012252m^{-1} = 0.08622m^{-1}$$

- $\in_{sm}$ = Strain at extreme tension fiber

$$\in_{sm} = \phi_u (d - c)$$

$$\in_{sm} = 0.08622m^{-1}(0.429m - 0.144m) = 0.0246$$

- $\in_{cu}$ = Strain at extreme compression fiber

$$\in_{cu} = \phi_u (c)$$

$$\in_{cu} = 0.08622m^{-1}(0.144m) = 0.0124$$

Appendix A-2

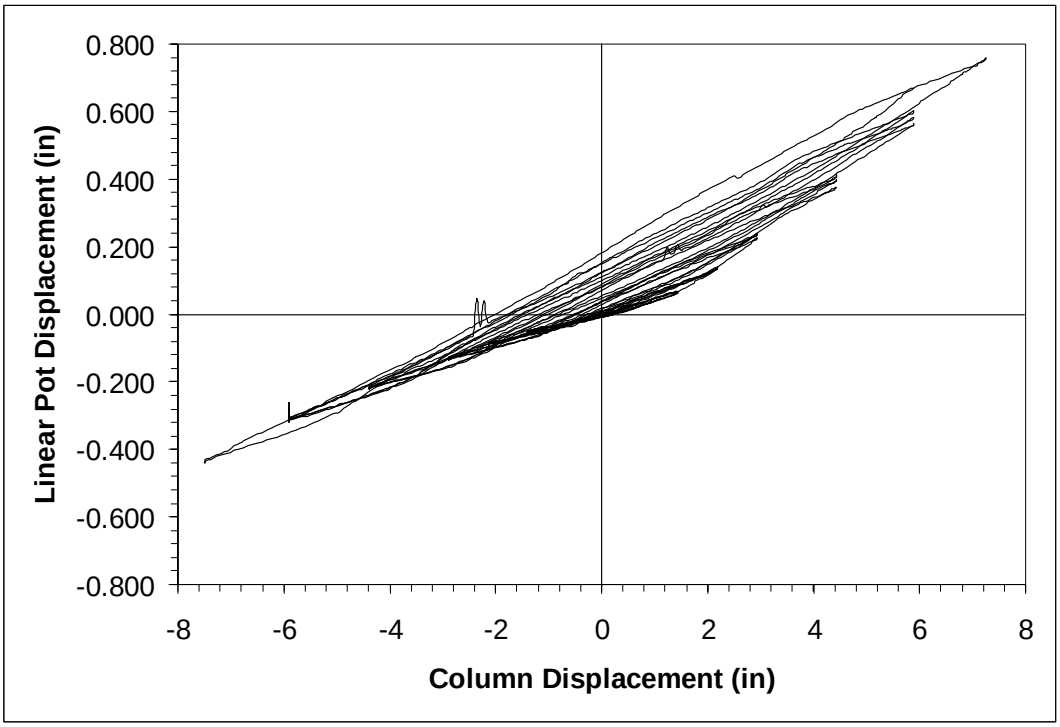

Figure A-2.1 Linear Pot History First 8 inches North Side

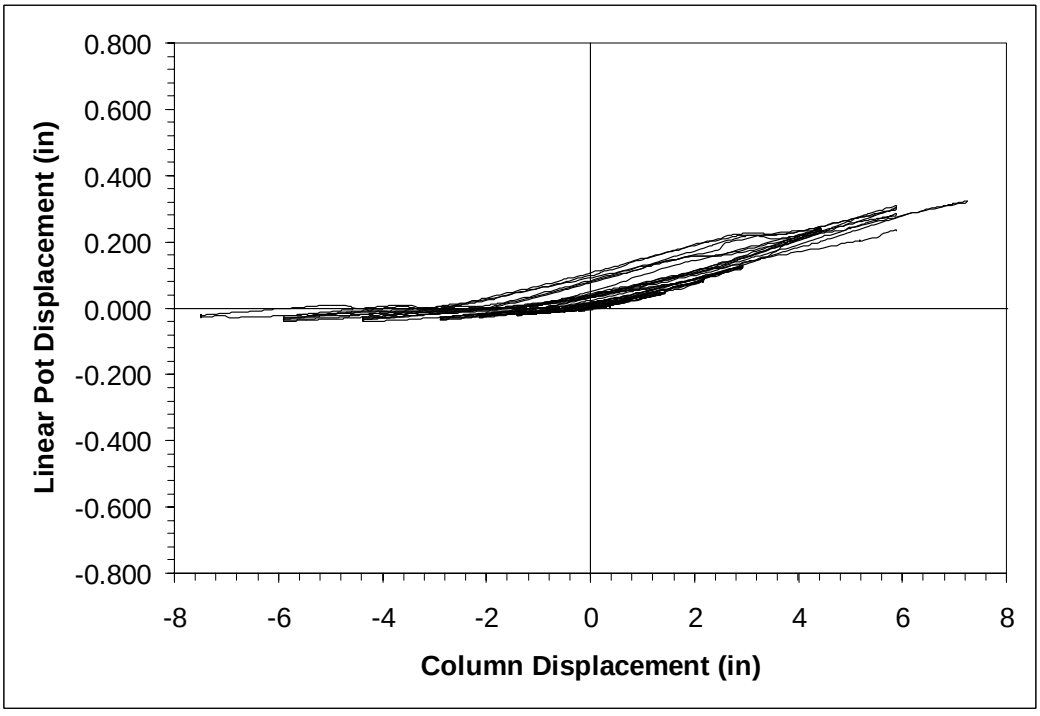

Figure A-2.2 Linear Pot History Second 8 inches North Side

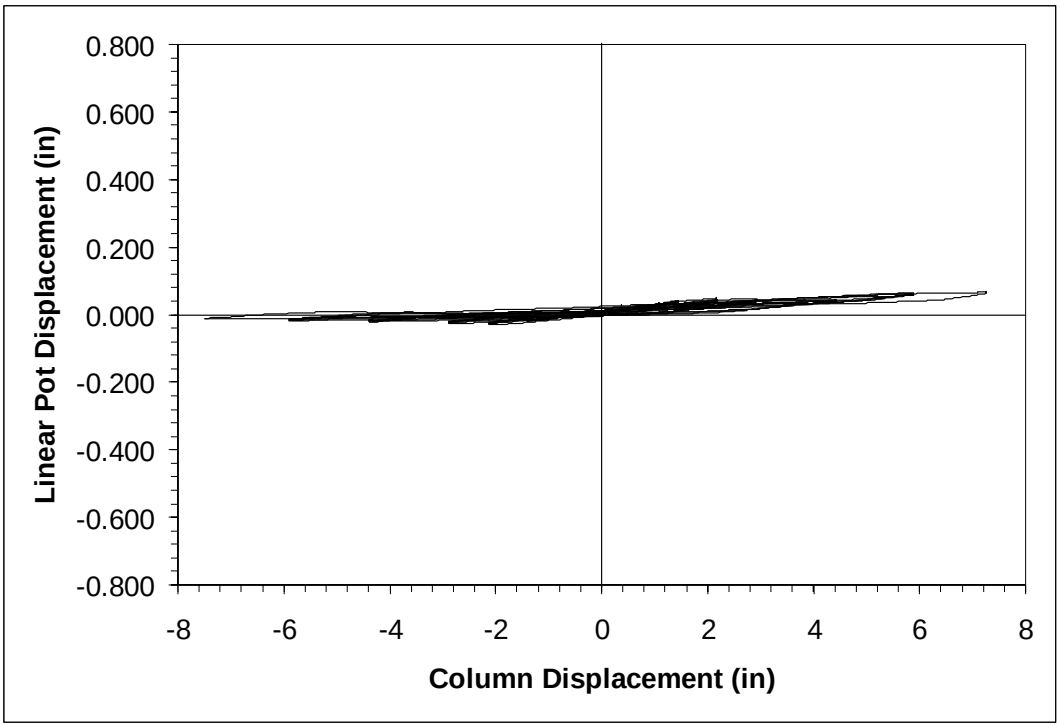

Figure A-2.3 Linear Pot History Third 8 inches North Side

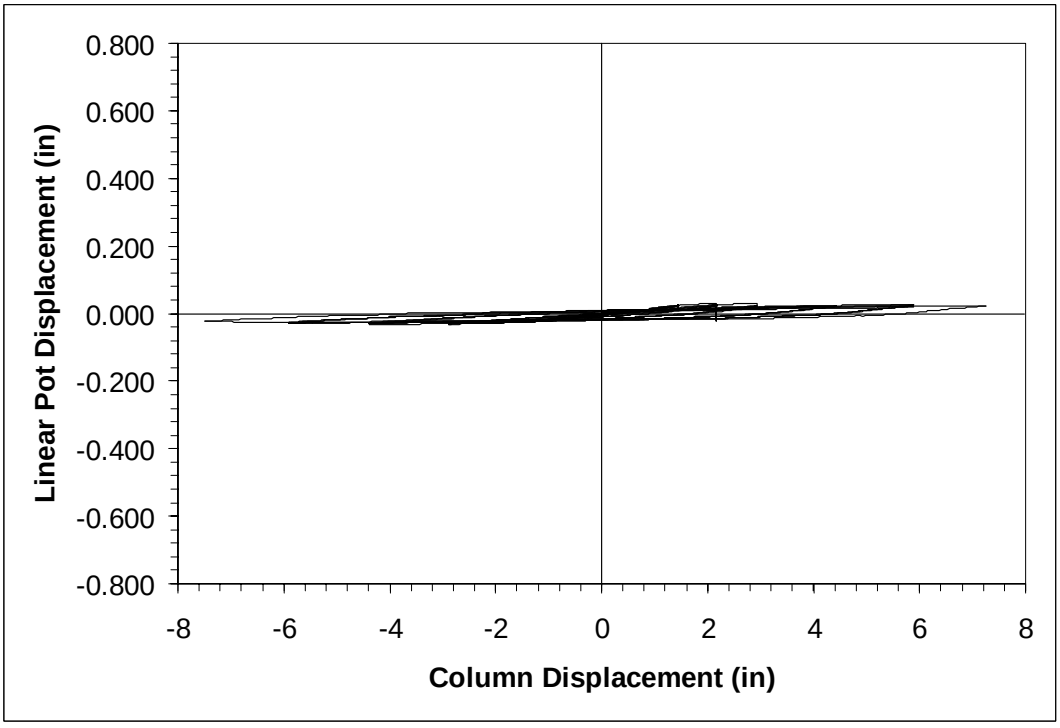

Figure A-2.4 Linear Pot History Fourth 8 inches North Side

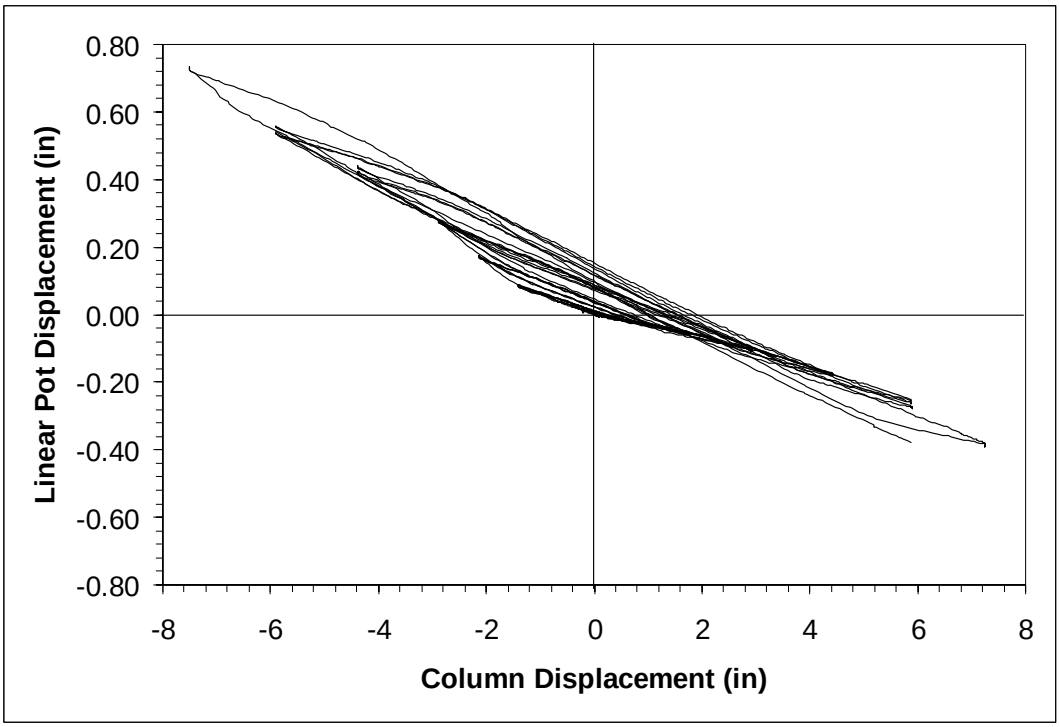

Figure A-2.5 Linear Pot History First 8 inches South Side

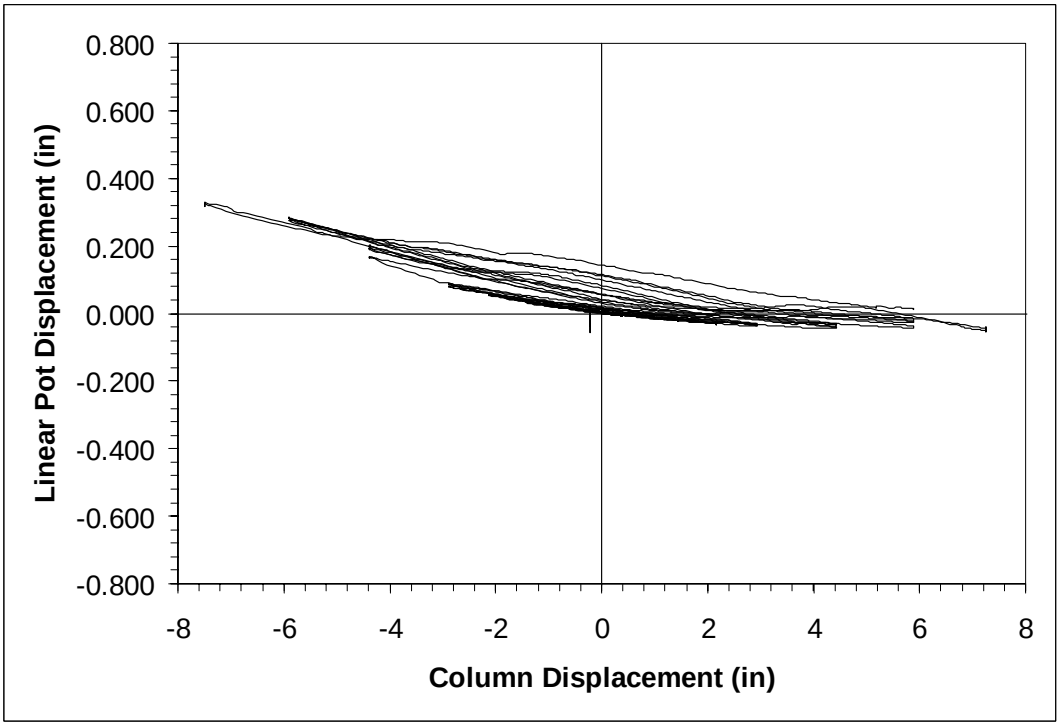

Figure A-2.6 Linear Pot History Second 8 inches South Side

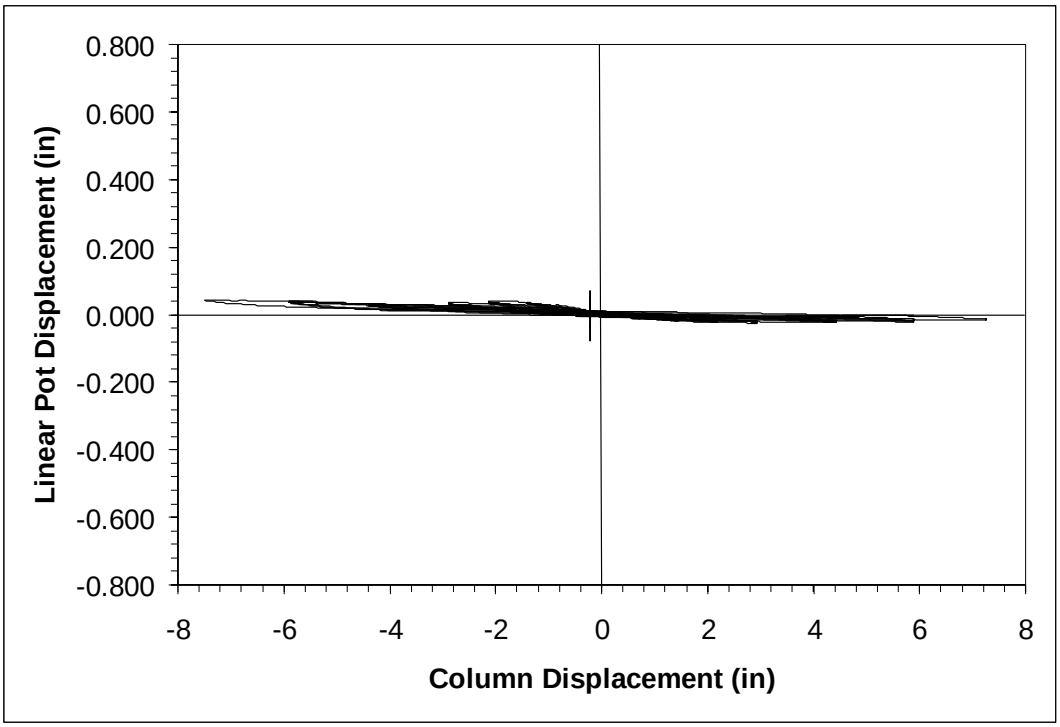

Figure A-2.7 Linear Pot History Third 8 inches South Side

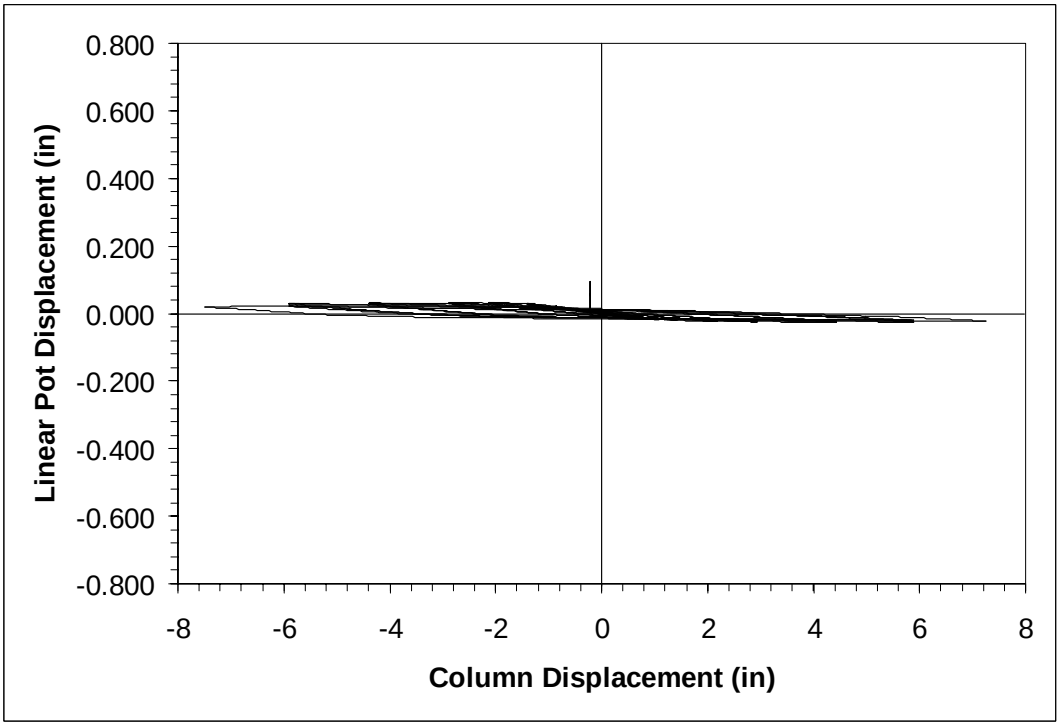

Figure A-2.8 Linear Pot History Fourth 8 inches South Side

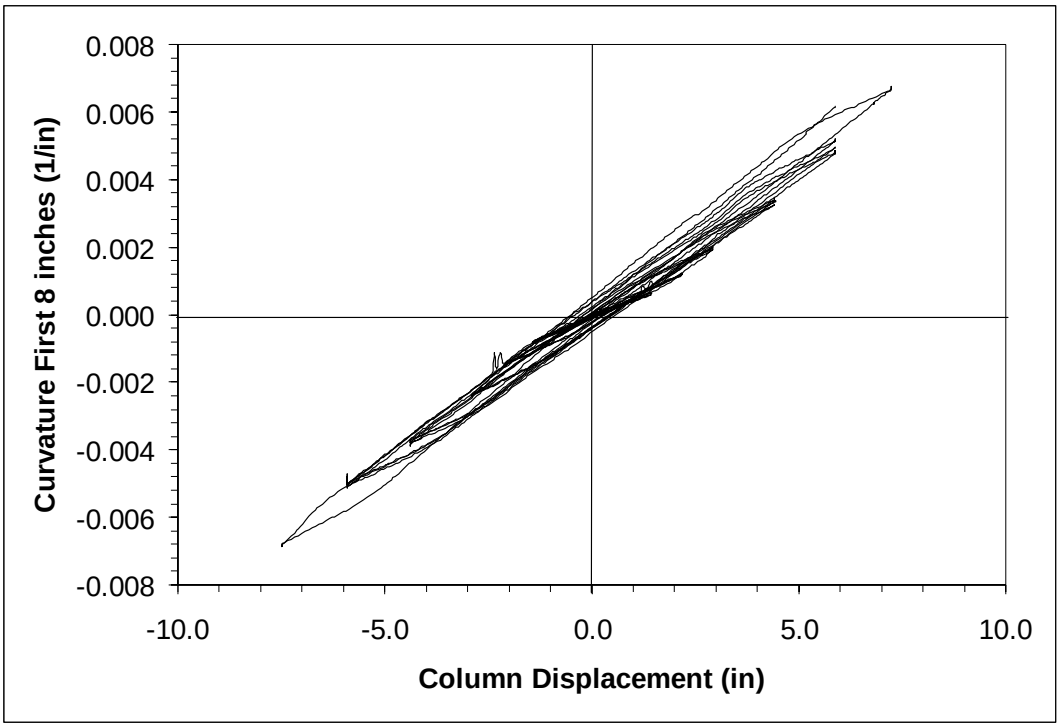

Figure A-2.9 Curvature over the First 8 inches of the Column

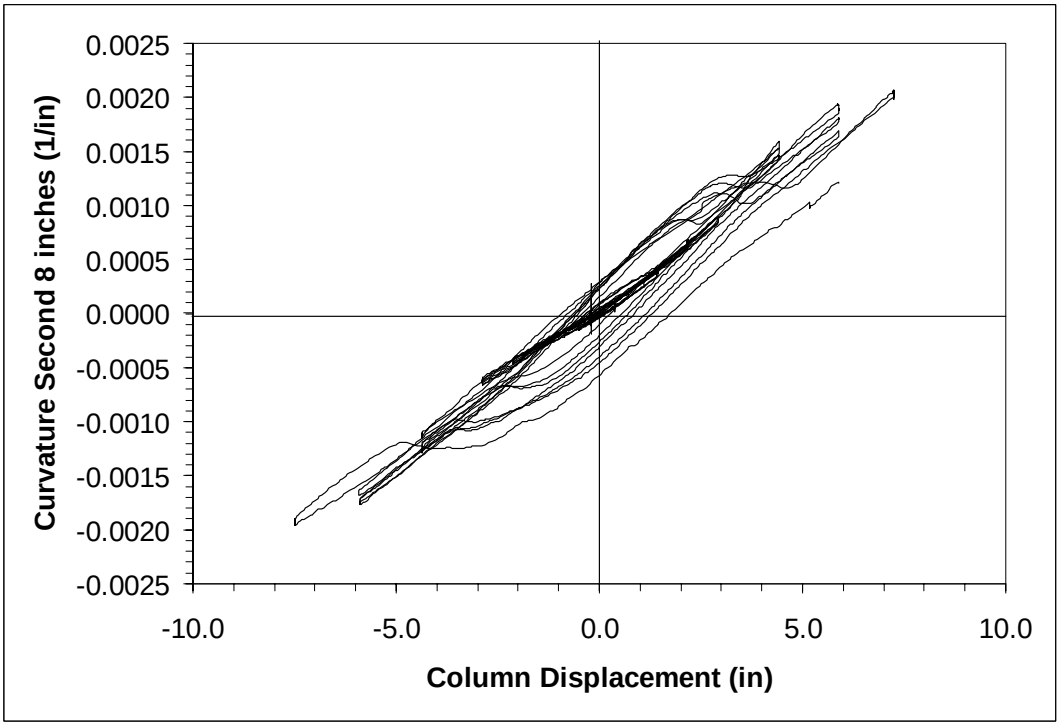

Figure A-2.10 Curvature over the Second 8 inches of the Column

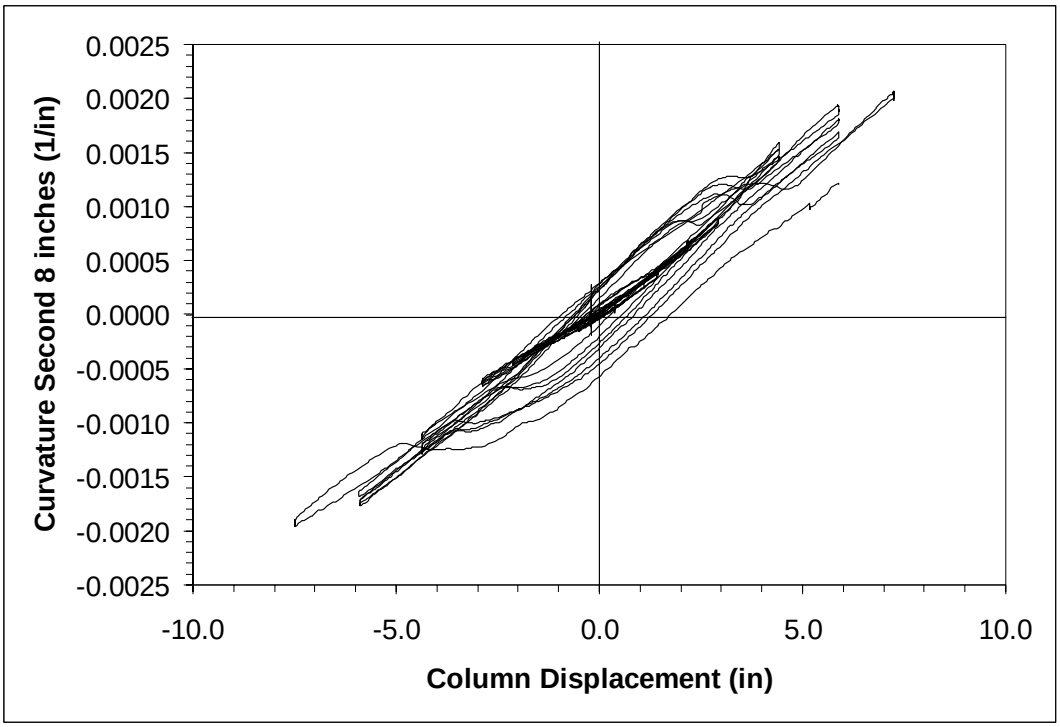

Figure A-2.11 Curvature over the Third 8 inches of the Column

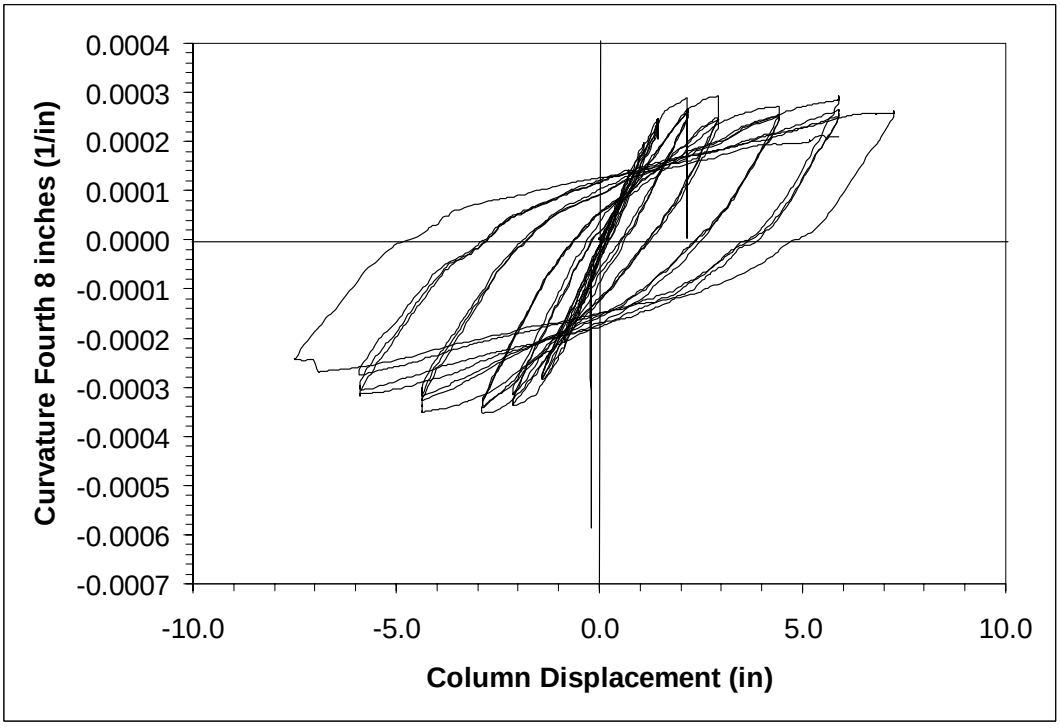

Figure A-2.12 Curvature over the Fourth 8 inches of the Column

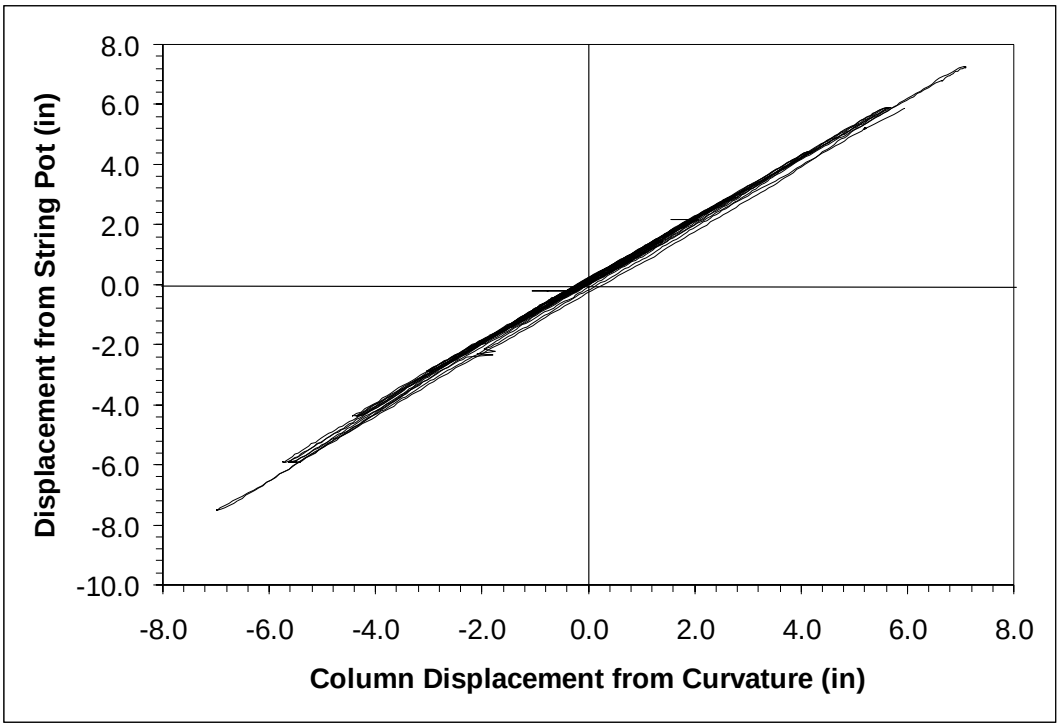

Figure A-2.13 String Pot Displacement versus Displacement from Curvature

Appendix A-3

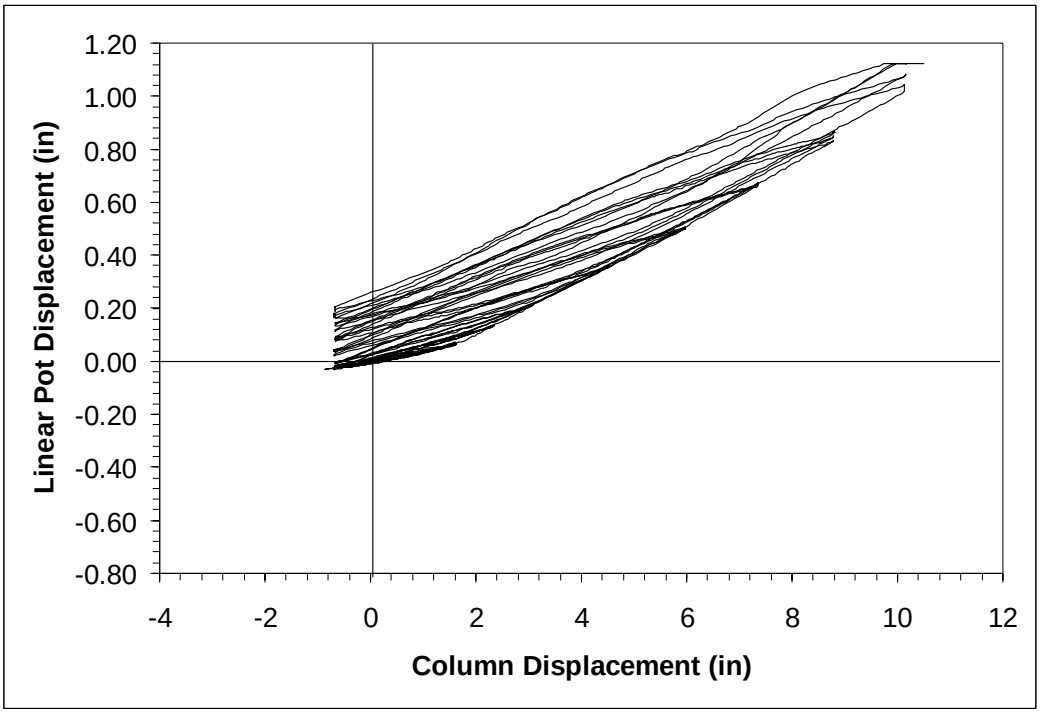

Figure A-3.1 Linear Pot History First 8 inches North Side

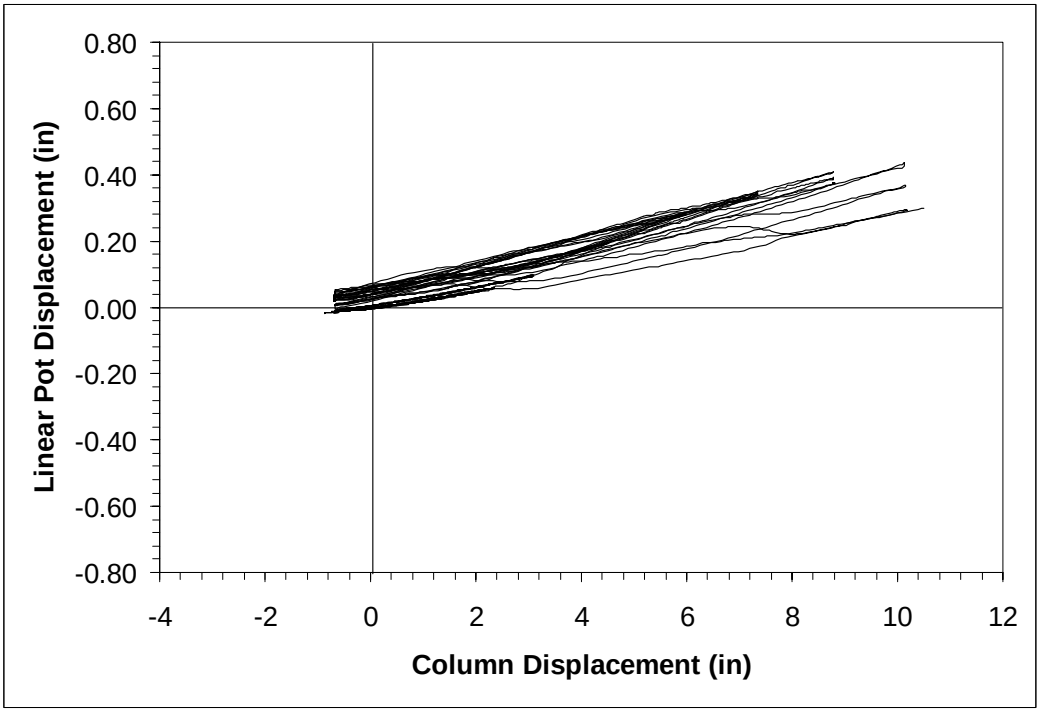

Figure A-3.2 Linear Pot History Second 8 inches North Side

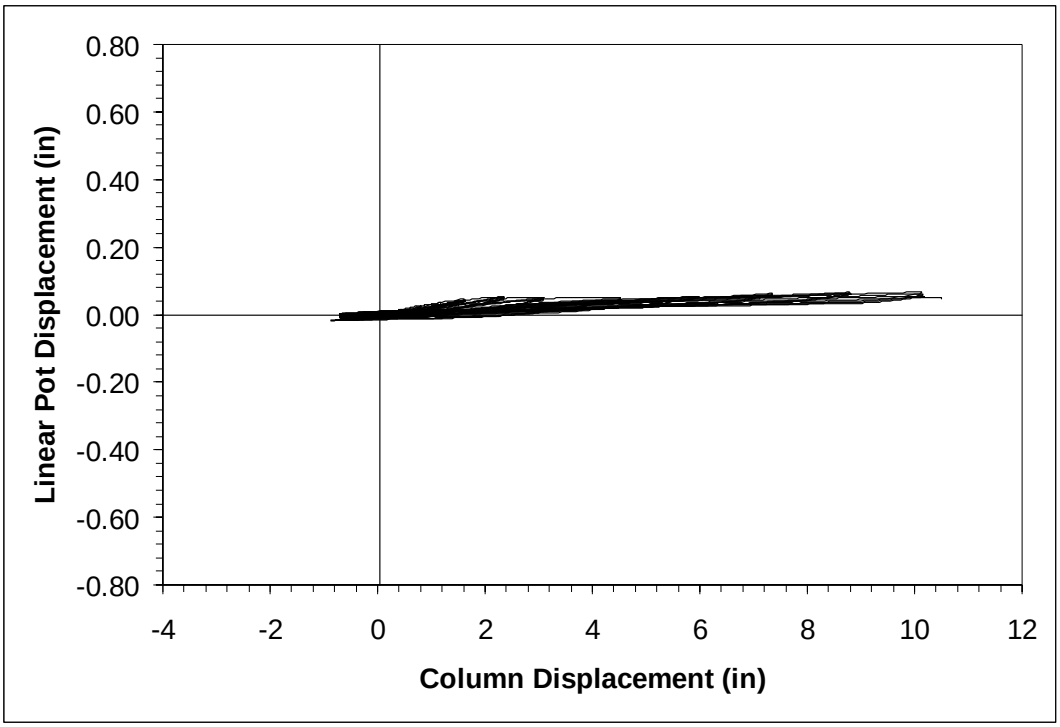

Figure A-3.3 Linear Pot History Third 8 inches North Side

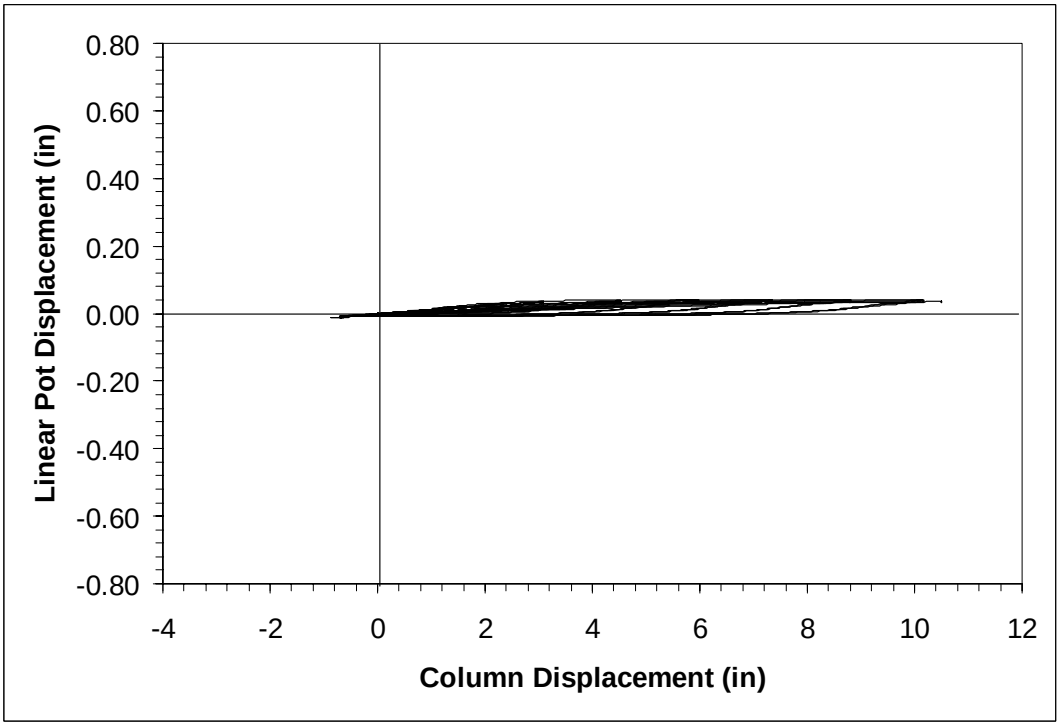

Figure A-3.4 Linear Pot History Fourth 8 inches North Side

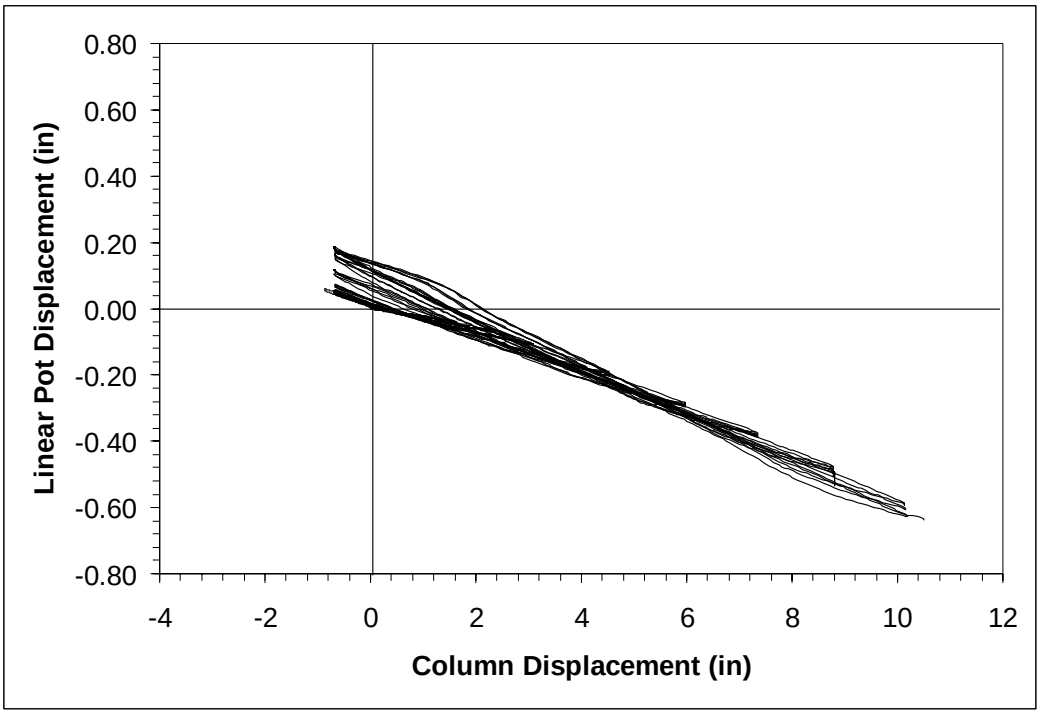

Figure A-3.5 Linear Pot History First 8 inches South Side

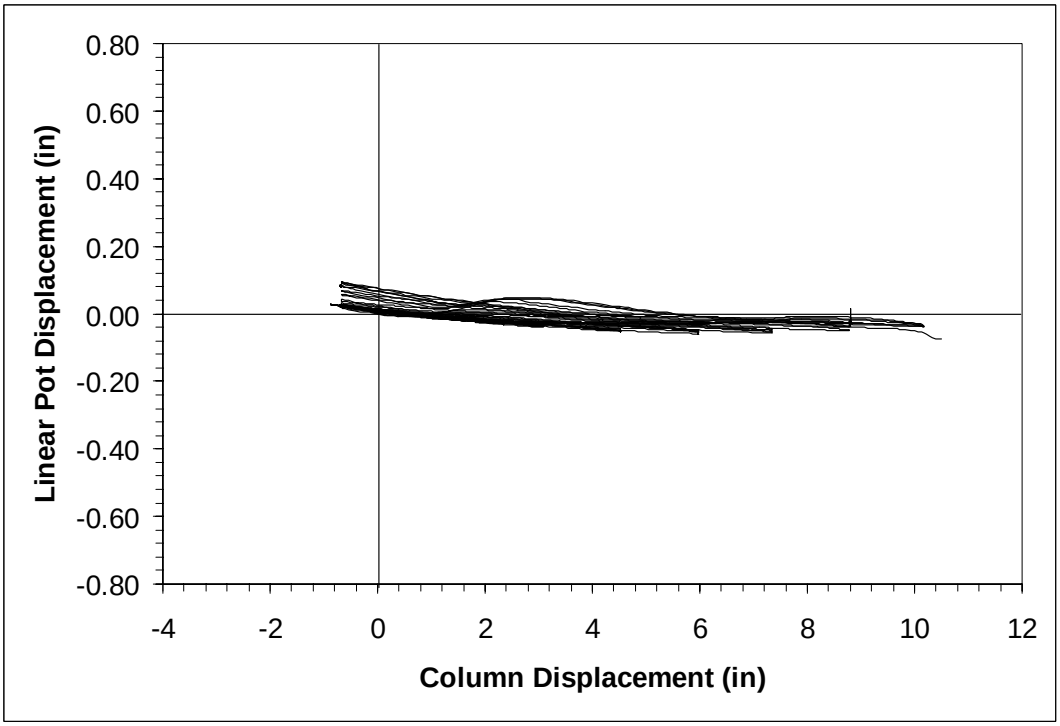

Figure A-3.6 Linear Pot History Second 8 inches South Side

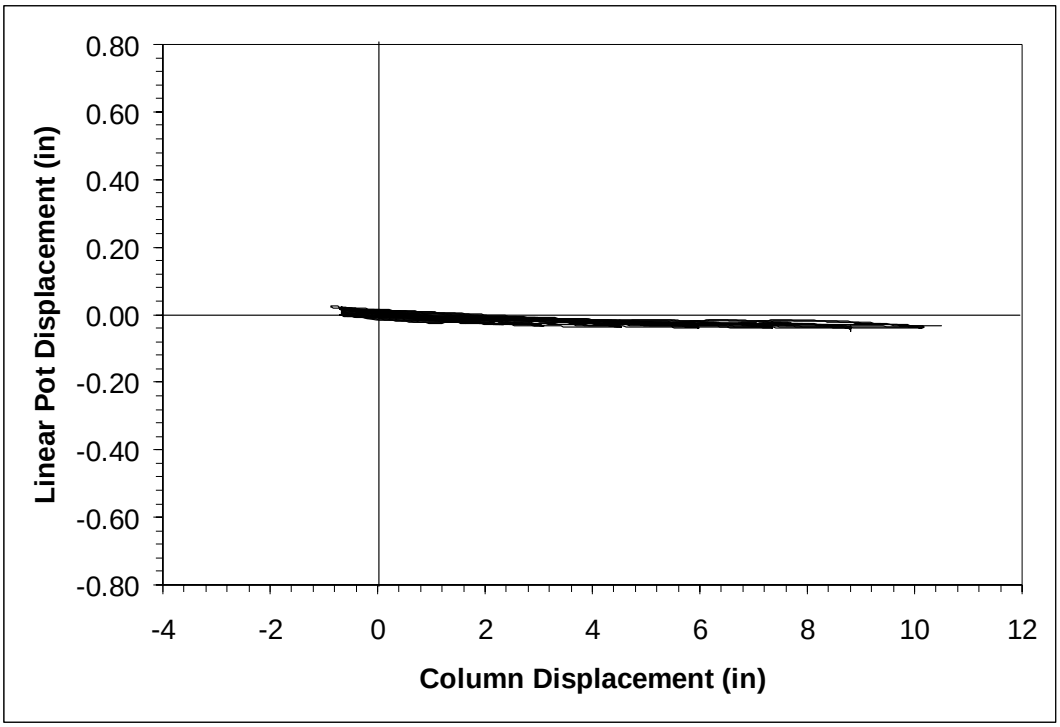

Figure A-3.7 Linear Pot History Third 8 inches South Side

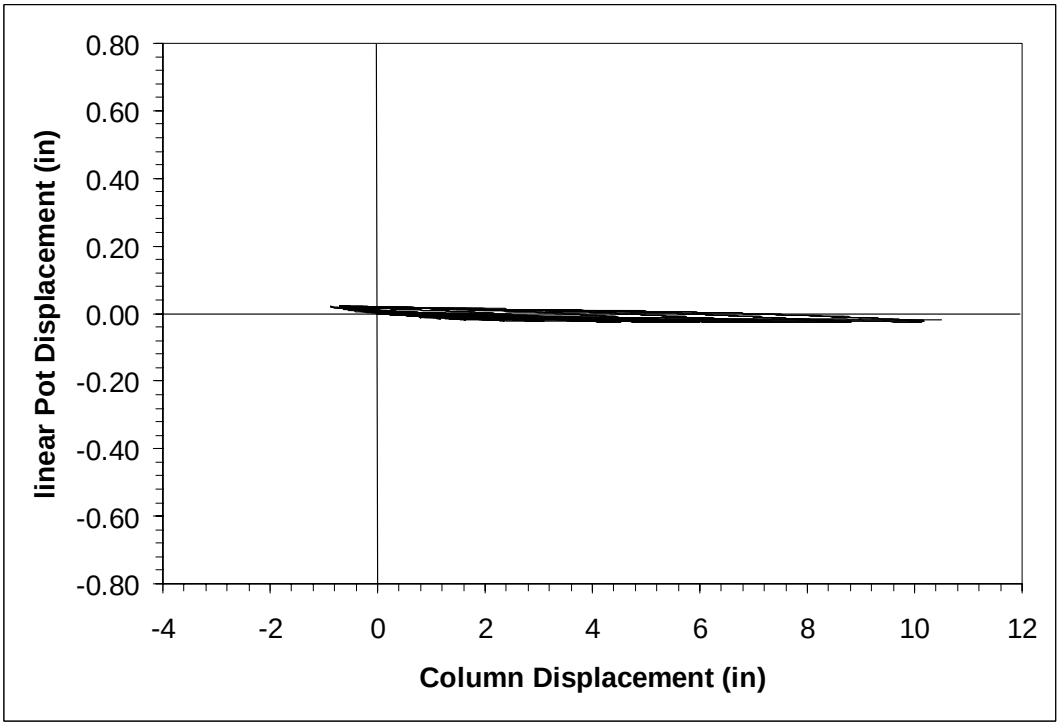

Figure A-3.8 Linear Pot History Fourth 8 inches South Side

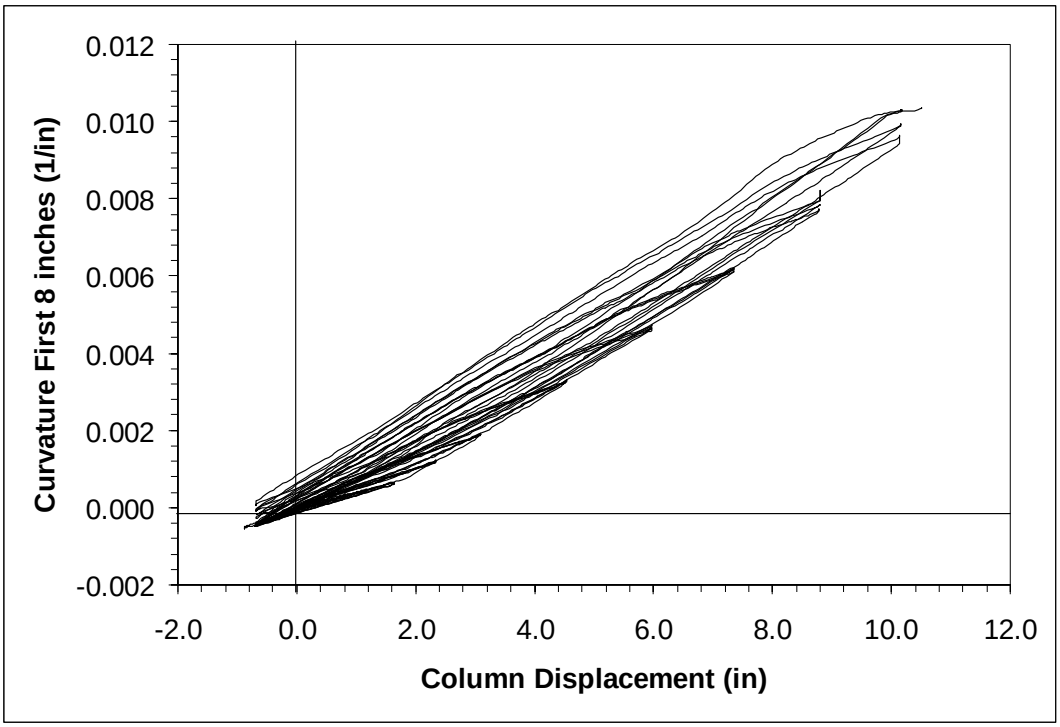

Figure A-3.9 Curvature over the First 8 inches of the Column

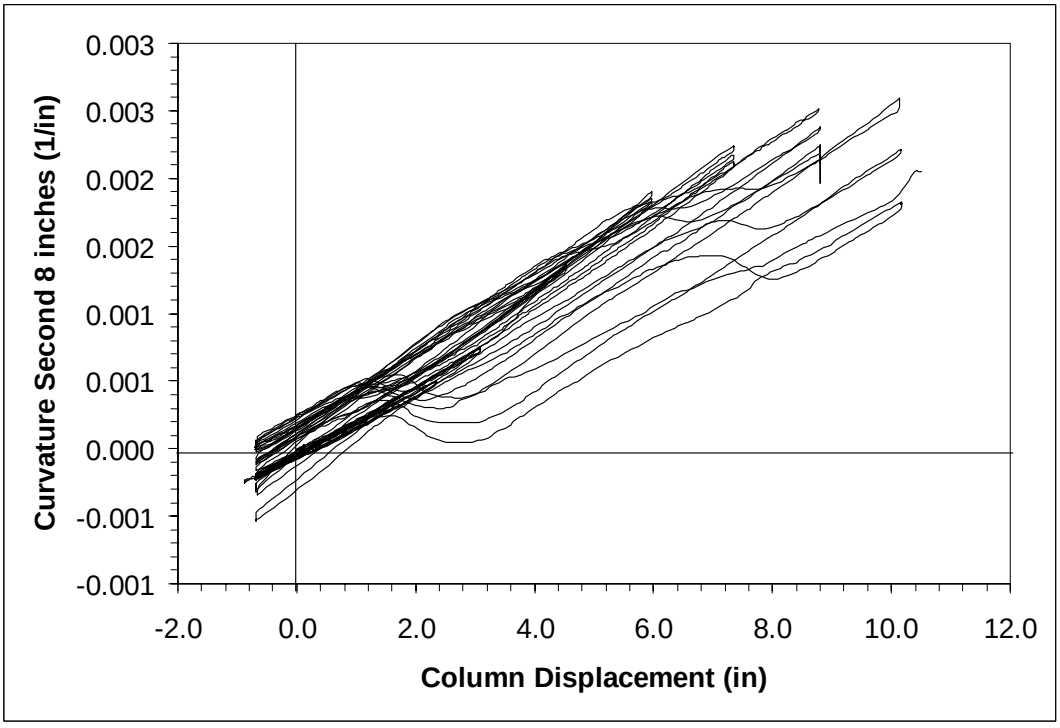

Figure A-3.10 Curvature over the Second 8 inches of the Column

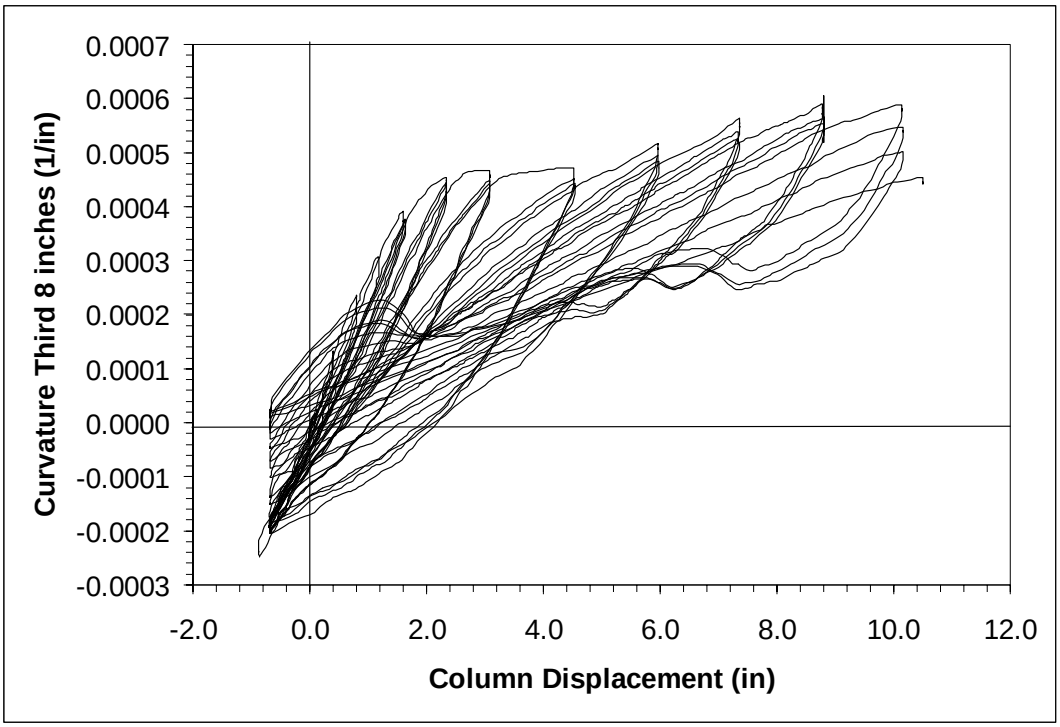

Figure A-3.11 Curvature over the Third 8 inches of the Column

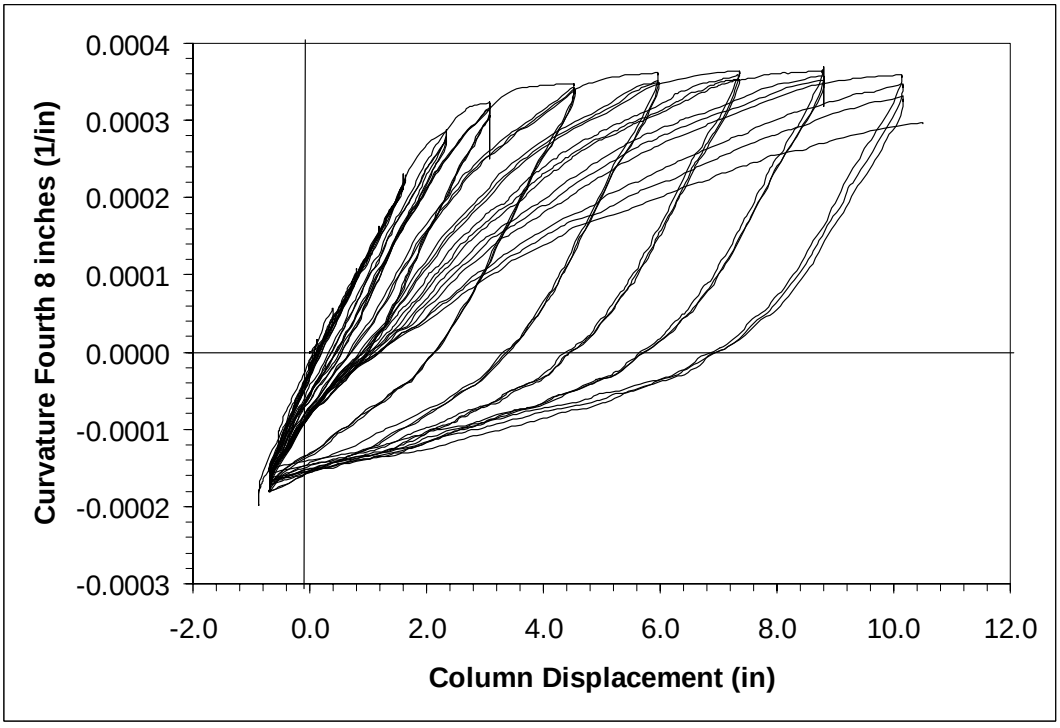

Figure A-3.12 Curvature over the Fourth 8 inches of the Column

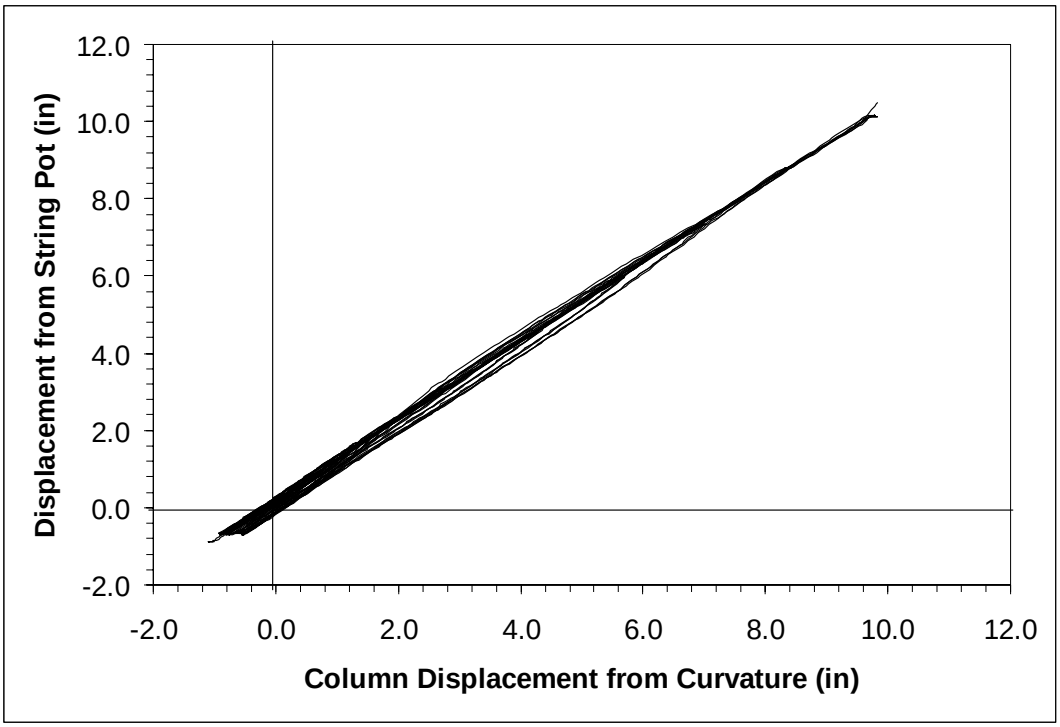

Figure A-3.13 String Pot Displacement versus Displacement from Curvature

Appendix A-4

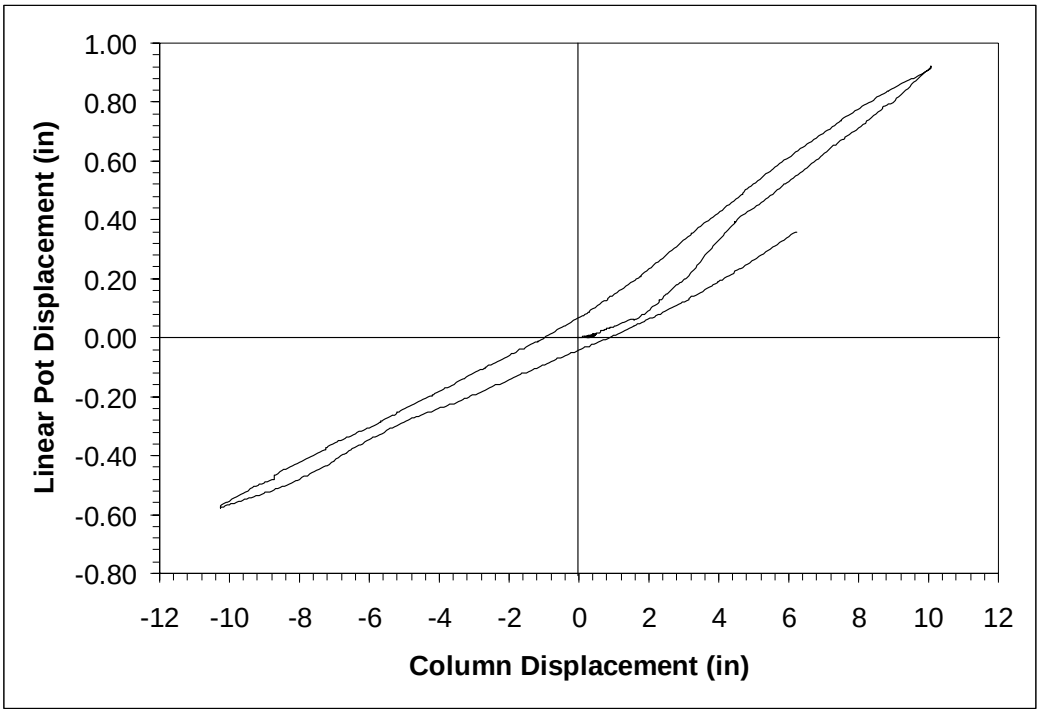

Figure A-4.1 Linear Pot History First 8 inches North Side

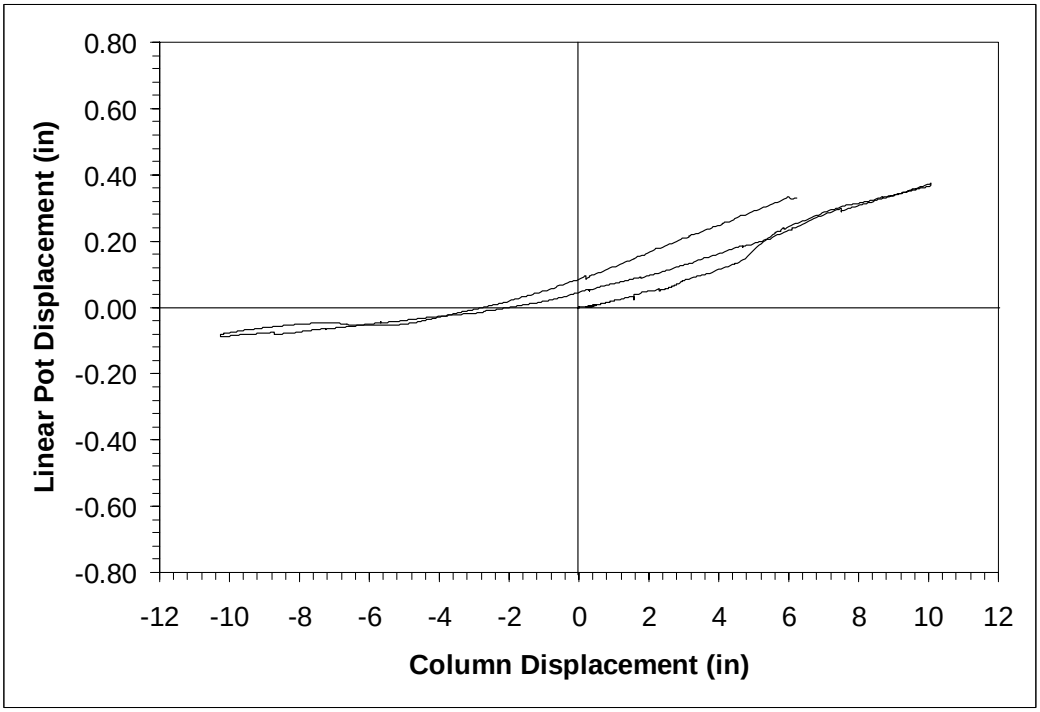

Figure A-4.2 Linear Pot History Second 8 inches North Side

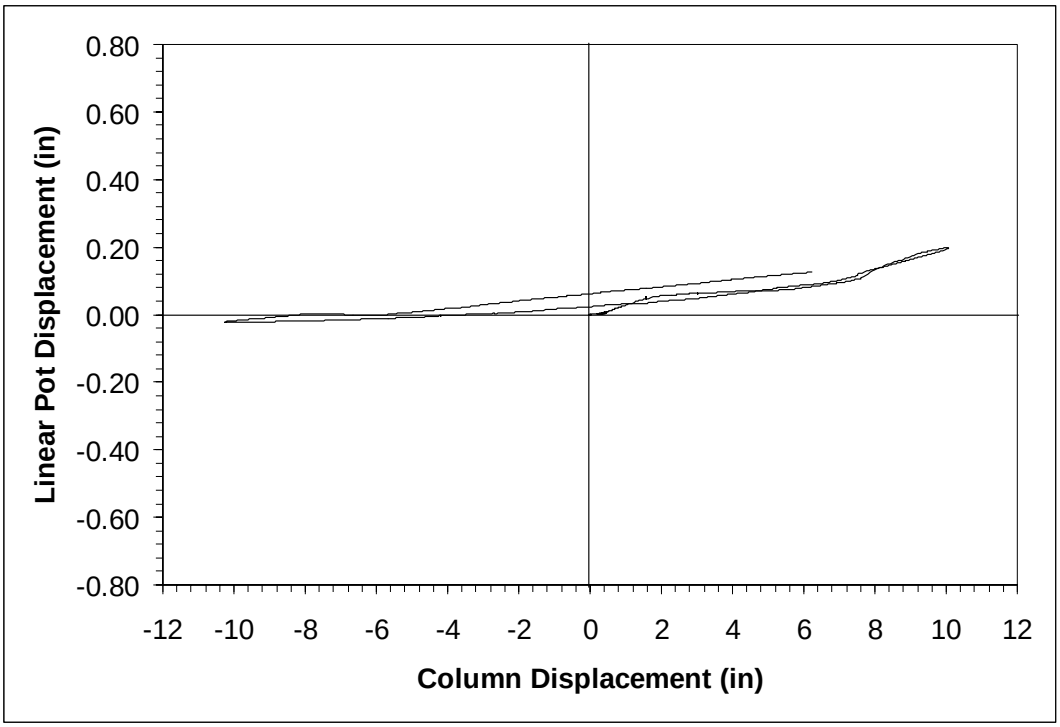

Figure A-4.3 Linear Pot History Third 8 inches North Side

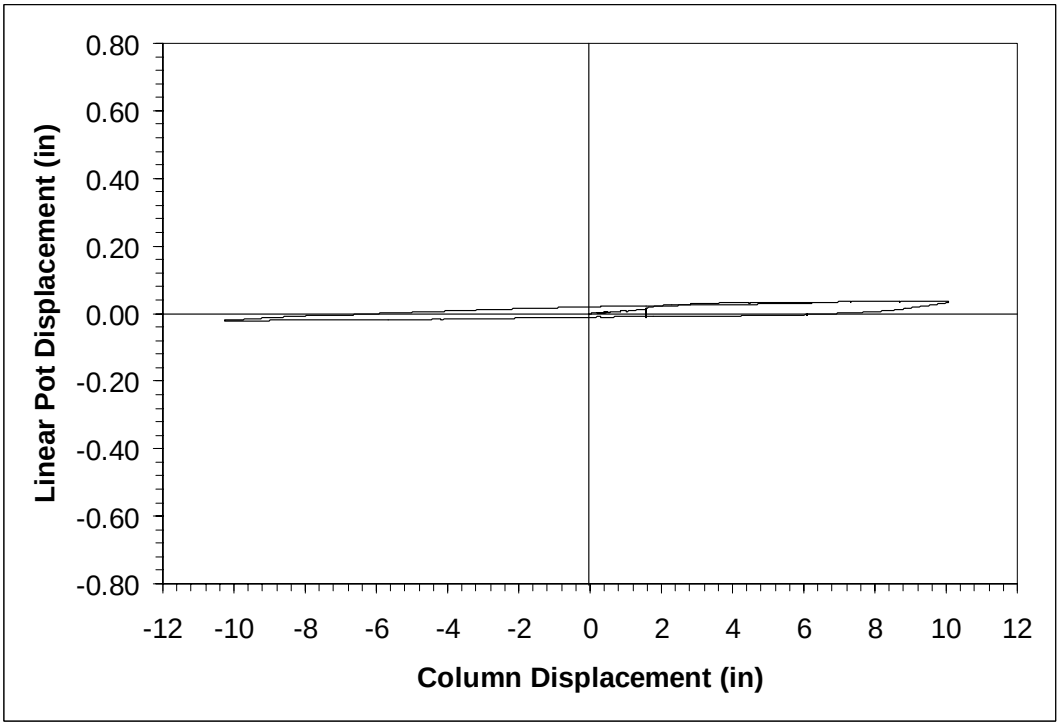

Figure A-4.4 Linear Pot History Fourth 8 inches North Side

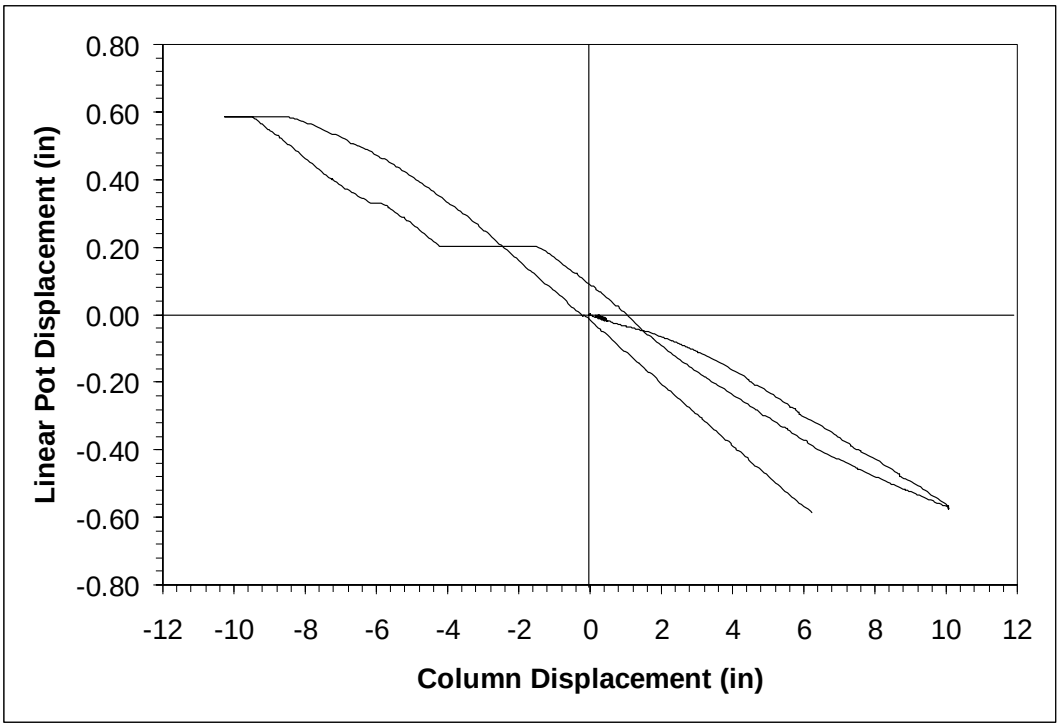

Figure A-4.5 Linear Pot History First 8 inches South Side

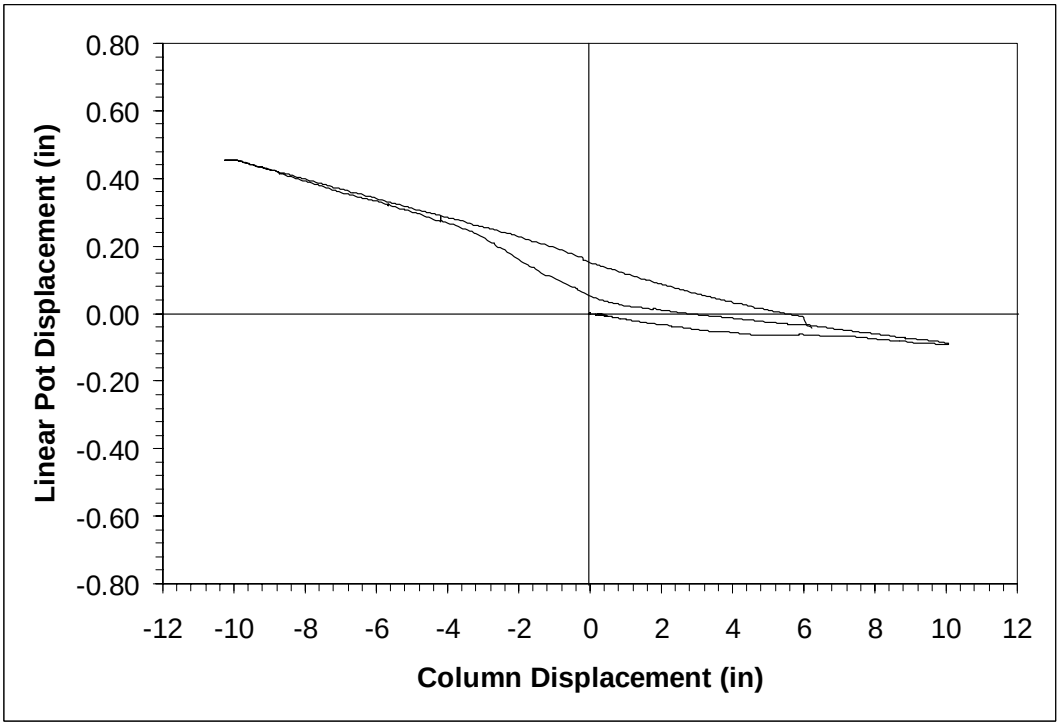

Figure A-4.6 Linear Pot History Second 8 inches South Side

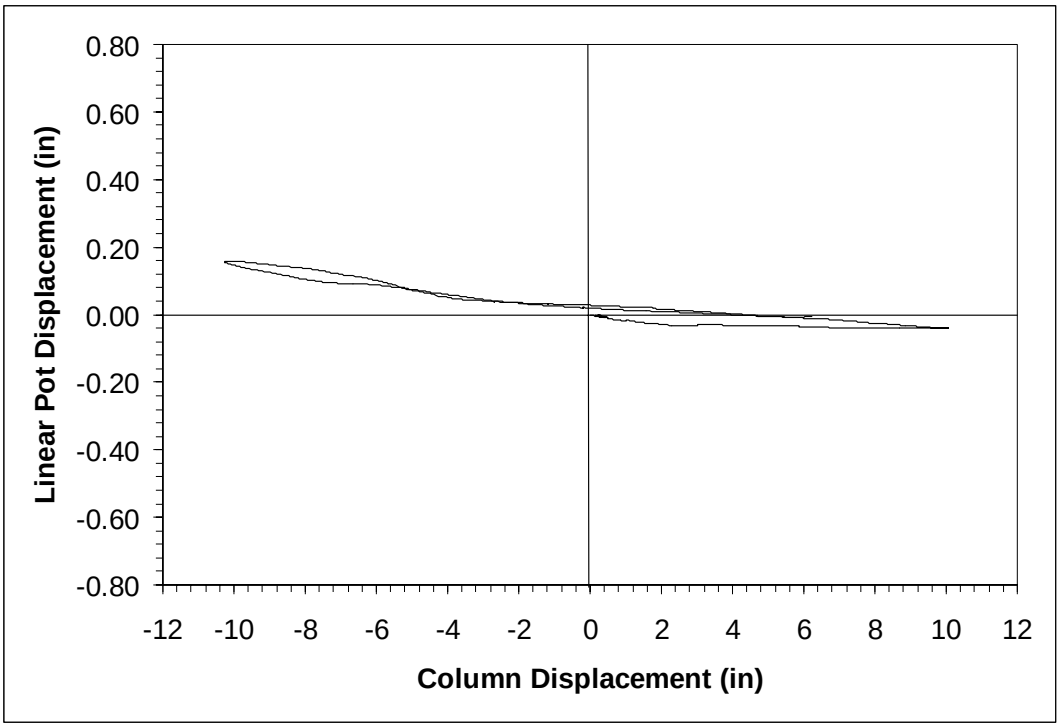

Figure A-4.7 Linear Pot History Third 8 inches South Side

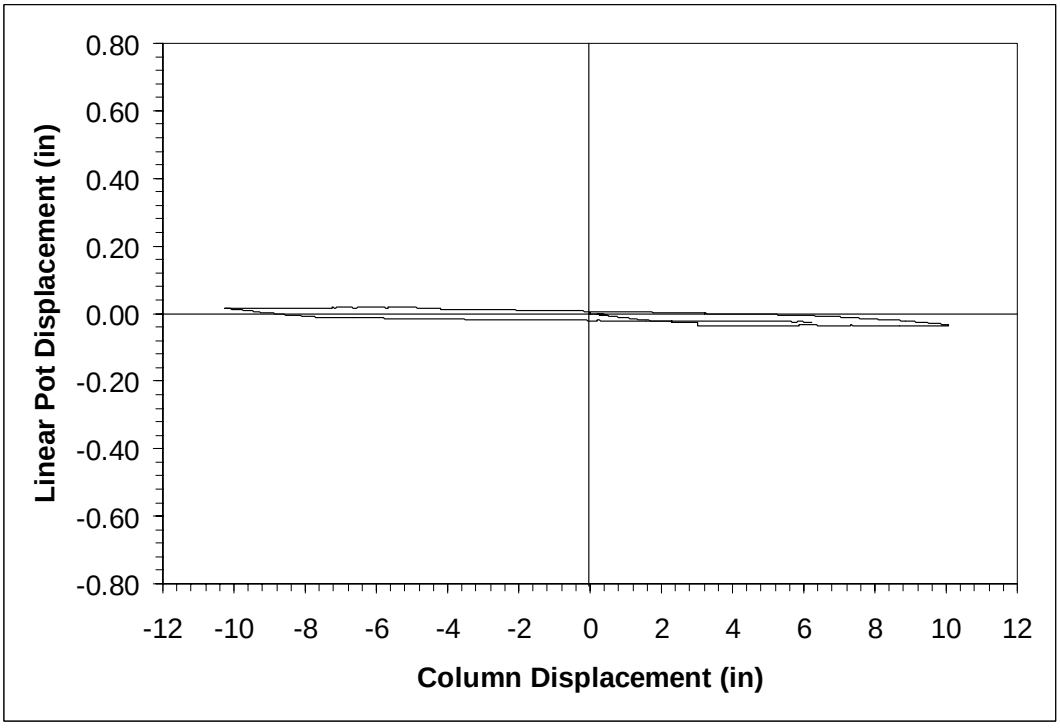

Figure A-4.8 Linear Pot History Fourth 8 inches South Side

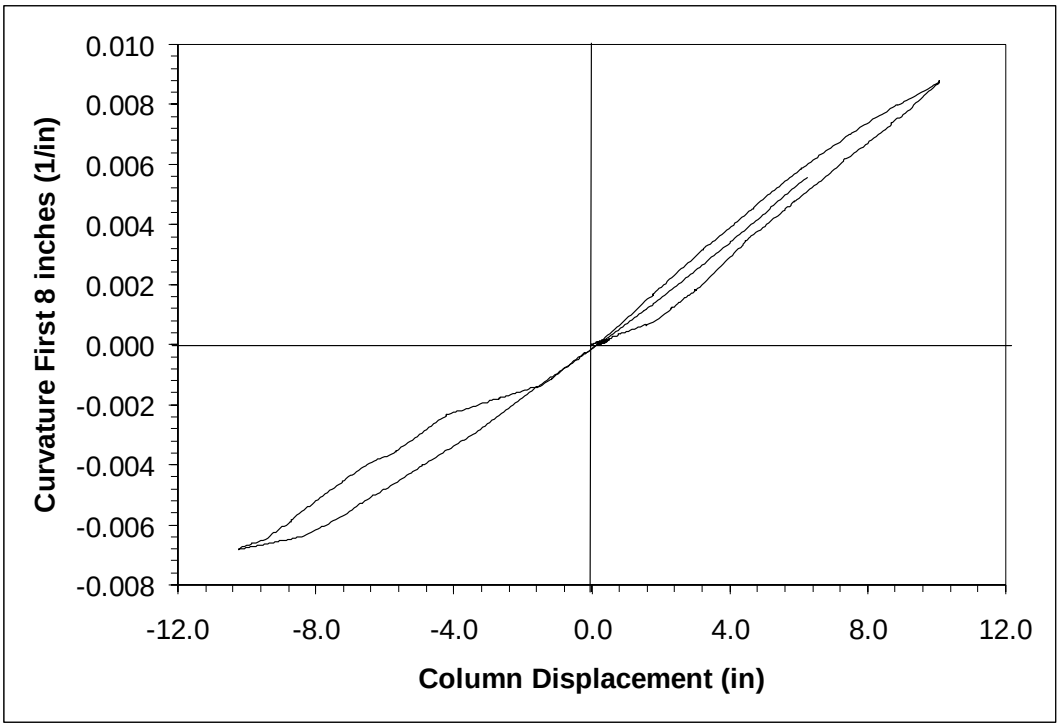

Figure A-4.9 Curvature over the First 8 inches of the Column

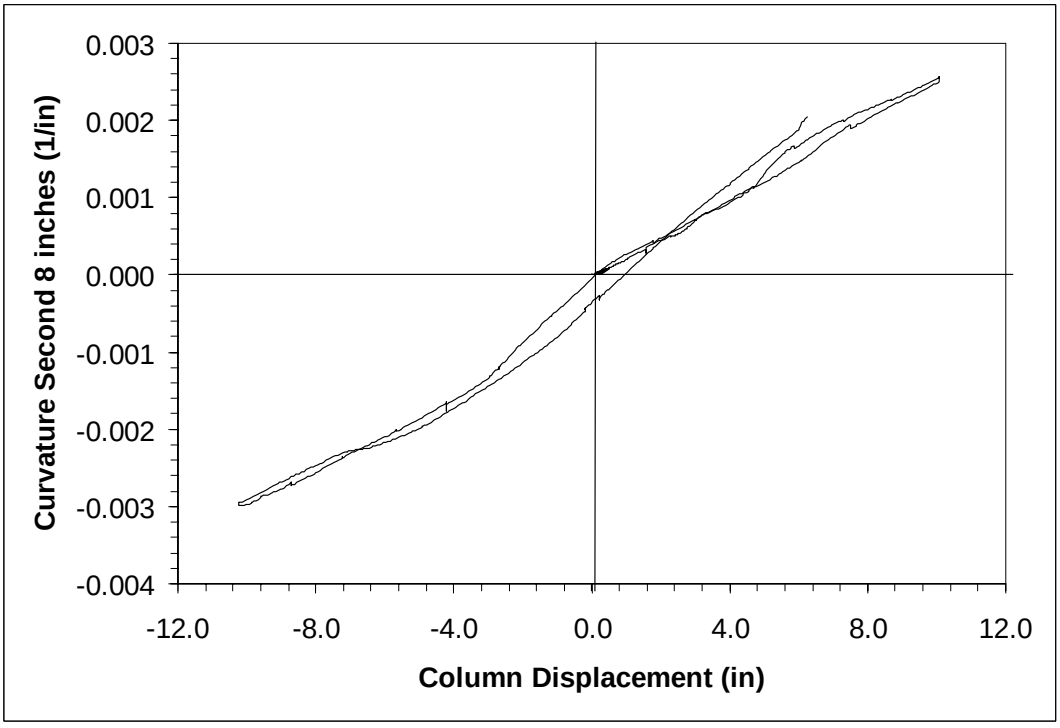

Figure A-4.10 Curvature over the Second 8 inches of the Column

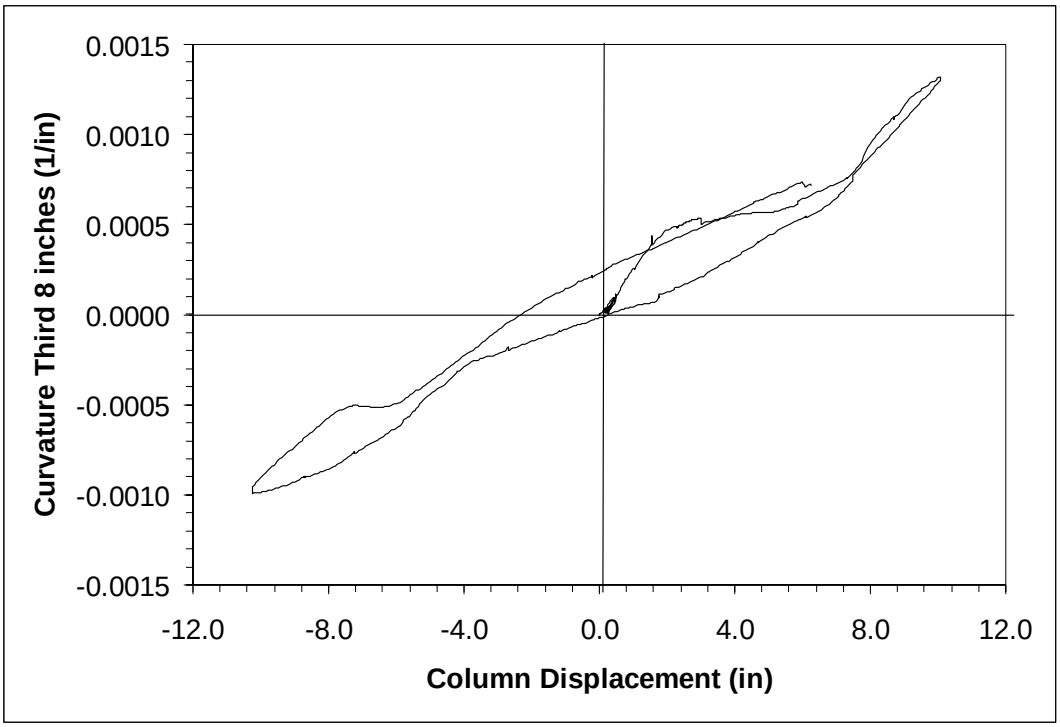

Figure A-4.11 Curvature over the Third 8 inches of the Column

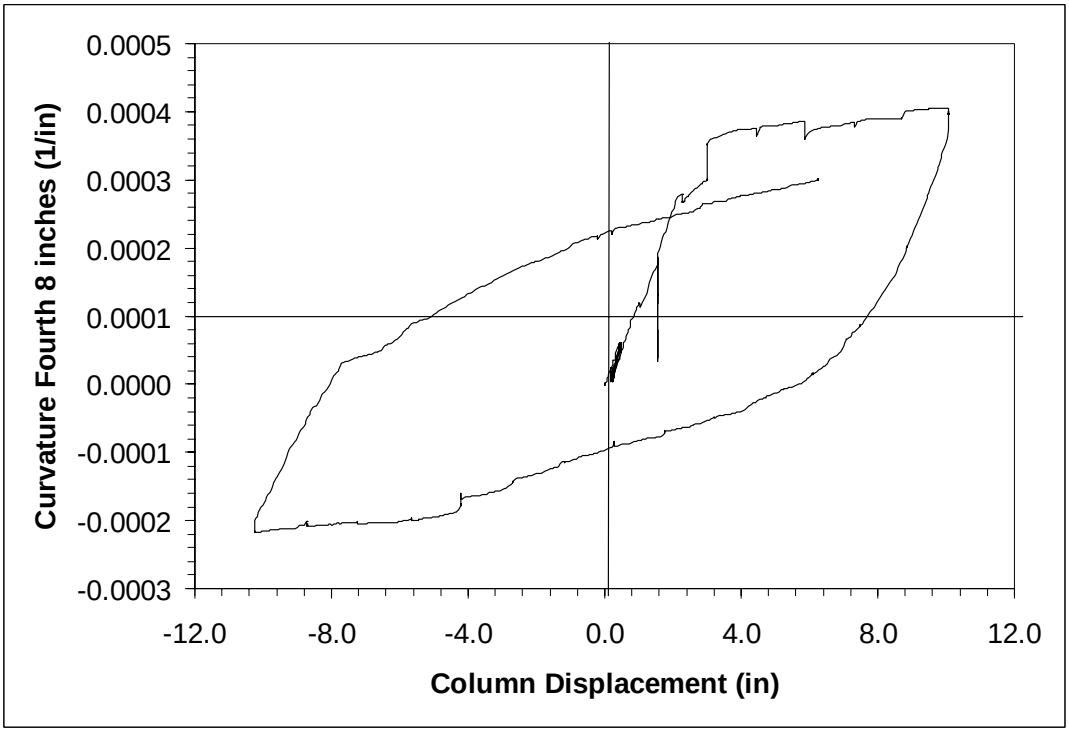

Figure A-4.12 Curvature over the Fourth 8 inches of the Column

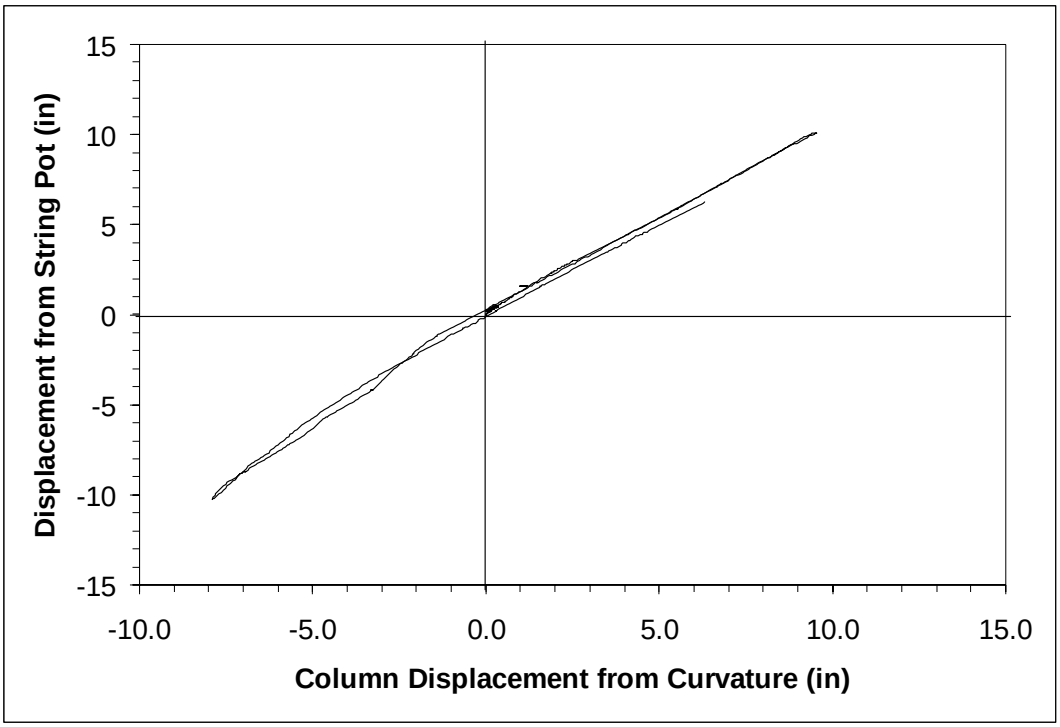

Figure A-4.13 String Pot Displacement versus Displacement from Curvature

Appendix A-5

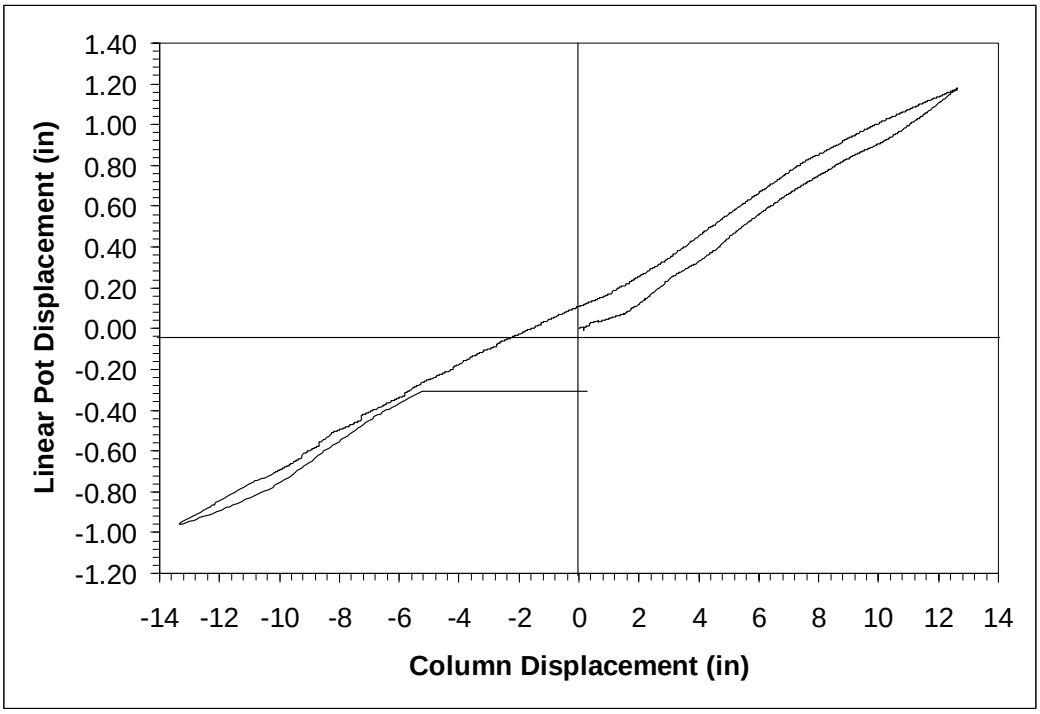

Figure A-5.1 Linear Pot History First 8 inches North Side

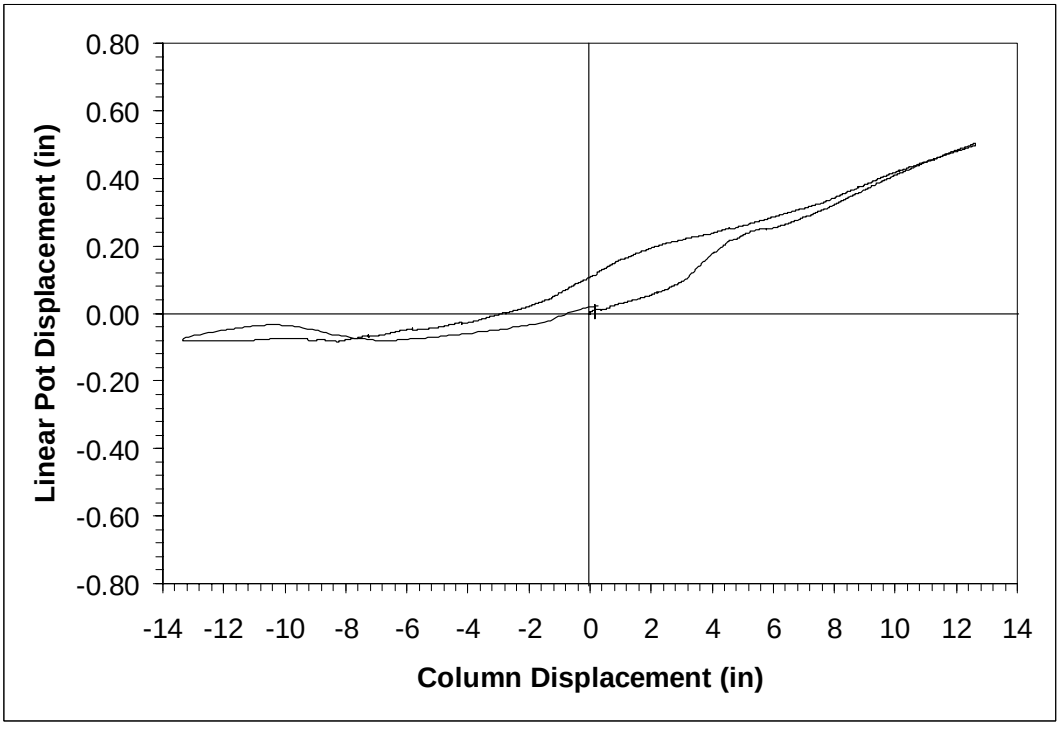

Figure A-5.2 Linear Pot History Second 8 inches North Side

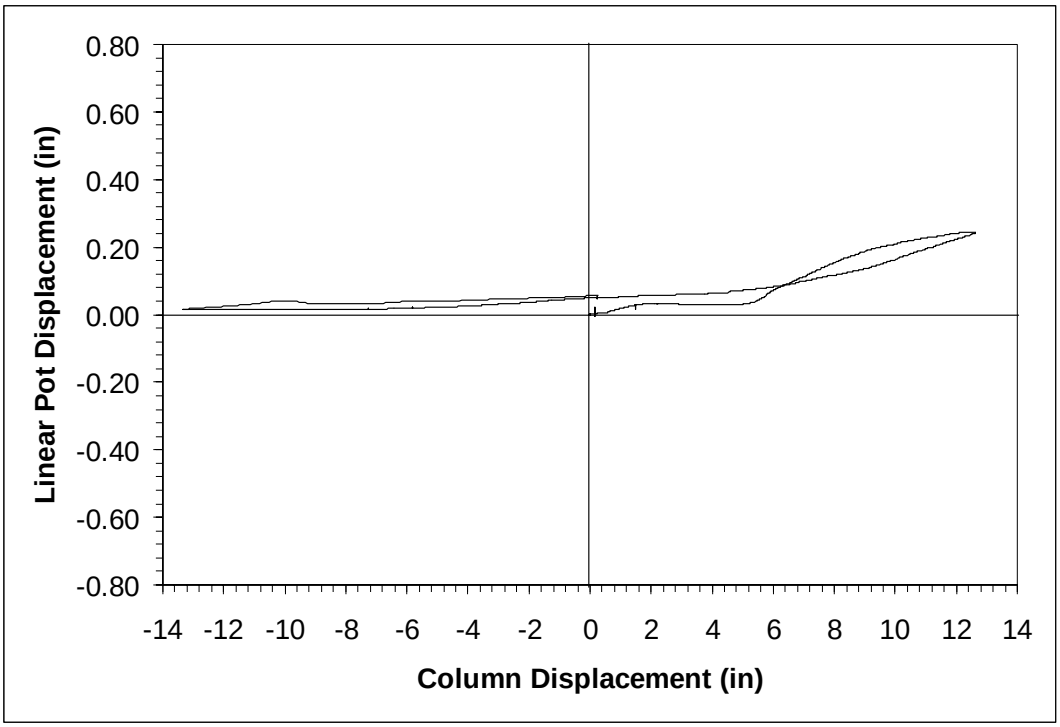

Figure A-5.3 Linear Pot History Third 8 inches North Side

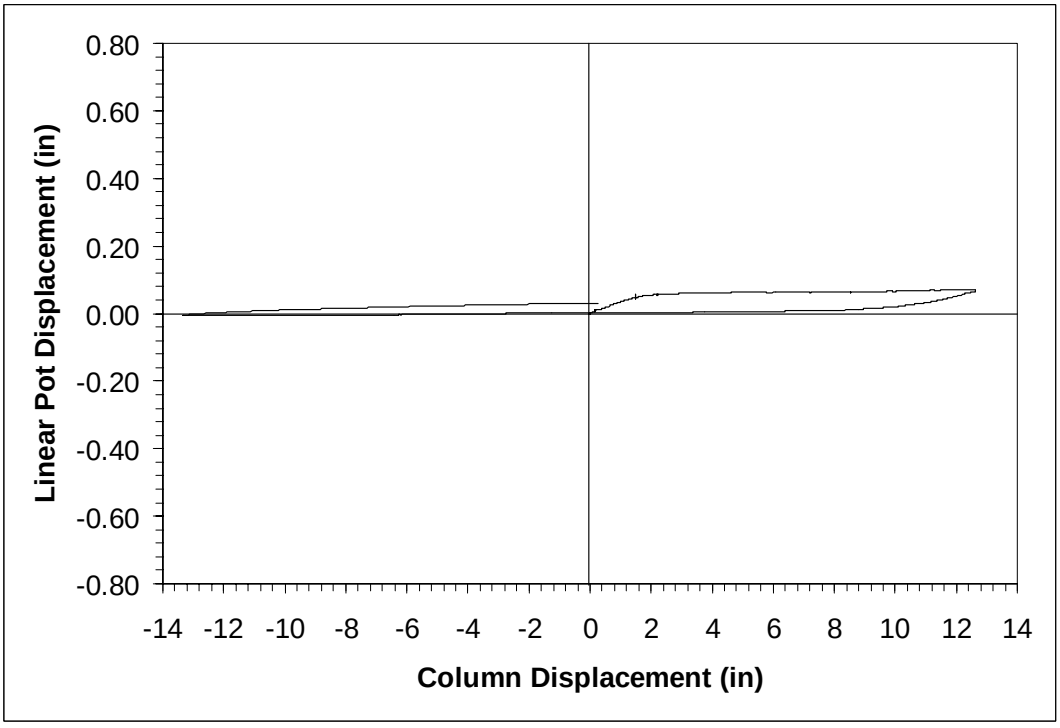

Figure A-5.4 Linear Pot History Fourth 8 inches North Side

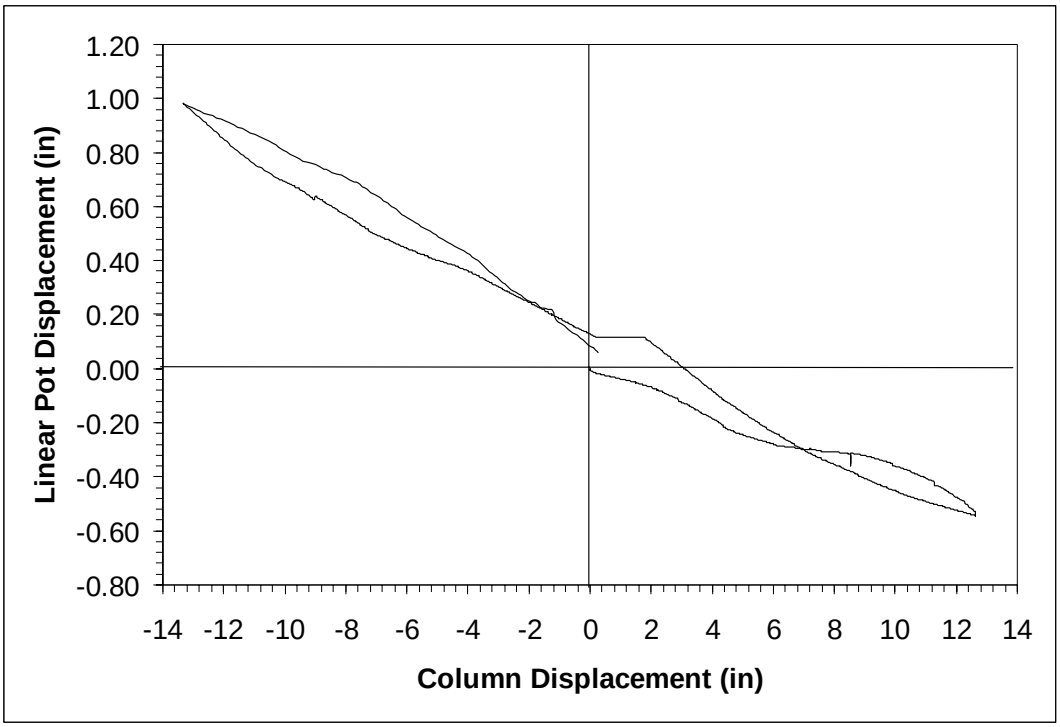

Figure A-5.5 Linear Pot History First 8 inches South Side

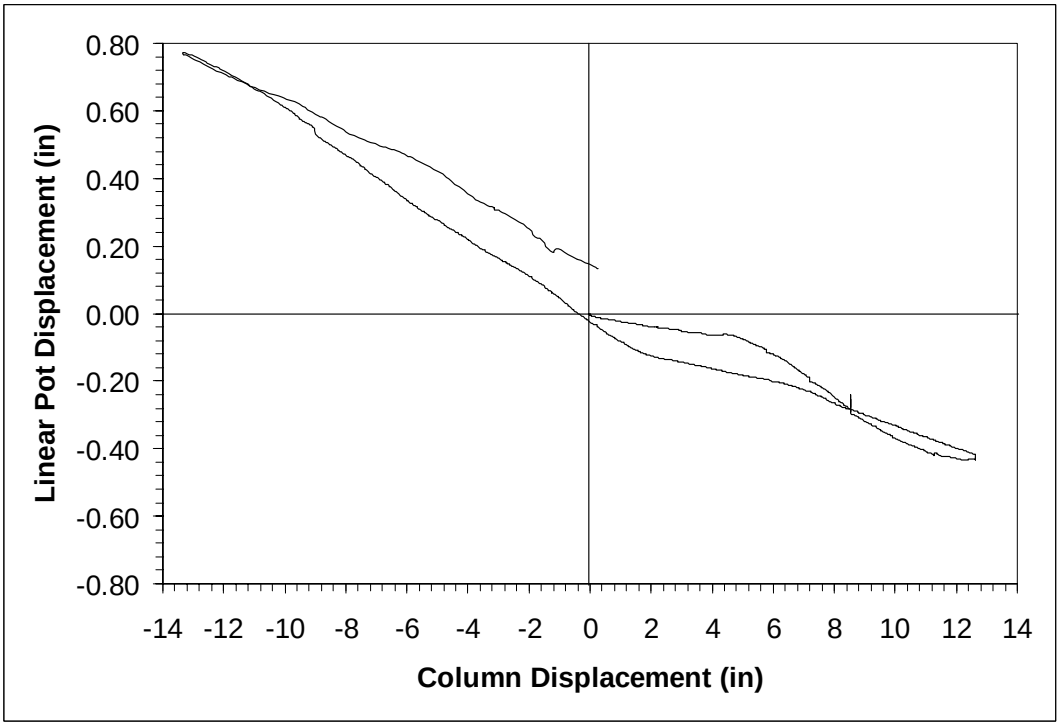

Figure A-5.6 Linear Pot History Second 8 inches South Side

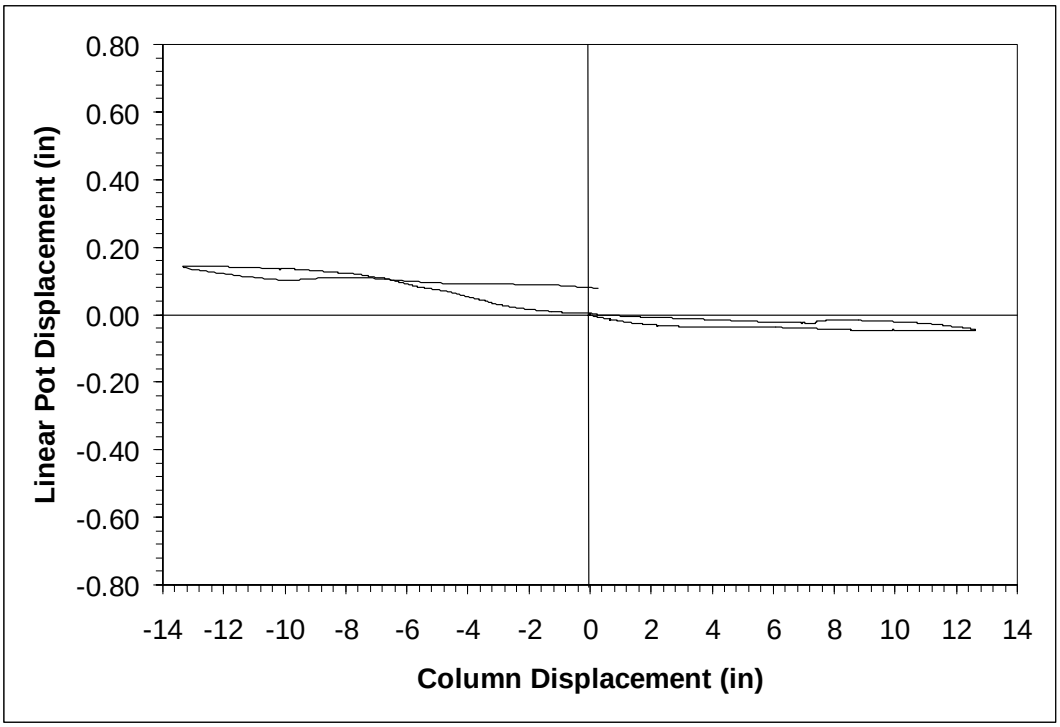

Figure A-5.7 Linear Pot History Third 8 inches South Side

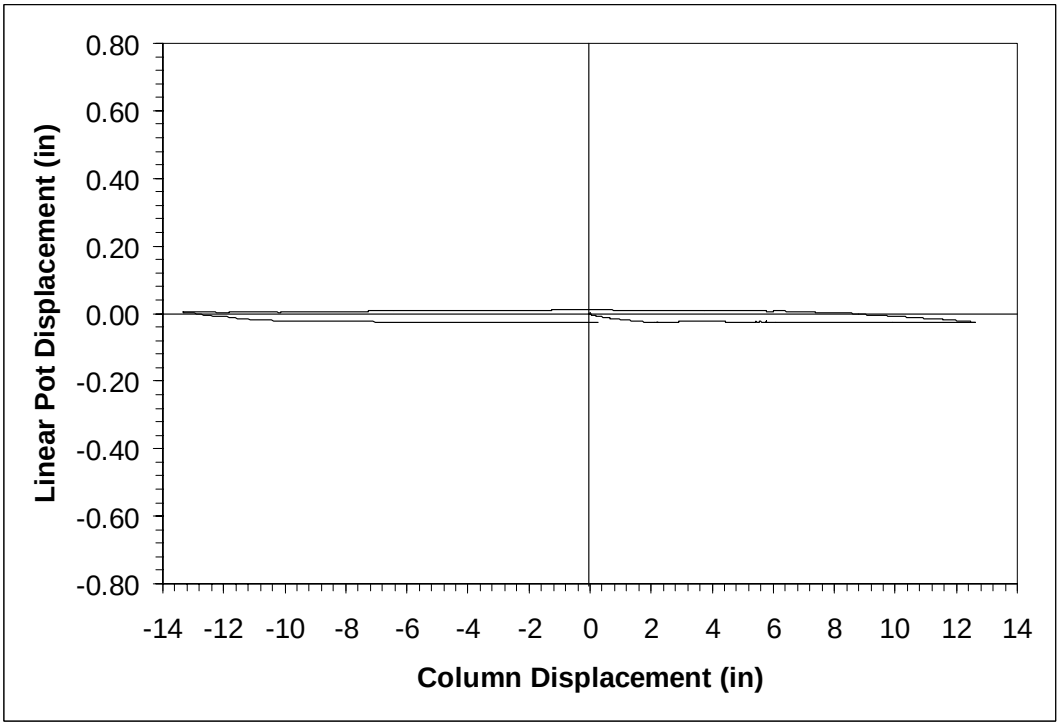

Figure A-5.8 Linear Pot History Fourth 8 inches South Side

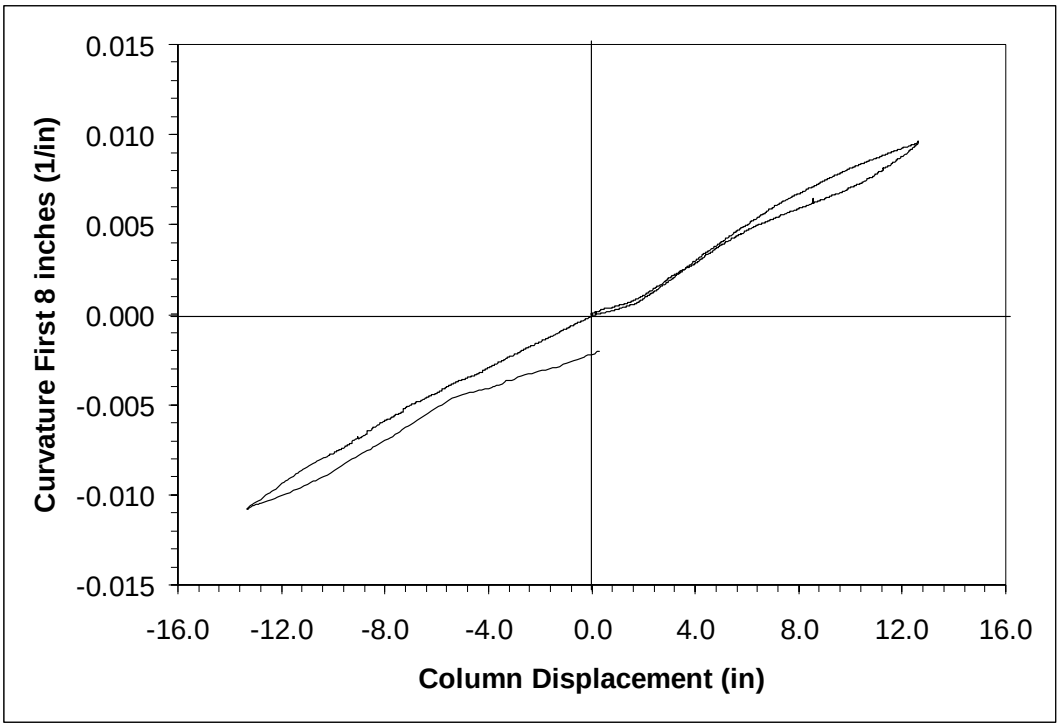

Figure A-5.9 Curvature over the First 8 inches of the Column

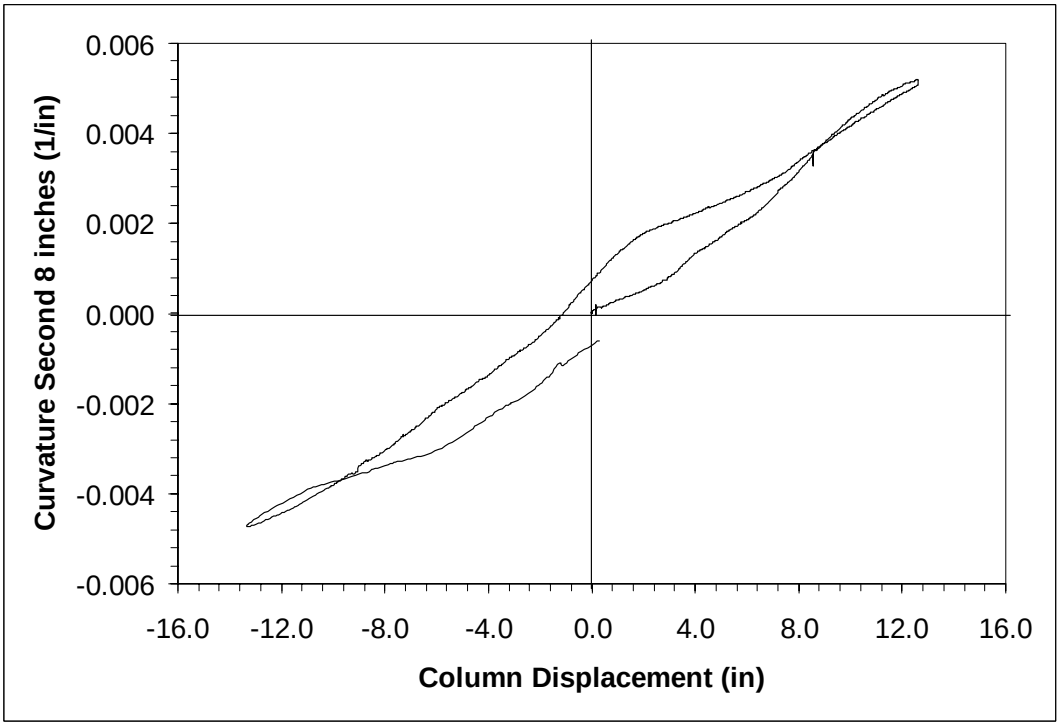

Figure A-5.10 Curvature over the Second 8 inches of the Column

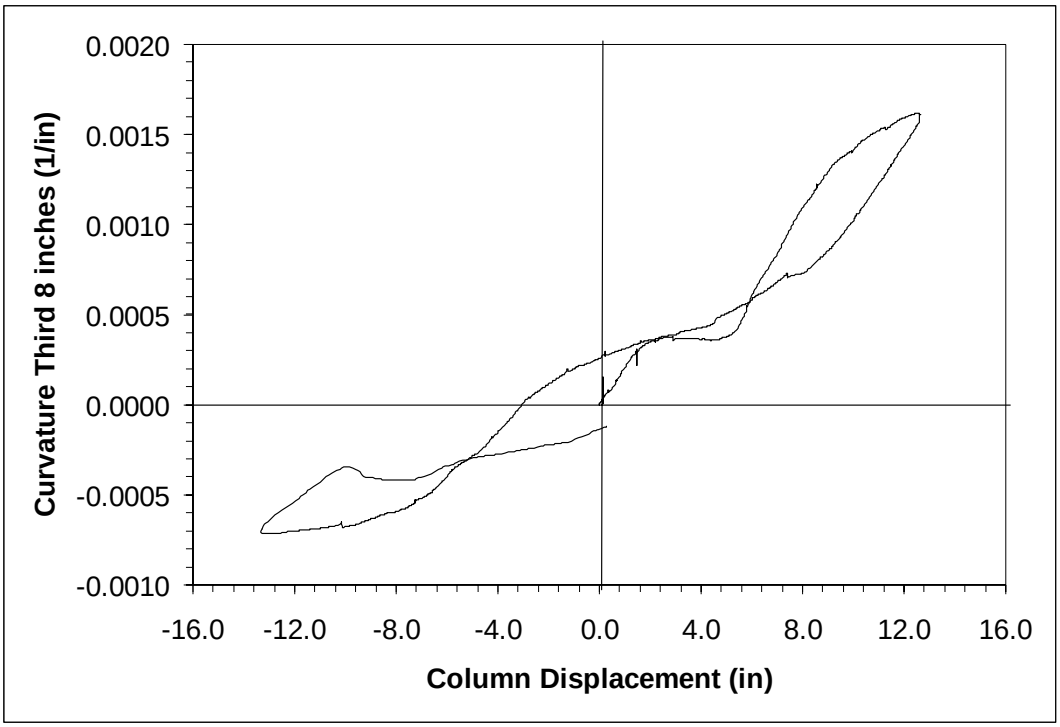

Figure A-5.11 Curvature over the Third 8 inches of the Column

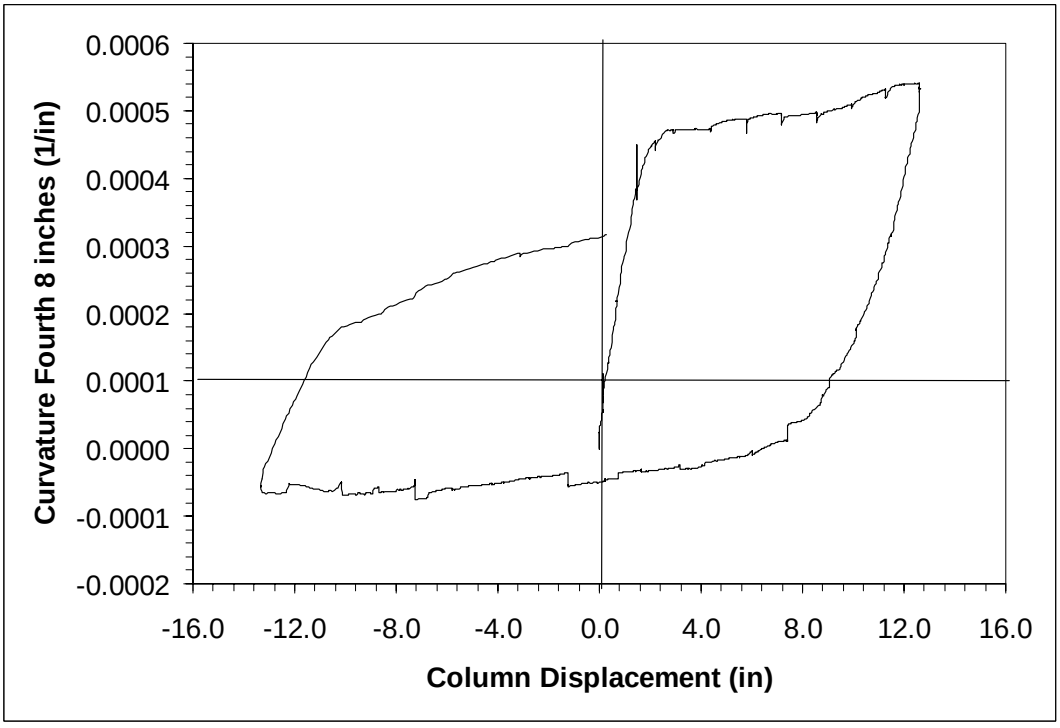

Figure A-5.12 Curvature over the Fourth 8 inches of the Column

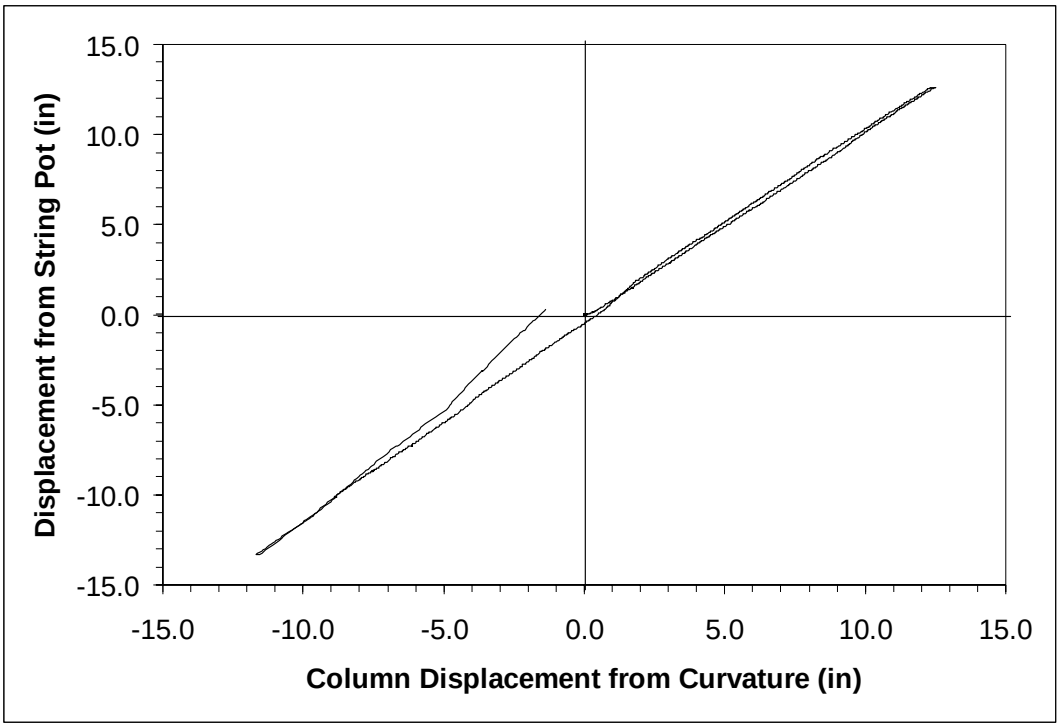

Figure A-5.13 String Pot Displacement versus Displacement from Curvature